**Contract No:**

This document was prepared in conjunction with work accomplished under Contract No. 89303321CEM000080 with the U.S. Department of Energy (DOE) Office of Environmental Management (EM).

**Disclaimer:**

This work was prepared under an agreement with and funded by the U.S. Government. Neither the U.S. Government or its employees, nor any of its contractors, subcontractors or their employees, makes any express or implied:

1 ) warranty or assumes any legal liability for the accuracy, completeness, or for the use or results of such use of any information, product, or process disclosed; or
2 ) representation that such use or results of such use would not infringe privately owned rights; or
3) endorsement or recommendation of any specifically identified commercial product, process, or service.

Any views and opinions of authors expressed in this work do not necessarily state or reflect those of the United States Government, or its contractors, or subcontractors.

# Refinement of Salt Dissolution Inhibitor Requirements - Final Report

**J. T. Boerstler**

July 2021

SRNL-STI-2021-00116, Revision 1

**DISCLAIMER**

# Refinement of Salt Dissolution Inhibitor Requirements - Final Report

J. T. Boerstler

July 2021

# REVIEWS AND APPROVALS

AUTHORS:

_____
J. T. Boerstler, Materials Technology Division
Environmental and Legacy Management Directorate                    Date

TECHNICAL REVIEW:

_____
B. J. Wiersma, Materials Technology Division, Reviewed per E7 2.60
Environmental and Legacy Management Directorate                    Date

_____
R. E Fuentes, Materials Technology Division
Environmental and Legacy Management Directorate                    Date

_____
K. B. Martin, Process Safety and Regulatory
Savannah River Remediation                                         Date

APPROVAL:

_____
A. D. Cozzi, Manager, Materials Technology Division                Date
Environmental and Legacy Management Directorate

_____
F. M. Pennebaker, Director, Chemical Processing
Environmental and Legacy Management Directorate                    Date

_____
C. Ridgeway, Manager, Process Safety and Regulatory
Savannah River Remediation                                         Date

# ACKNOWLEDGEMENTS

# Executive Summary

At Savannah River Site (SRS), High-Level Waste is stored in below-grade carbon steel tanks. This waste in part consists of sludge, salt cake, and/or supernate. Preparation of this waste for future processing involves dissolution of the salt cake layer. The salt dissolution process can create conditions that leave the carbon steel tanks susceptible to localized corrosion. The salt to be dissolved contains high concentrations of nitrate, that once released, create an environment that may be conducive to pitting corrosion and/or stress corrosion cracking (SCC) of carbon steel.

The salt dissolution process also liberates interstitial liquid trapped between the salt crystals. This liquid is initially high in nitrite and hydroxide concentration. High pH and greater ratios of nitrite to nitrate act as inhibitors to minimize corrosion of carbon steel in high nitrate environments. However, as dissolution proceeds, the concentration of nitrate will increase, while the hydroxide and nitrite concentration of the interstitial liquid will deplete and become insufficient to prevent the onset of corrosion attack. Tank blending and addition of inhibitors are used to ensure adequate concentrations of hydroxide and nitrite. However, this is not desirable during salt dissolution as it can reduce process efficiency and increase the amount of waste that needs processing.

It has been proposed that these corrosion control limits be revisited to evaluate the corrosion susceptibility of carbon steel in environments that more closely resemble current operating conditions at SRS. An experimental matrix was designed to evaluate the use of the pitting factor for supernate chemistries characteristic to SRS, particularly during the salt dissolution process. Two electrochemical methods were identified to determine the susceptibility of A537 and A285 low-carbon steels to pitting corrosion with this chemistry envelope at temperatures up to 75 °C. The predominant electrochemical test method was Cyclic Potentiodynamic Polarization (CPP) studies. Through CPP, the pitting factor was used, based on Hanford Site corrosion studies, to accurately identify pitting susceptibility within the compositional range studied with some conservatism. Additionally, sulfate was determined to have no statistically significant influence, at concentrations up to 0.6 M, on pitting behavior in more concentrated solutions where other aggressive species govern pitting susceptibility. Where CPP was inconclusive, Modified ASTM G192 was successfully used to evaluate pitting susceptibility conditions and allowed for a pass/fail result to be determined. In all cases, the pitting factor was determined to be applicable to the simulants tested, with this metric accurately predicting incidences in which pitting occurred. Based upon the findings in this work, a pitting factor of 1.2 is being proposed to build in a safety factor and remain consistent with the Hanford Site approach. Additionally, a minimum pH limit of 12 is proposed to ensure carbon steel passivity and localized corrosion the primary degradation mechanism.

Susceptibility to SCC was evaluated using a reduced matrix of tests at 75 °C. No failures due SCC were observed at open circuit. In addition, tests polarized anodically by 200 mV only resulted in failures for trials with pitting factors less than 0.86. However, a test with a passing condition based upon the pitting factor metric (pitting factor = 1.40) did exhibit a failure with an applied potential of +300 mV vs. OCP. This result is contrary to the prediction based upon the pitting factor, however, a polarization of 300 mV, or even 200 mV, from open circuit is substantial. The relationship between these testing parameters and service environment/conditions and the desired level of conservatism in the metric should be further evaluated in the determination of the significance of this result. While the pitting factor accurately predicted susceptibility to SCC at temperatures up to 75 °C and with positive overpotentials up to 200 mV, the relatively small sample matrix and failure of a passing pitting factor with a 300 mV polarization resulted in an inconclusive determination of whether the pitting factor may be used for predicting susceptibility to SCC at temperatures between 50 °C and 75 °C. As such, additional testing is recommended to evaluate the validity of the pitting factor for SCC susceptibility prediction at temperatures between 50 °C and 75 °C.

# TABLE OF CONTENTS

# LIST OF TABLES

# LIST OF FIGURES

# LIST OF ABBREVIATIONS

A285        A285 Low-Carbon Steel

A537        A537 Low-Carbon Steel

ASTM        American Society for Testing and Materials

CPP         cyclic potentiodynamic polarization

MOC         material(s) of construction

OCP         open circuit potential

SCC         stress corrosion cracking

SCE         saturated calomel electrode

SiC         silicon carbide

SRS         Savannah River Site

SSRT        slow strain rate testing

## 1.0 Introduction

At Savannah River Site (SRS), High-Level Waste is stored in below-grade tanks constructed of carbon steel. This waste is composed of sludge, salt cake, and/or supernate. In part, preparation of this waste for future processing involves dissolution of the salt cake layer. The salt dissolution process can create conditions that leave the carbon steel tanks susceptible to a number of corrosion processes. The salt to be dissolved contains high concentrations of nitrate, that once released, create an environment that may be conducive to pitting corrosion and/or stress corrosion cracking (SCC) of carbon steel.

The salt dissolution process also liberates interstitial liquid trapped between the salt crystals. This liquid is initially high in nitrite and hydroxide concentration. High pH and greater ratios of nitrite to nitrate act as inhibitors to minimize corrosion of carbon steel in high nitrate environments. However, as dissolution proceeds the concentration of nitrate will increase while the hydroxide and nitrite concentration of the interstitial liquid will deplete and become insufficient to prevent the onset of corrosion attack. Tank blending and addition of inhibitors are used to ensure adequate concentrations of hydroxide and nitrite. However, this is not desirable during salt dissolution as it can reduce process efficiency and increase the amount of waste that needs processed.

An administrative control program is in place that dictates the amount of inhibitors required for tank chemistries based on the concentration of nitrate present [1]. This program is based on experimental programs that have evaluated the susceptibility of A537 carbon steel to pitting corrosion and SCC in high nitrate concentration solutions with low concentrations of inhibitors [2-4]. The nitrate and inhibitor concentrations examined in these works are shown in Table 1-1. It has been proposed that these corrosion control limits be revisited to evaluate the corrosion susceptibility of carbon steel in environments that more closely resemble current operating conditions during salt dissolution.

**Table 1-1: Compositional Ranges for Previous Testing [2-4]**

| Species | Concentration Range [M] | Temperature Range [°C] |
|---------|-------------------------|------------------------|
| Nitrate | 5.5 - 8.5 | |
| Nitrite | 0.01 - 0.1 | |
| Hydroxide | 0.01 - 0.1 | |
| Chloride | 0.1 | |
| Sulfate | 0.1 | 50 |
| Aluminate | 0.5 | |
| Carbonate | 0.1 | |
| Phosphate | 0.05 | |

The compositional range of inhibiting species (nitrite and hydroxide) in these works are lower than current salt dissolution tank chemistries. Sulfate concentrations have also recently been observed to be higher than the 0.1 M that was previously evaluated. In addition, it is desirable to expand the temperature range to 75 °C from 50 °C, to potentially allow for continued mixing during salt dissolution campaigns.

To evaluate the susceptibility of carbon steel to pitting corrosion and SCC in conditions more resembling the salt dissolution environment, corrosion testing was conducted at higher inhibitor concentrations and more realistic operating temperatures, shown in Table 1-2.

**Table 1-2: Compositional Ranges for Proposed Testing**

| Species | Concentration Range [M] | Temperature Range [°C] |
|---|---|---|
| Nitrate | 0.0 - 7.0 or saturation | |
| Nitrite | 0.0 - 1.2 | |
| Hydroxide | 0.0 - 1.2 | |
| Chloride | 0.0 - 0.4 | 25-75 |
| Sulfate | 0.0 - 0.6 | |
| Aluminate | 0.5 | |
| Carbonate | 0.1 | |
| Phosphate | 0.05 | |

Coupons of A537 and A285 were subjected to cyclic potentiodynamic polarization (CPP) electrochemical experiments to help determine their pitting corrosion vulnerability in salt dissolution supernate simulants and other tank farm simulant chemistries at temperatures ranging from 25-75 °C. In some cases, CPP provided inconclusive results as to the susceptibility to pitting corrosion in a given chemistry. In such cases, a Modified ASTM G192 test was used to further evaluate the pitting behavior of the material and ultimately draw conclusions on its susceptibility. This method employs galvanostatic and potentiostatic holds that differ from the constant ramp rate of the potential for CPP, allowing the system time to reach a steady state and elucidate details that may be missed during CPP analysis. The pitting factor was determined to accurately predict instances of pitting within the chemistry envelope evaluated, and control limits based upon this approach are proposed.

As supernate temperatures begin to exceed 50 °C, an increased susceptibility to SCC may be present. Therefore, a targeted matrix was developed to evaluate the validity of the pitting factor for prediction of susceptibility to SCC at 75 °C. Round tensile samples of A537 and A285 were subjected to slow strain rate testing (SSRT). A test cell constructed around a tensile sample allowed for exposure to waste tank simulants during mechanical testing. A slow strain rate was used to allow time for electrochemical processes to take place and to not have their contributions become indiscernible. Tests were conducted at open circuit (no polarization) and with an anodic overpotential to account for potential changes in open circuit potential that are possible over decades-long exposures.

## 2.0 Experimental Procedure

### 2.1 Long Term Open Circuit Potential Measurement

Open circuit potential (OCP) is the potential at which the anodic and cathodic reactions taking place on a material in a given environment are equal and the net current is equal to zero. Changes in surface condition, chemistry, and kinetics of electrochemical reactions can result in a shift in OCP over time. If such a shift were substantial and in the positive direction, an increase in pitting susceptibility may occur. For this reason, the evolution of the OCP for A537 carbon steel in waste tank simulants at various inhibitor levels was observed over time to determine if an increased susceptibility to pitting corrosion could exist, although, OCP alone cannot be used to make this determination.

An insulated wire was affixed to 1-inch by 3-inch coupons of A537 carbon steel with silver epoxy to serve as a lead wire for electrochemical measurements. This connection was then covered with acrylic to prevent intrusion of solution interrupting the electrical connection. Each coupon was placed in a beaker containing

simulated waste tank simulants with varying inhibitor levels.  The composition of the simulants is shown in Table 2-1.

**Table 2-1:  Composition of Waste Tank Simulants used for Long Term OCP Measurements**

| Species | Concentration [M] |
|---------|-------------------|
| Nitrate | 7 or saturation |
| Nitrite | 0.01 - 0.5 |
| Hydroxide | 0.01 - 0.6 |
| Chloride | 0.1 |
| Sulfate | 0.1 |
| Aluminate | 0.5 |
| Carbonate | 0.1 |
| Phosphate | 0.05 |

Solution was added to the beakers containing the carbon steel coupons until the liquid reached approximately a half inch above the electrical connection.  Beakers were then sealed with plastic film and the solution temperatures were maintained at 30 or 50 °C using a hot plate.  OCP measurements were recorded each day using a potentiostat and a saturated calomel reference electrode.  Additional supernate was added when necessary to account for evaporative losses.

2.2 Cyclic Potentiodynamic Polarization (CPP) of Carbon Steel Coupons

A common method used to assess the pitting susceptibility of an alloy in a given environment is CPP.  The resulting polarization curve from a CPP can be found in Figure 2-1 for reference. This method involves polarizing the sample anodically through the passive regime until breakdown occurs, due to the onset of pitting, and/or reaching transpassive conditions, then polarizing cathodically until the scan returns to the corrosion potential.  From this process, a number of assessments can be made about the susceptibility of the material to pitting corrosion in that environment.  The first characteristic value is the breakdown potential or pitting potential.  This is typified by the large increase in current from the passive current that occurs as a result of increased anodic dissolution rates.  The next characteristic that can be assessed is the nature of the hysteresis. A positive hysteresis, the reverse scan having higher current than the forward scan at the same potential value, indicates that pitting has occurred, and pits continue to grow even below the breakdown potential.  A negative or no hysteresis likely indicates that no localized corrosion has occurred, or pit growth is no longer stable when the potential decreases.  Lastly, the repassivation potential could be obtained if solution conditions are such that repassivation of active pits can occur.  This parameter may not be possible to obtain if chemistries conducive to repassivation are not present or if repassivation occurs below the corrosion potential.

The OCP or corrosion potential of the material, along with the repassivation potential and breakdown potential, can be used to assess the severity of the material's susceptibility to pitting corrosion in a given environment.  The relative positions of the corrosion and breakdown potentials indicates how much the material must be polarized to support stable pit growth into the material.  If the breakdown potential is close to the corrosion potential, pitting is more likely in the event of polarization of the material or if there is an increase in the OCP of the material with exposure time.  The relative positions of the breakdown and repassivation potentials essentially indicates the range over which initiated pits will continue to grow, if pits are present.  Therefore, materials with repassivation potentials closer to the breakdown potential are desirable.  Lastly, the relationship of the corrosion potential and the repassivation potential is an indicator of the likelihood of pitting in a material.  If the repassivation potential is near the corrosion potential, there is an increased likelihood that the repassivation potential could be exceeded, and pits that initiated will continue to grow so long as the potential remains above the repassivation potential.
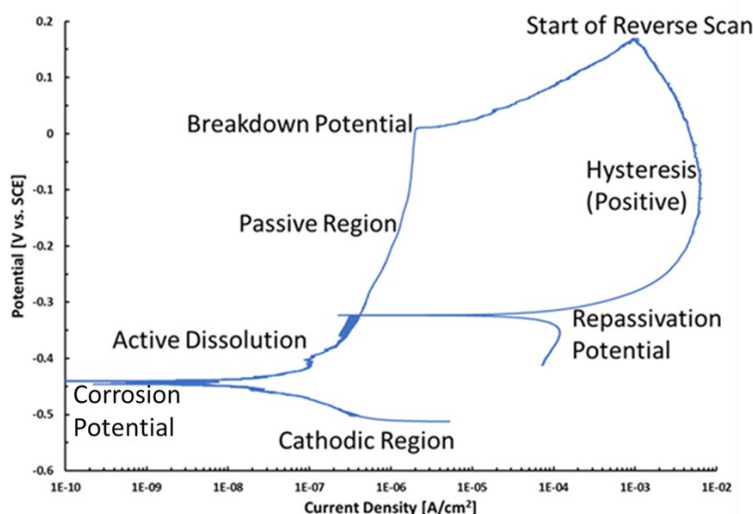
**Figure 2-1: Example of CPP curve with regions and values of interest labelled.**

The forward scan begins in the cathodic region and continues until the start of the reverse scan. The corrosion potential and breakdown potential can be determined in this region. The reverse scan begins at the end of the forward scan and ends once the potential is equal to the corrosion potential. The nature of the hysteresis (positive, negative, or mixed) along with the repassivation potential, when applicable, can be determined from this portion of the curve.

Three outcomes are possible based upon the presence or absence of stable localized corrosion during the polarization. The first is a positive hysteresis, which is shown in Figure 2-2.
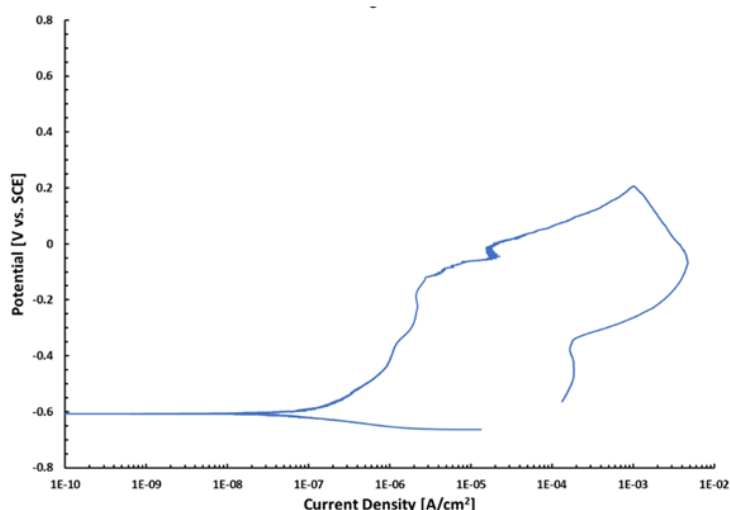


**Figure 2-2: Example of a positive hysteresis, defined as the current density from the reverse scan being greater than that of the forward scan.**

A positive hysteresis is defined by the current of the reverse scan being greater than that of the forward scan. With these cases, the current density of the reverse scan should remain higher than the passive current

density within the potential range of the passive region with the exception of decreases in current associated with repassivation, illustrated in Figure 2-1.  This is indicative of stable localized corrosion taking place, which could be the result of pitting or crevice corrosion.  Crevice corrosion can occur due to aggressive conditions forming in the narrow space between the sample and the acrylic mount.  The crevice creates an occluded region where the localized chemistry can become different from the bulk chemistry as metal ions dissolve, creating a charge imbalance, and attracting negatively charged anions, some aggressive, into the crevice region.  This can result in increasingly aggressive conditions that result in accelerated dissolution of the base material.  If the positive hysteresis is the result of crevice corrosion, this does not indicate a failure, as the result is due to an artifact of experimental design.  A failure is determined if the following three conditions are met:

1.  A positive or mixed hysteresis was present on the CPP curve.
2.  Pitting, not crevice, corrosion was observed on the sample surface.
3.  Repassivation potential was not observed or the difference between repassivation potential and corrosion potential is less than 200 mV.

Pitting corrosion can only occur at potentials above the repassivation potential.  Below this potential, any pits that were present would be passivated, meaning that a passive film is stable, and no further dissolution would occur.  Therefore, the difference between the corrosion potential and the repassivation potential indicates how likely pitting corrosion would occur for a given material in an environment.  A difference of more than 200 mV indicates that conditions favorable for pitting to occur are not anticipated absent any outside influence polarizing the surface substantially beyond typical OCP drift.

A negative hysteresis is defined by the current density on the reverse scan being less than the current on the forward scan.  An example is shown in Figure 2-3.


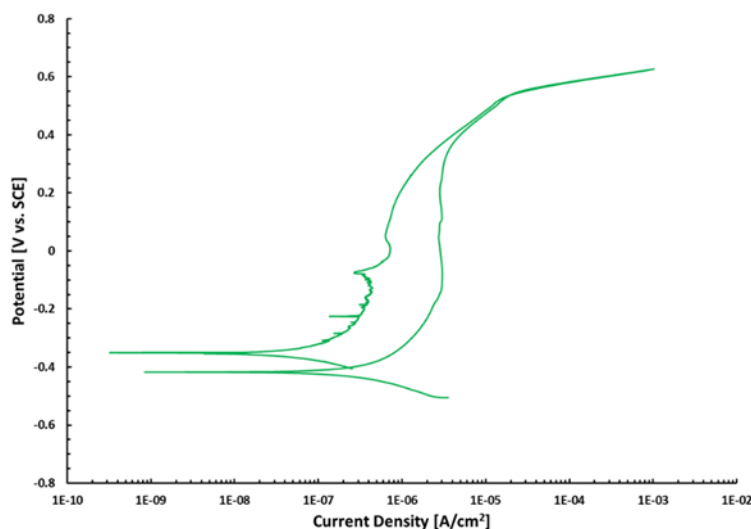
**Figure 2-3**:  **Example of a negative hysteresis, defined as the current density from the reverse scan being less than that of the forward scan.**

A negative hysteresis indicates that stable localized corrosion has not occurred during polarization.  Neither pitting nor crevice corrosion was present in these cases.  As such, trials with a negative hysteresis are defined as a pass condition.

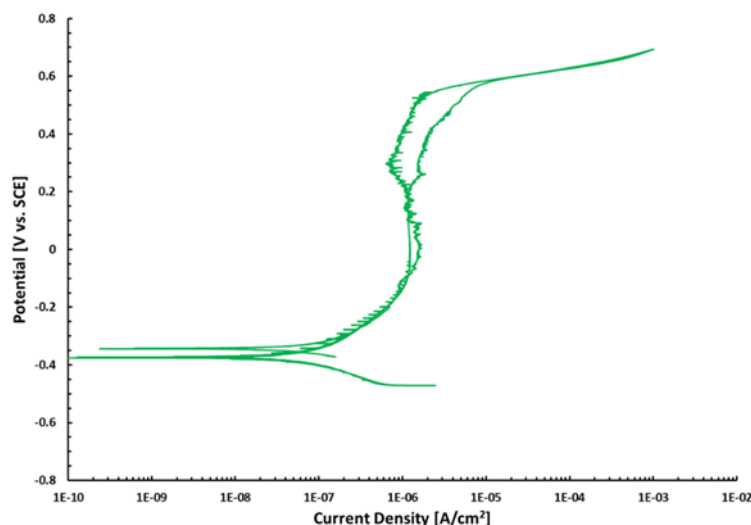The final potential outcome is a mixed hysteresis, shown in Figure 2-4.



**Figure 2-4: Example of a mixed hysteresis, defined as the current density from the reverse scan exhibiting behavior of both a positive and negative hysteresis.**

A mixed hysteresis represents a condition in which the current density during the reverse scan displays behavior of both positive and negative hysteresis during portions of the reverse scan. This could occur due to localized corrosion to a lesser extent or because of changes to the sample surface during the forward scan that result in slightly different kinetics for dissolution on the reverse scan. These instances require further examination to determine whether a passing or failing condition for susceptibility to pitting corrosion has occurred. First, the sample was examined for the presence of pitting or crevice corrosion. If this examination was still inconclusive, meaning there is no clear indication of pitting or crevice corrosion, the sample was subjected then to a Modified ASTM G192 test, which will be discussed further in the next section.

Two types of carbon steel were examined to characterize the pitting behavior of Type IIIA and Type II waste tank materials of construction, A537 and A285, respectively. Disks (exposed area of approximately 2 cm$^2$) or squares (approximately 0.75-inch by 0.75-inch) were cut from bar or rectangular bar stock using a slow speed saw. Insulated lead wires were affixed to the back side of coupons with conductive silver epoxy to create an electrical connection outside of the test cell. The wired coupons were then cold mounted using acrylic to protect the electrical connection, exposing only the top face of the coupon, and to provide a means of handling the coupons for further sample preparation. Samples were ground to 800-grit using progressively higher grit silicon carbide (SiC) paper with water as lubrication to obtain a flat, uniform surface. The final grinding step was conducted within one hour of testing to prevent the development of corrosion products on the test surface from residual moisture or atmospheric condition. Finally, the samples were rinsed with ethyl alcohol and blown dry to remove any residual organic material and water from the sample surface. An example of each sample is shown below in Figure 2-5.

**Figure 2-5: Example of A537 (top) and A285 (bottom) electrodes used for CPP experiments.**

750 mL of test solution was batched for each test. Test solutions were made the same day as testing to prevent precipitation of salts at room temperature during storage. In general solutions were made at their respective test temperature with stirring using a magnetic stir bar on a hotplate/stirrer. However, exceptions were made dependent upon solution chemistry. The dissolution of sodium nitrate is endothermic, therefore, solutions containing higher nitrate concentrations (greater than 4 M) would have the temperature increased when necessary to account for the endothermic process and aid in complete dissolution. Another exception was due to the dissolution behavior of sodium sulfate. In high nitrate solutions, it was observed that sodium sulfate did not readily dissolve. In addition, sodium sulfate differs from the other solution constituents in that the solubility is highest between 30 and 40 °C then decreases with increasing temperature. For this reason, the temperature of the test solution would be lowered, if necessary, to accommodate the solubility characteristics of sodium sulfate. In some cases, precipitation of salts was observed for highly concentrated solutions. As many of these solutions represent salt dissolution conditions, this was considered acceptable as operating conditions would represent an equilibrium, or at least steady state, between the supernate and precipitated salt layer.

The prepared solution was then added to a test vessel with ports for the working electrode or sample, a salt bridge containing a reference electrode, two graphite rods to serve as counter electrodes, and thermocouples to monitor test temperature and prevent overheating of the solution. The solution was heated on a hotplate with stirring until a steady test temperature was achieved. The hotplate contained an additional thermocouple to provide feedback for maintaining test temperature. After test temperature was achieved, the sample, counter electrodes, and salt bridge containing the reference electrode and a 0.1 M sodium nitrate solution were inserted into the test cell. Two graphite counter electrodes were used to promote more even current distribution to the working electrode. A saturated calomel electrode (SCE) was used as the reference electrode.

After the proper test conditions were established and the test apparatus was prepared, an OCP delay was initiated. The potential was measured once per second for a total of two hours. This was followed by the CPP experiment. The following parameters for the polarization were used:

| | |
|---|---|
| Scan rate: | 0.167 mV/s |
| Initial potential: | -0.1 V versus open circuit potential |
| Final potential: | 1.2 V versus reference electrode |
| Current density limit: | 1 mA/cm$^2$ |
| Reverse scan rate: | 0.167 mV/s |
| End potential: | 0.0 V versus open circuit potential |

The forward scan proceeded until either the final potential or the current density limit was reached, which was the current density limit in all cases. At this point the scan direction was reversed, and the reverse scan proceeded until the OCP at the beginning of the test was reached. The applied potential and the measured current were monitored for the duration of the cyclic polarization. After completion of the test, the sample was removed from the test solution, rinsed with deionized water, and dried. Samples were visually inspected for the presence of pitting and crevice corrosion and then placed in a desiccator for storage.

## 2.3 Modified ASTM G192

Results from CPP experiments were not always conclusive. In such cases, a secondary test method was used to clarify the pitting susceptibility of the material. Modified ASTM G192 is a test method by which the protection potential or repassivation potential can be determined [6]. This method involves potentiodynamically polarizing the sample until a potential or current density limit is reached (similar to the forward scan of CPP tests), galvanostatically maintaining that current to allow for stable pit growth, and then finally progressing through a series of potentiostatic holds where the applied potential is reduced in a step-wise manner until the current density becomes less than the current density measured on the forward scan. Sample preparation and setup for this test were carried out in an identical manner as the CPP tests through the two-hour OCP delay. The following test parameters were used:

Potentiodynamic

| | |
|---|---|
| Initial potential: | -0.1 V vs. open circuit potential |
| Final potential: | 1.5 V vs. reference electrode |
| Current density limit: | 50 µA/cm$^2$ |
| Scan Rate: | 0.1667 mV/s |

Galvanostatic

| | |
|---|---|
| Hold current density: | 50µA/cm$^2$ |
| Hold time: | 240 min |

Potentiostatic Staircase

| | |
|---|---|
| Potential step decrement: | 25 mV |
| Potential hold time: | 120 min |

The potential and the current were monitored for the duration of the test for all steps. After completion of the test, the sample was removed from the test solution, rinsed with deionized water, and dried. The sample was visually inspected for the presence of pitting and crevice corrosion and then placed in a desiccator for storage.

## 2.4 Slow Strain Rate Testing (SSRT)

Tensile tests are a common means by which the mechanical strength of a material may be assessed. In many cases this involves applying tensile stress to a sample in an ambient environment, at room temperature and exposed to air. For many applications this type of testing is satisfactory, however, material-

environment interactions can greatly impact mechanical performance in some situations. One such example is when a material is susceptible to SCC in its intended service environment, as potentially exists in the storage of High-Level Waste in carbon steel tanks. Cracking can initiate at a variety of locations in a material under mechanical stress: welds, mechanical flaws, corrosion pits, secondary phase particles, or any other feature acting as a stress concentrator. These susceptibilities can be further exacerbated in the presence of an aggressive environment and the interaction between mechanical stress and localized corrosion leads to accelerated crack growth. As is the case with pitting corrosion, a crack creates an occluded environment, one in which chemistry within the crack may differ significantly from the bulk due to lack of mixing. This can lead to acidification and concentration of aggressive species within the crack tip region, resulting in accelerated dissolution of the material at the crack tip. This can lead to premature failure in a material that otherwise should exhibit ductile behavior. To examine this susceptibility, SSRT can be combined with a test cell that enables exposure of the test specimen to waste tank simulants during mechanical testing.

A537 and A285 tensile specimens with round cross-sectional areas were used in the SSRT tests. The expected range of ultimate tensile strength in an ambient environment for the two materials is 450-585 MPa and 380-515 MPa, respectively. The approximate dimensions of the gage area were 1 inch in length with a diameter of either 0.25 inches or 0.16 inches. The exact dimensions of each specimen were recorded prior to testing for use in calculations to determine stress and strain during the mechanical testing. As shown in Figure 2-6, the gage length was measured from shoulder to shoulder (where the diameter begins to increase) and the gage diameter was measured in three positions and averaged to account for any variation in gage thickness. An insulated wire was then affixed to an unexposed portion of the test specimen for electrochemical tests during exposure.
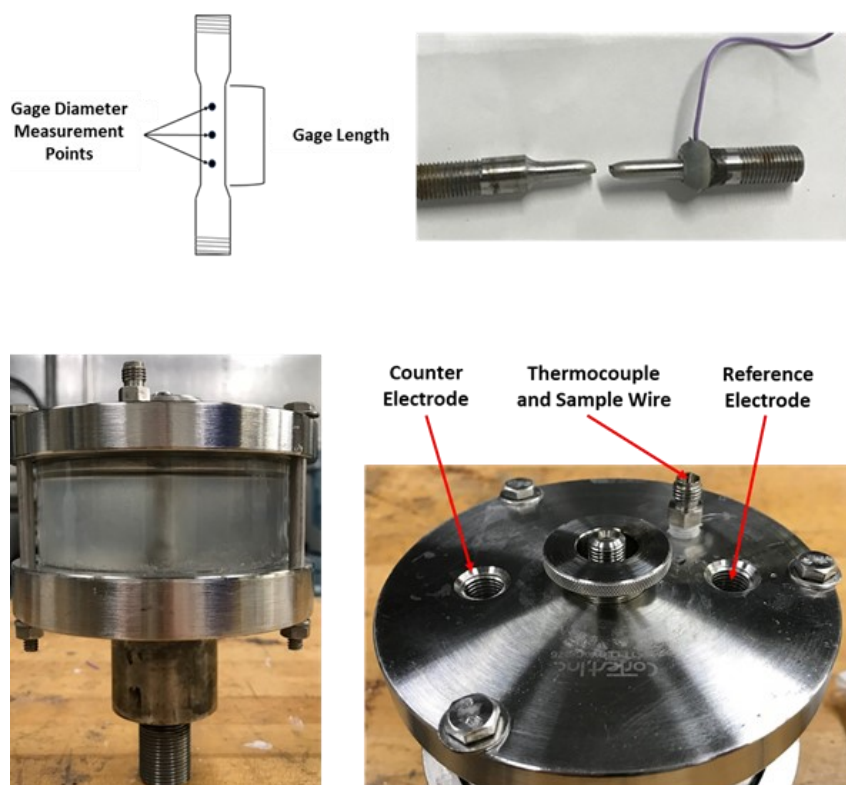


**Figure 2-6: Diagram of tensile specimens used for SSRT with points for measuring gage dimensions as well as test cell and sample showing affixed wire for electrochemical measurements.**

An Instron 8862 load frame and Instron Stress Corrosion Cracking Program Version 6.3.3 were used for all mechanical testing. After measurements of the specimens were taken, a test cell was constructed around the specimen to allow exposure to simulated waste tank supernate during tensile testing. The test cell consisted of lower and upper plates, a cylindrical cell wall, and gaskets and O-rings for seals. The lower plate contained only an opening for tensile specimen. The top plate was constructed with openings for the tensile specimen, a counter electrode (if desired), a salt bridge for a reference electrode, and thermocouples. After assembly the test cell with specimen were loaded into the load frame by threads on both ends of the tensile specimen. Test solution was then added to the cell, followed by the thermocouples, salt bridge (containing 0.1 M sodium nitrate) and a saturated calomel reference electrode, and a graphite counter electrode, if necessary. Heating tape was affixed to the test cell and then the solution was heated to 75 °C for all tests. This temperature was maintained for 24 hours prior to mechanical testing, with OCP being monitored in some cases during the delay. After the 24 hour delay completed, slack was taken out of the system by manually adjusting the position of the test specimen until a force increase was observed. Once the test preparation was completed, the mechanical test would begin. A constant extension rate of $10^{-6}$ inches per second was used for these slow strain rate tests. Elongation of the specimen would continue until failure occurred, a fracture of the specimen into two pieces. Position and force were recorded throughout the duration of the mechanical testing. Additionally, OCP could be obtained at any point unless the test was being conducted with an overpotential. In tests with overpotentials, a potentiostat was used to potentiostatically polarize the tensile specimen in conjunction with a counter electrode and reference electrode inserted into the test cell. The potentiostatic polarization would last for the duration of the tensile test, with potential and current being measured throughout. After exposure, samples were removed from the load frame and test cell and cleaned with water and a soft brush to remove loosely adherent corrosion products. The samples were dried in air and fracture surfaces were visually observed for indications of brittle fracture or cracking. Images from the visual observations can be found in Appendix B and the electronic laboratory notebook for the project [7].

2.5 Quality Assurance

Data used in this report were recorded in the electronic laboratory notebook system, notebook number G1720-00424-01.

Requirements for performing reviews of technical reports and the extent of review are established in manual E7 2.60. SRNL documents the extent and type of review using the SRNL Technical Report Design Checklist contained in WSRC-IM-2002-00011, Rev. 2.

## 3.0 Results and Discussion

3.1 Long Term Open Circuit Potential Measurement

The results of the long term open circuit measurement experiments are shown below in Figure 3-1.
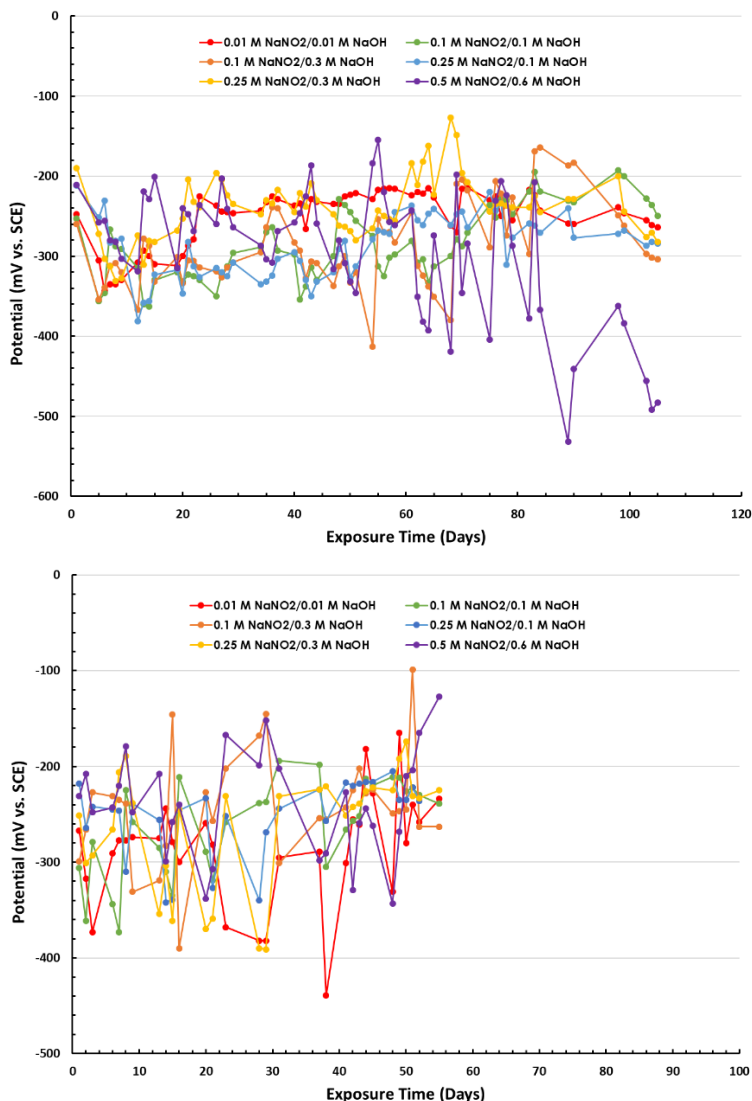
**Figure 3-1: Results of Long Term OCP Measurement at 30 °C (top) and 50 °C (bottom)**

The data from the 30 °C trials indicated that OCP did not drift substantially over the 100 day exposure, with day-to-day variations but the final OCP typically being slightly more negative than the initial OCP value. The result of a largely stable or decreasing OCP with time does not lead to increased susceptibility to pitting corrosion with time, as the repassivation potential is not anticipated to be exceeded with increased exposure time if applicable. The data from the 50 °C trials exhibited a similar trend, with final OCP being near that of the original OCP in most cases.

It must also be noted that difficulties arose in the testing of OCP evolution. The simulants used in this study were designed to represent salt dissolution conditions in which precipitation has occurred and supernates are exceedingly concentrated (up to 7 M nitrate). This resulted in solutions that readily precipitated after mixing when solution preparation had ceased. As a result, the beakers became increasingly filled with precipitated salts with increased exposure time, particularly at higher temperatures. While this condition may have well portrayed the salt dissolution environment, this resulted in the termination of the 50 °C trials shortly after day 50 as reliable measurement of OCP was no longer possible. Similar, but less extensive, issues were encountered during the 30 °C trials, potentially leading to inaccurate results in those trials as

well. As a result of these complications and trends not conveying an increase in OCP with exposure duration, this data was not considered in the evaluation of pitting susceptibility.

3.2 Cyclic Polarization of Carbon Steel Coupons

The experimental matrix used for CPP testing is shown below in Table 3-1. Trials 1 to 15 represent a range of simulated salt dissolution simulant chemistries. This matrix was statistically designed to span the compositional range of salt dissolution chemistries with nitrate concentration up to 7 M or saturation and increased inhibitor concentrations up to 0.6 and 0.5 M for hydroxide and nitrite, respectively. Aluminate, carbonate, and phosphate concentrations were held constant across the chemistry envelope, with these values found in Table 1-2. Trials 16 to 33 represent a screening matrix based upon work conducted for the mitigation of pitting and SCC of Hanford double-shell tanks [8]. In general, nitrate concentrations are lower, maximum inhibitor concentrations are higher, and chloride is present in higher quantities. In addition, sulfate concentration was also expanded from a maximum of 0.2 M to a maximum of 0.6 M to evaluate its influence on pitting corrosion. This second group of screening trials represents more general SRS tank farm chemistries. Both matrices were also expanded to include temperature up to 75 °C. The table also includes a metric called the pitting factor which is used to determine the susceptibility of the material to pitting corrosion in a given environment. The pitting factor is calculated by a ratio of inhibitor species (hydroxide and nitrite) to aggressive species (nitrate and halides) that are weighted based upon logistic regression of the influence of these species on pitting that resulted from CPP experimental campaigns [8]. The equation for the pitting factor is shown below.

$$\text{Pitting Factor} = \frac{8.06\,[\text{OH}^-] + 1.55\,[\text{NO}_2^-]}{[\text{NO}_3^-] + 16.7\,[\text{Cl}^-]}$$

A pitting factor of greater than 2 indicates an environment in which pitting is not anticipated. A pitting factor of less than 1 indicates a condition in which the probability of pitting is high and can occur. Pitting factor values between 1 and 2 represent conditions in which the probability of pitting is low and minor pitting could potentially occur. This metric was determined based upon tank chemistries at Hanford Site; therefore, it is being evaluated in this study for applicability to Savannah River Site waste tank chemistries. It should be noted that fluoride concentration is a factor in the calculation of the pitting factor as it applies to Hanford control programs. However, fluoride concentrations within waste streams at Savannah River are not significant enough to affect the calculation of the pitting factor and were not considered in this work.

**Table 3-1: Chemistry envelope developed for evaluation of pitting corrosion in salt dissolution environments expanded for increased sulfate concentrations.**

| Trial | Nitrate [M] | Hydroxide [M] | Nitrite [M] | Sulfate [M] | Chloride [M] | Temperature [°C] | Pitting Factor |
|---|---|---|---|---|---|---|---|
| 1 | 7 | 0.6 | 0.5 | 0.6 | 0.1 | 75 | 0.65 |
| 2 | 4 | 0.6 | 0.01 | 0.6 | 0.1 | 75 | 0.86 |
| 3 | 4 | 0.01 | 0.5 | 0 | 0.1 | 75 | 0.15 |
| 4 | 7 | 0.01 | 0.01 | 0.6 | 0 | 75 | 0.01 |
| 5 | 4 | 0.6 | 0.01 | 0 | 0.1 | 30 | 0.86 |
| 6 | 4 | 0.01 | 0.5 | 0 | 0 | 75 | 0.21 |
| 7 | 4 | 0.01 | 0.01 | 0.6 | 0 | 30 | 0.02 |
| 8 | 7 | 0.01 | 0.01 | 0 | 0.1 | 30 | 0.01 |
| 9 | 7 | 0.6 | 0.01 | 0 | 0 | 75 | 0.69 |
| 10 | 7 | 0.6 | 0.5 | 0 | 0 | 30 | 0.80 |
| 11 | 4 | 0.6 | 0.5 | 0.6 | 0 | 30 | 1.40 |
| 12 | 7 | 0.01 | 0.5 | 0.6 | 0.1 | 30 | 0.10 |
| 13 | 5.5 | 0.305 | 0.255 | 0.3 | 0.05 | 53 | 0.45 |
| 14 | 5.5 | 0.305 | 0.255 | 0.3 | 0.05 | 53 | 0.45 |
| 15 | 5.5 | 0.305 | 0.255 | 0.3 | 0.05 | 53 | 0.45 |
| | | | | | | | |
| 16 | 2.75 | 0.3 | 0.6 | 0.1 | 0.2 | 35 | 0.55 |
| 17 | 0.94 | 1.2 | 0.2 | 0.01 | 0.24 | 35 | 2.02 |
| 18 | 0 | 1.2 | 1.2 | 0.2 | 0 | 35 | NA |
| 19 | 0 | 1.2 | 1.2 | 0.6 | 0.4 | 25 | 1.73 |
| 20 | 5.5 | 1.2 | 1.2 | 0.6 | 0 | 75 | 2.10 |
| 21 | 0 | 1.2 | 0 | 0.6 | 0 | 75 | NA |
| 22 | 5.5 | 0 | 0 | 0.6 | 0.4 | 75 | 0.00 |
| 23 | 0 | 1.2 | 0 | 0.6 | 0.4 | 75 | 1.45 |
| 24 | 0 | 0 | 1.2 | 0.6 | 0.4 | 25 | 0.28 |
| 25 | 5.5 | 1.2 | 1.2 | 0.6 | 0 | 25 | 2.10 |
| 26 | 5.5 | 0 | 0 | 0.6 | 0.4 | 25 | 0.00 |
| 27 | 0 | 1.2 | 0 | 0.6 | 0 | 25 | NA |
| 28 | 5.5 | 0 | 1.2 | 0.6 | 0 | 25 | 0.34 |
| 29 | 0 | 1.2 | 0 | 0.6 | 0 | 25 | NA |
| 30 | 0 | 0 | 1.2 | 0.6 | 0.4 | 75 | 0.28 |
| 31 | 5.5 | 1.2 | 1.2 | 0.6 | 0 | 75 | 2.10 |
| 32 | 5.5 | 0 | 0 | 0.6 | 0 | 75 | 0.00 |
| 33 | 0 | 1.2 | 1.2 | 0.6 | 0.4 | 75 | 1.73 |

Table 3-2 shows the results for the CPP experiments in terms of the hysteresis behavior and whether or not pitting was observed. The composition of each trial in terms of the species of interest and the pitting factor is also displayed. Additionally, Table 3-3 displays whether each condition was a pass or fail based upon the criteria described above. The CPP curves for all trials that are used for these determinations are provided in the Appendix A.

**Table 3-2: Composition, pitting factor, and results (hysteresis and presence of pitting) for each of the 33 trials for A537 and A285 carbon steel.**

**Red indicates pitting or a positive hysteresis. Green indicates no pitting or a negative hysteresis. A question mark (?) indicates that degradation occurred near the acrylic/metal interface that could not be attributed clearly to either crevice or pitting corrosion. Rows highlighted in yellow indicate an opposite hysteresis between A537 and A285.**

| Trial | Temp | PF | Nitrate | Hydroxide | Nitrite | Sulfate | Chloride | Pit? | | Hysteresis | |
|---|---|---|---|---|---|---|---|---|---|---|---|
| | | | | | | | | A537 | A285 | A537 | A285 |
| 1 | 75 | 0.65 | 7 | 0.6 | 0.5 | 0.6 | 0.1 | Y | Y | Pos | Pos |
| 2 | 75 | 0.86 | 4 | 0.6 | 0.01 | 0.6 | 0.1 | Y | Y | Pos | Pos |
| 3 | 75 | 0.15 | 4 | 0.01 | 0.5 | 0 | 0.1 | Y | Y | Pos | Pos |
| 4 | 75 | 0.01 | 7 | 0.01 | 0.01 | 0.6 | 0 | Y | Y | Pos | Pos |
| 5 | 30 | 0.86 | 4 | 0.6 | 0.01 | 0 | 0.1 | Y | N | Pos | Neg |
| 6 | 75 | 0.21 | 4 | 0.01 | 0.5 | 0 | 0 | Y | Y | Pos | Pos |
| 7 | 30 | 0.02 | 4 | 0.01 | 0.01 | 0.6 | 0 | Y | N | Pos | Neg |
| 8 | 30 | 0.01 | 7 | 0.01 | 0.01 | 0 | 0.1 | Y | Y | Pos | Pos |
| 9 | 75 | 0.69 | 7 | 0.6 | 0.01 | 0 | 0 | Y | Y | Pos | Pos |
| 10 | 30 | 0.80 | 7 | 0.6 | 0.5 | 0 | 0 | N | N | Neg | Neg |
| 11 | 30 | 1.40 | 4 | 0.6 | 0.5 | 0.6 | 0 | N | N | Neg | Neg |
| 12 | 30 | 0.10 | 7 | 0.01 | 0.5 | 0.6 | 0.1 | Y | N | Pos | Mix |
| 13 | 53 | 0.45 | 5.5 | 0.305 | 0.255 | 0.3 | 0.05 | Y | Y | Pos | Pos |
| 14 | 53 | 0.45 | 5.5 | 0.305 | 0.255 | 0.3 | 0.05 | Y | Y | Pos | Pos |
| 15 | 53 | 0.45 | 5.5 | 0.305 | 0.255 | 0.3 | 0.05 | Y | Y | Pos | Pos |
| 16 | 35 | 0.55 | 2.75 | 0.3 | 0.6 | 0.1 | 0.2 | Y | Y | Pos | Mix |
| 17 | 35 | 2.02 | 0.94 | 1.2 | 0.2 | 0.01 | 0.24 | ? | N | Pos | Neg |
| 18 | 35 | NA | 0 | 1.2 | 1.2 | 0.2 | 0 | N | N | Neg | Neg |
| 19 | 25 | 1.73 | 0 | 1.2 | 1.2 | 0.6 | 0.4 | N | N | Neg | Neg |
| 20 | 75 | 2.10 | 5.5 | 1.2 | 1.2 | 0.6 | 0 | N | N | Neg | Neg |
| 21 | 75 | NA | 0 | 1.2 | 0 | 0.6 | 0 | N | N | Neg | Neg |
| 22 | 75 | 0.00 | 5.5 | 0 | 0 | 0.6 | 0.4 | Y | Y | Pos | Pos |
| 23 | 75 | 1.45 | 0 | 1.2 | 0 | 0.6 | 0.4 | N | N | Neg | Neg |
| 24 | 25 | 0.28 | 0 | 0 | 1.2 | 0.6 | 0.4 | Y | Y | Pos | Pos |
| 25 | 25 | 2.10 | 5.5 | 1.2 | 1.2 | 0.6 | 0 | N | N | Neg | Neg |
| 26 | 25 | 0.00 | 5.5 | 0 | 0 | 0.6 | 0.4 | Y | Y | Pos | Pos |
| 27 | 25 | NA | 0 | 1.2 | 0 | 0.6 | 0 | N | N | Neg | Neg |
| 28 | 25 | 0.34 | 5.5 | 0 | 1.2 | 0.6 | 0 | N | N | Neg | Neg |
| 29 | 25 | NA | 0 | 1.2 | 0 | 0.6 | 0 | N | N | Neg | Neg |
| 30 | 75 | 0.28 | 0 | 0 | 1.2 | 0.6 | 0.4 | N | N | Neg | Mix |
| 31 | 75 | 2.10 | 5.5 | 1.2 | 1.2 | 0.6 | 0 | N | N | Neg | Neg |
| 32 | 75 | 0.00 | 5.5 | 0 | 0 | 0.6 | 0 | Y | Y | Pos | Pos |
| 33 | 75 | 1.73 | 0 | 1.2 | 1.2 | 0.6 | 0.4 | N | N | Neg | Neg |

**Table 3-3:  Results (Pass/Fail) for all CPP trials for A537 and A285 carbon steels. A question mark (?) indicates that degradation occurred near the acrylic/metal interface that could not be attributed clearly to either crevice or pitting corrosion.**

| Trial | A537 | A285 |
|-------|------|------|
| 1 | Pass | Fail |
| 2 | Fail | Fail |
| 3 | Fail | Fail |
| 4 | Fail | Fail |
| 5 | Fail | Pass |
| 6 | Fail | Fail |
| 7 | Fail | Pass |
| 8 | Fail | Fail |
| 9 | Pass | Pass |
| 10 | Pass | Pass |
| 11 | Pass | Pass |
| 12 | Fail | Pass |
| 13 | Fail | Fail |
| 14 | Fail | Fail |
| 15 | Fail | Fail |
| 16 | Fail | Fail |
| 17 | ? | Pass |
| 18 | Pass | Pass |
| 19 | Pass | Pass |
| 20 | Pass | Pass |
| 21 | Pass | Pass |
| 22 | Fail | Fail |
| 23 | Pass | Pass |
| 24 | Fail | Fail |
| 25 | Pass | Pass |
| 26 | Fail | Fail |
| 27 | Pass | Pass |
| 28 | Pass | Pass |
| 29 | Pass | Pass |
| 30 | Pass | Pass |
| 31 | Pass | Pass |
| 32 | Fail | Fail |
| 33 | Pass | Pass |

Trials 10, 11, 18, 19, 20, 21, 23, 25, 27, 28, 29, 30, 31, and 33 were determined to be passes based upon a negative hysteresis and no pitting observed for both materials.  Additionally, Trials 1 and 9 for A537 and Trials 5, 7, 9, 12, and 17 for A285 were considered passes based upon the same criteria or a difference between the corrosion potential and repassivation potential greater than 200 mV.  With the exception of Trial 17, the rest were fails based upon the presence of pitting determined visually and/or by a positive hysteresis.  Trial 17 for A537 was ultimately determined to be a passing condition after further examination, which will be discussed in the following section.  In general, A537 was determined to be more susceptible to pitting corrosion than A285 based upon the number of conditions in which fails occurred.  This behavior was likely owing to the slight compositional differences between the two materials, shown in Table 3-4.

While very similar in composition, A537 contains slightly more manganese than A285. This increase in manganese results in a higher number of manganese sulfide inclusions in A537, which serve as a common initiation site for pitting to occur. This decreased barrier to pit initiation leads to increased pitting susceptibility for A537. Tanks constructed of A537 are stress relieved, however, this is not anticipated to significantly affect the pitting behavior but can contribute to degradation mechanisms in which mechanical stress is a factor, such as SCC. Also displayed in Table 3-4 is the composition of AAR TC218 Rail Car Steel. This material was used in the Hanford work alluded to throughout the discussion of this work [8]. This analog for tank steel for Hanford double shell tanks allows for slightly more phosphorus and sulfur than A537 and A285 carbon steels but does not differ compositionally in a way that is anticipated to significantly impact the pitting behavior.

**Table 3-4: Composition (weight percent) of A537, A285, and AAR TC128 Rail Car Steel.**

|  | C | Mn | P | S | Si | Fe |
|---|---|---|---|---|---|---|
| A537 | 0.24 (max.) | 0.7 to 1.60 | 0.025 (max.) | 0.025 (max.) | 0.15 to 0.5 | Balance |
| A285 | 0.28 (max.) | 0.9 (max.) | 0.025 (max.) | 0.025 (max.) | - | Balance |
| AAR TC128 Rail Car Steel | 0.24 (max.) | 0.9 (max.) | 0.035 (max.) | 0.04 (max.) | 0.13 to 0.33 | Balance |

These pass/fail results were used to analyze the predictive capability of the pitting factor in addition to examining the influence of sulfate concentration on pitting behavior. The presence of pitting compared to the pitting factor is displayed in Figure 3-2.



**Figure 3-2: Chart displaying the pitting factor of trials with pitting and no pitting. Note: Trial 17 was shown to not exhibit pitting conclusively after further analysis.**

These results indicate a few key points. First, no instances of pitting were observed with a pitting factor greater than 2. Even at the intermediate range between 1 and 2, no pitting occurred. The highest pitting factor to exhibit pitting was at a value of 0.86. This indicates that a pitting factor minimum of 1 would be conservative for the mitigation of pitting corrosion for the compositional ranges examined. Second, several trials with a pitting factor of less than 2, or even less than 1, were shown to not exhibit pitting. This again illustrated conservatism in the predictive capability of the pitting factor with many chemistries that would be deemed non-compliant not actually displaying pitting susceptibility. This generally occurred in environments where one or both inhibiting species were in high concentrations for their given matrix, but nitrate concentrations were sufficient to drive the pitting factor calculation below 1. Therefore, it was concluded that the predictive capability of the pitting factor within the chemistry envelope and temperature range studied was adequate if not conservative.
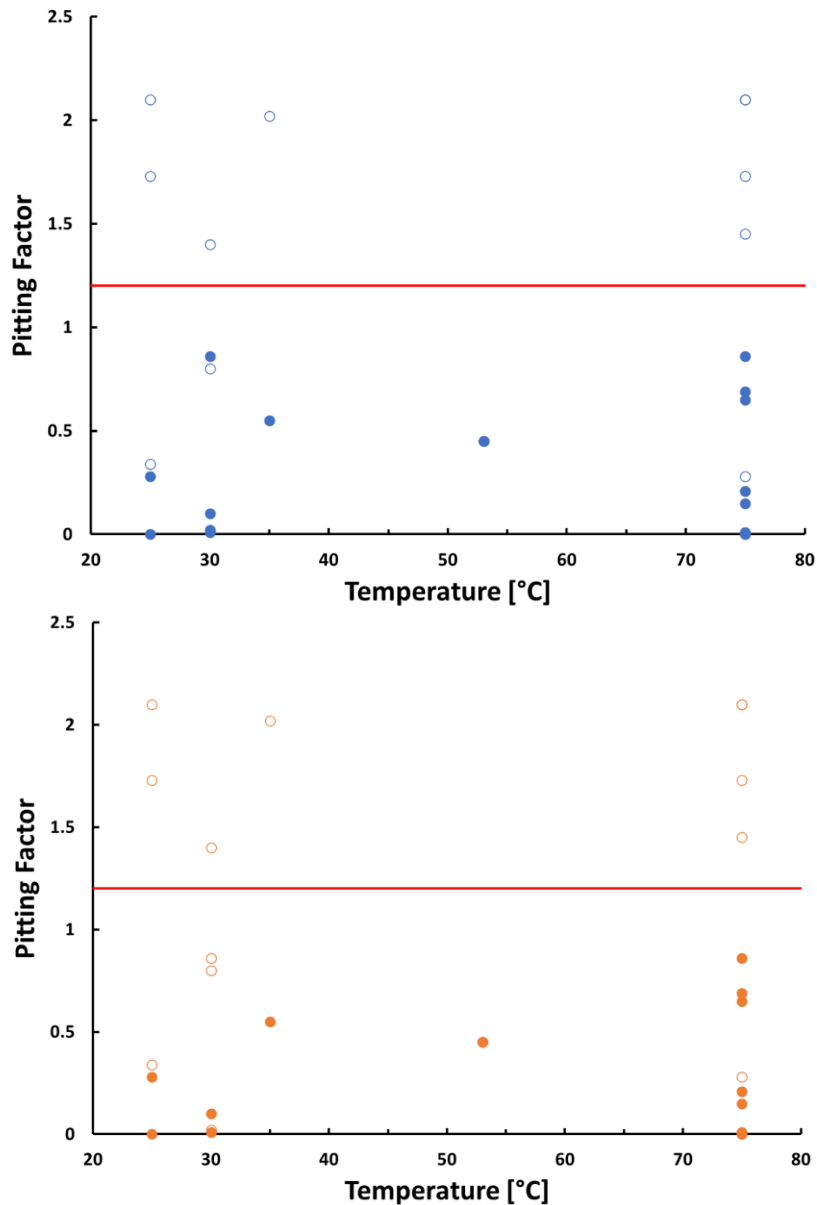


**Figure 3-3: Plots of showing the influence of temperature on pitting incidence for A537 carbon steel (top) and A285 carbon steel (bottom). Open markers indicated trials in which no pitting was observed. The red line indicates the proposed 1.2 control limit for pitting factor.**

While no instances of pitting were observed at pitting factors above 1, the region containing trials less than 1.2 (predicted failures) was evaluated to determine if temperature had an effect on pitting incidence. As can be seen in Figure 3-3, there was no observable temperature effect in the region defined by pitting factor greater than 1.2, with all tests resulting in no pitting. However, the trials with pitting factor less than 1.2 that did not pit seem to indicate an influence on temperature. Out of a total of eight such cases, six of the cases with no pitting and pitting factor less than 1.2 occurred at temperatures of 30 °C or less. The remaining two cases occurred at 75 °C. These results indicate a higher likelihood of pitting incidence within the region defined by pitting factor less than 1.2 at elevated temperatures. It is important to note that this finding does not affect the validity of the pitting factor used as predictive metric or defining a control limit, as no instances of pitting are observed at any temperature at pitting factor greater than 0.86. However, it represents an indication that increased operating temperatures and exposure to low pitting factor chemistries present an increased risk of pitting incidence.

The influence of sulfate concentration on pitting susceptibility was also evaluated. Sulfate is not acknowledged explicitly as an aggressive species in the pitting factor, which includes nitrite, hydroxide, nitrate, and halides. However, sulfate can be influential on pitting in carbon steels in dilute solutions, so there was a driving force to determine whether this susceptibility was applicable to more highly concentrated solutions within the test matrix. Figure 3-4 shows the influence of sulfate on pitting compared to the pitting factor.
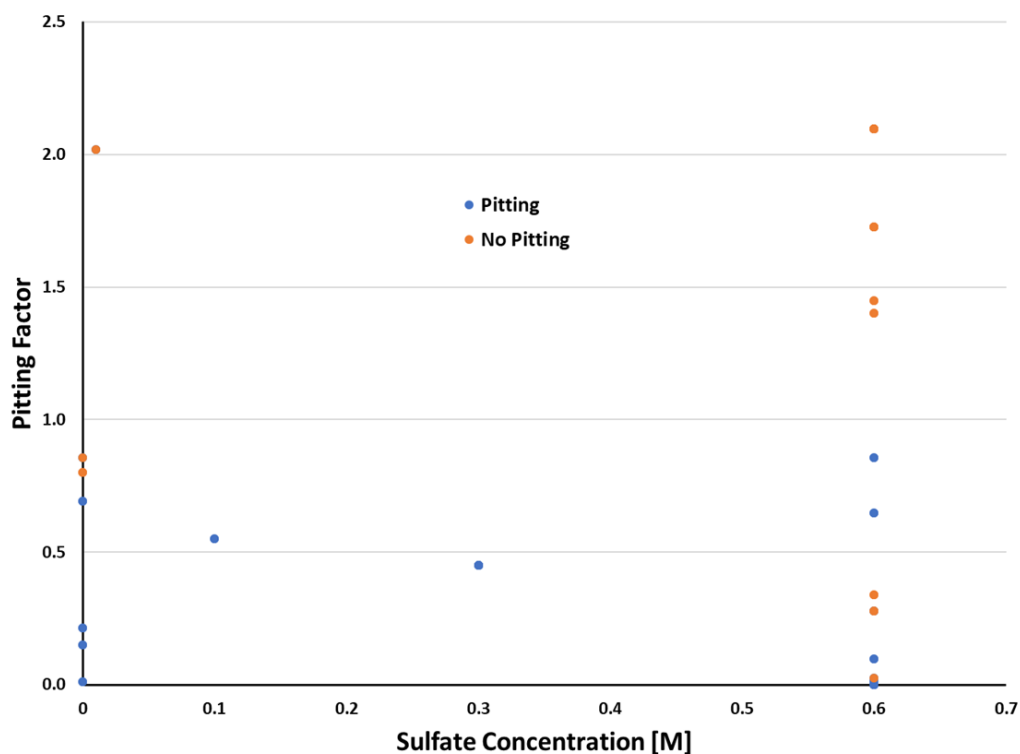


**Figure 3-4: Influence of sulfate concentration and pitting factor on pitting behavior for CPP of A537 carbon steel.**

No correlation between sulfate concentration and pitting was determined. Cases of pitting were observed at all sulfate concentrations between 0 and 0.6 M. Additionally, cases without pitting were observed at

both high concentrations of sulfate and when sulfate was absent. More important was the pitting factor of each of these trials. As was observed for the complete data set, no pitting occurred at any sulfate concentration with a pitting factor greater than 0.86. While sulfate can contribute to pitting in some instances, its effect was considered to be minimal compared to the other aggressive species present. Even in solutions with no other aggressive species present, such as Trials 21 and 27, intermediate to high concentrations of sulfate did not result in pitting.

In addition, statistical analysis of all variables within the test matrices was conducted to determine the relative influence of each variable on the outcome (pass or fail). For this analysis, four submatrices were evaluated individually: Trials 1-15 for A537 (A537-SD), Trials 16-33 for A537 (A537-HT), Trials 1-15 for A285 (A285-SD), and Trials 16-33 for A285 (A285-HT). A Likelihood Ratio Chi Square test was conducted on these matrices to determine the relative influence of nitrate, hydroxide, nitrite, sulfate, and chloride concentrations on a pass or failure. The results are listed below in Table 3-5.

**Table 3-5: Results of Likelihood Ratio Chi Square statistical analysis for determining the influence of chemical species on pitting susceptibility.**

| A537-SD | | | | A285-SD | | |
|---|---|---|---|---|---|---|
| Source | L-R Chi Square | Prob > Chi Square | | Source | L-R Chi Square | Prob > Chi Square |
| Nitrate | 7.60E-08 | 0.9998 | | Nitrate | 9.07E-04 | 0.9760 |
| Hydroxide | 35.13 | <.0001* | | Hydroxide | 7.64 | 0.0057* |
| Nitrite | 4.65E-08 | 0.9998 | | Nitrite | 0 | 1.0000 |
| Sulfate | 1.95E-08 | 0.9999 | | Sulfate | 1.44E-04 | 0.9904 |
| Chloride | 4.05E-07 | 0.9995 | | Chloride | 13.29 | 0.0003* |

| A537-HT | | | | A285-HT | | |
|---|---|---|---|---|---|---|
| Source | L-R Chi Square | Prob > Chi Square | | Source | L-R Chi Square | Prob > Chi Square |
| Nitrate | 1.18E-07 | 0.9997 | | Nitrate | 1.18E-07 | 0.9997 |
| Hydroxide | 7.27 | 0.0070* | | Hydroxide | 7.27 | 0.0070* |
| Nitrite | 20.78 | <.0001* | | Nitrite | 20.78 | <.0001* |
| Sulfate | 1.10E-07 | 0.9997 | | Sulfate | 1.10E-07 | 0.9997 |
| Chloride | 2.19E-07 | 0.9996 | | Chloride | 2.19E-07 | 0.9996 |

Two values are presented in Table 3-5. The Likelihood Ratio Chi Square Value (L-R Chi Square) indicates a likelihood that a given variable influences the outcome more than the case where none of the variables have any effect on the result, i.e., the result is random and independent of the parameters. A L-R Chi Square value of greater than 0.05 indicates some level of correlation between a given parameter and the outcome of the test. The second value is the Prob > Chi Square, which indicates the probability that Chi Square value larger than the L-R Chi Square value is achievable assuming the hypothesis that all variables are unrelated and do not affect the outcome. Essentially this illustrates the probability that the calculated correlation between a variable and the outcome could be observed by chance if no real influence was present. This means that variables with a Prob > Chi Square at or near 1 exhibit no meaningful influence that could be distinguished from random chance. In general, this analysis shows that inhibitor levels (in particular hydroxide) had the greatest impact on the pass/fail result of the CPP test. Chloride was shown to exhibit a statistically significant influence in one subset of the test matrix; however, this result is not maintained when the entire test matrix is considered. The potential for sulfate to be considered as an additional aggressive species as discussed previously was also explored. As indicated by the Prob > Chi Square values in Table 3-5, there is a probability less than 1% in each subset of the matrix that sulfate concentration had an influence greater than any random, unrelated variable. Therefore, within the compositional range studied (up to 0.6 M), sulfate concentration was not predicted to have any meaningful influence on pitting susceptibility.

### 3.3 Modified ASTM G192

A conclusive result was not always attainable with CPP alone.  This was the case with Trial 17 for A537 carbon steel.  CPP results from this trial can be found in Figure 3-5.  The initial CPP test (a) displayed a positive hysteresis, though the current density on the reverse scan was less than an order of magnitude different from the passive current density.  Localized attack was observed on the sample surface; however, this attack was confined to at or near the interface between the acrylic and metal.  Observation of the sample was inconclusive as to whether the attack initiated on the boldly exposed surface or within the crevice region.  Therefore, the trial was repeated to elucidate whether attack could be attributed to experimental artifact.  This CPP (b) revealed a negative hysteresis and no indications of localized attack.  With conflicting results between the two tests, a separate electrochemical technique was used to determine the pitting characteristics of A537 exposed to the conditions of Trial 17.  Modified ASTM G192 has been used previously to determine the repassivation behavior of carbon steels in similar simulants [6].  This method predominantly differs from CPP in the time that the system remains at a given polarization.  The initial potentiodynamic step is largely the same as the forward scan during a CPP test.  While the CPP method uses a constant potential ramp rate on the forward scan immediately followed by the reverse scan, the Modified ASTM G192 method includes a 4-hour galvanostatic hold following the forward scan which allows any stable pits to grow at a stable current density.  This period is then followed by the potential being stepped down with the potential being held for two hours at each value.  These two-hour potentiostatic holds allow the system to reach a steady state, and either the current density increases, indicating stable pit growth, or remains constant or declines, indicating no localized corrosion.  This process continued until the measured current falls below the passive current density observed during the potentiodynamic scan performed during this test.  At the point where current density is less than the passive current density, the repassivation potential can be determined.  The results of this test can be found in Figure 3-6.
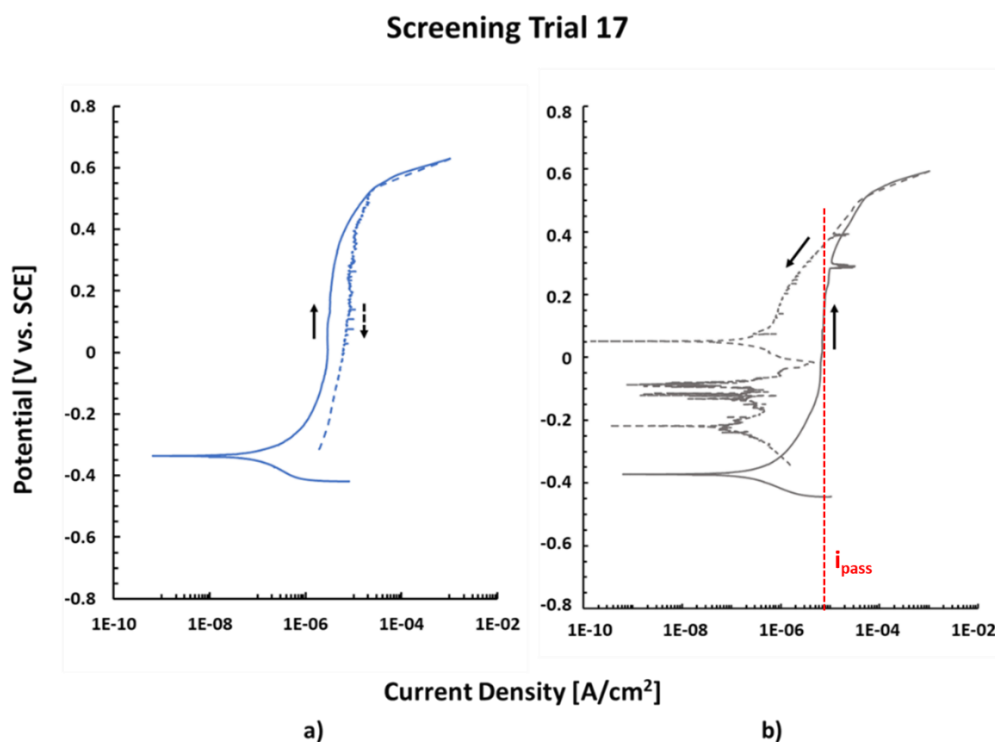


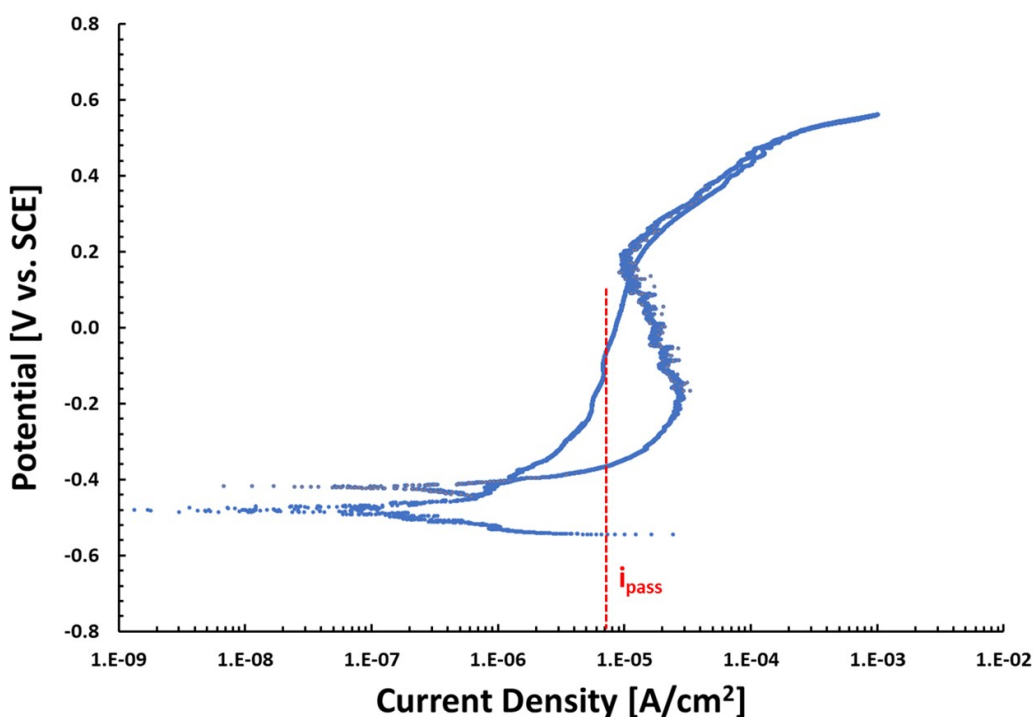**Figure 3-5:  CPP curves for Trial 17 for A537. a) initial CPP curve b) subsequent CPP curve.  The red dashed line indicates the passive current density used in the analysis of the Modified ASTM G192.**
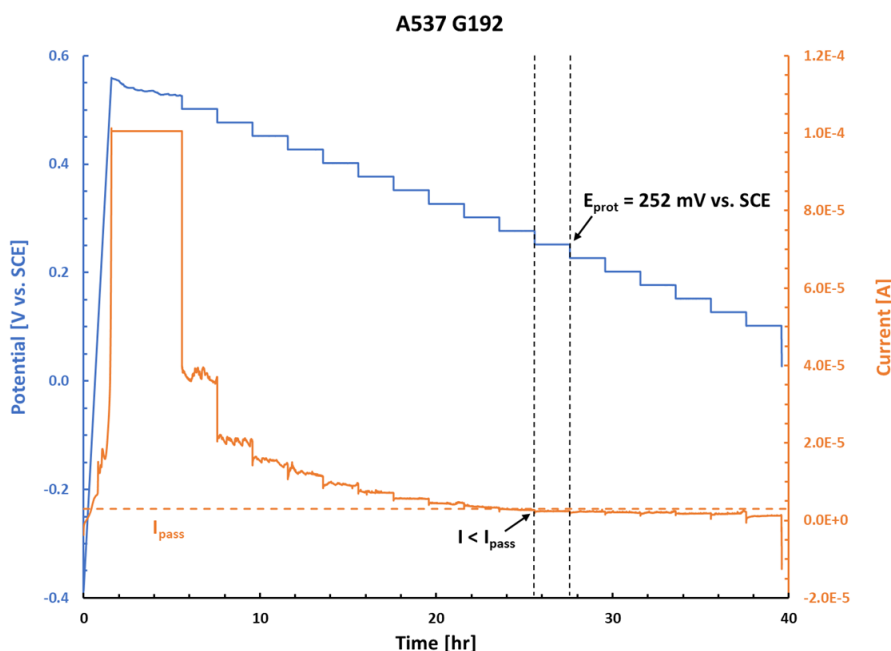
**Figure 3-6:  Modified ASTM G192 data for Trial 17 for A537**

Stable increases in current were not observed for any of the potentiostatic steps.  This indicated a lack of stable pit growth even during the initial potentiostatic holds.  However, the protection potential requires that the measured current density be less than the passive current density.  At a potential of 252 mV vs. SCE these two criteria were met, and a protection potential was established.  The difference between this potential and the corrosion potential was greater than 600 mV.  These results, coupled with the lack of any indications of localized corrosion upon visual inspection of the sample, resulted in a pass condition for Trial 17 for A537.  The positive hysteresis and localized corrosion observed in the initial CPP for Trial 17 were attributed to crevice corrosion that was the result of inadequate sample preparation.

3.4 <u>Slow Strain Rate Testing</u>

The matrix designed for evaluating the susceptibility to SCC is shown in Table 3-6.  As was the case for Table 3-1, aluminate, carbonate, and phosphate were held constant at the values shown in Table 1-2.  Trials 2, 5, 9, 10, 11, 16, and 17 are simulants that were repeated from the experimental matrix designed for the evaluation of pitting susceptibility, with the exception that sulfate concentration was lowered to a maximum of 0.3 M.  Due to the lack of stirring and duration of SSRT, along with the anticipation that sulfate would not significantly impact SCC, sulfate concentrations were lowered to increase the stability of the test solutions.  Trials 34 and 35 are new trials that were intended to fill in compositional gaps amongst the other trials.  Trial 34 was selected to establish a trial with high nitrate concentration and the maximum sulfate concentration.  Trials 9 and 10 also contained 5.5 M nitrate, but neither contained any sulfate.  Additionally, this chemistry provided a highly concentrated solution with a pitting factor well below 1, representing an aggressive condition.  Trial 35 was selected to evaluate a relatively dilute solution compared to the other trials in the matrix and a chemistry that is within the current corrosion control parameters for SRS.  This chemistry also provided a pitting factor of 2.88, indicating what should be a benign condition for pitting corrosion.  In addition to the trials outlined in this matrix, tests were also conducted in mineral oil to serve as a standard condition, as mineral oil provided a neutral environment for the carbon steels tested.

**Table 3-6: Composition and pitting factor for screening trials used in slow strain rate testing. All slow strain rate and supplementary electrochemical tests were conducted at 75 °C.**

| Trial | Nitrate [M] | Hydroxide [M] | Nitrite [M] | Sulfate [M] | Chloride [M] | Pitting Factor |
|-------|-------------|---------------|-------------|-------------|--------------|----------------|
| 2 | 4 | 0.6 | 0.01 | 0.3 | 0.1 | 0.86 |
| 5 | 4 | 0.6 | 0.01 | 0 | 0.1 | 0.86 |
| 9 | 5.5 | 0.6 | 0.01 | 0 | 0 | 0.88 |
| 10 | 5.5 | 0.6 | 0.5 | 0 | 0 | 1.02 |
| 11 | 4 | 0.6 | 0.5 | 0.3 | 0 | 1.40 |
| 16 | 2.75 | 0.3 | 0.6 | 0.1 | 0.2 | 0.55 |
| 17 | 0.94 | 1.2 | 0.2 | 0.01 | 0.24 | 2.02 |
| 34 | 5.5 | 0.3 | 0.6 | 0.3 | 0 | 0.61 |
| 35 | 1 | 0.3 | 0.3 | 0.3 | 0 | 2.88 |

Because Trials 34 and 35 were previously untested, supplementary tests were conducted to evaluate the electrochemical behavior. As was the case with Trials 1-33, a CPP was conducted to ascertain the pitting behavior. Results of the CPP tests for Trial 34 and Trial 35 can be found in Figures 3-7 and 3-8, respectively.
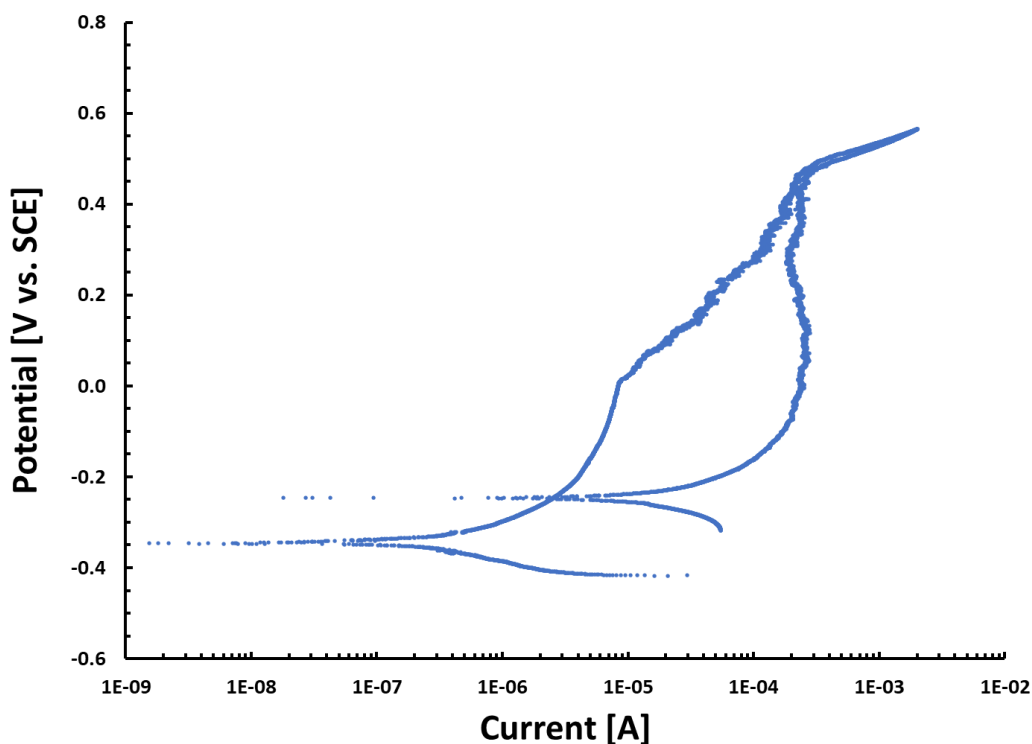


**Figure 3-7: CPP curve for Trial 34 for A537.**

**Figure 3-8: CPP curve for Trial 35 for A537. The red dashed line indicates the passive current density used in the analysis of the Modified ASTM G192.**

Based upon the pitting factor of 0.61, Trial 34 was anticipated to be a failure for pitting corrosion. As can be seen in Figure 3-7, the positive hysteresis coupled with a repassivation potential near the corrosion potential resulted in a fail condition. Pitting was observed on the sample surface as would be expected with a large, positive hysteresis. Trial 35, however, was inconclusive about whether the trial was a pass or fail. The CPP, shown in Figure 3-8, indicated a mixed hysteresis, where the hysteresis is originally negative but then becomes positive. Pitting was not observed, so it was not a clear pass or fail case. However, a Modified ASTM G192 was conducted so that a determination could be made. The results of this test are displayed in Figure 3-9. A change in potential was not observed during the galvanostatic hold and a definitive increase in current was not observed during the any of the potentiostatic steps, both indications that pitting or other localized forms of attack were not occurring. After the first potentiostatic step, a noticeable decrease in current was apparent throughout the duration of each step. This trend was maintained throughout the rest of the test until the current reached essentially zero. The protection potential, where current is no longer increasing and the measured current is less than the passive current, was determined to be at 217 mV vs. SCE. With a difference of approximately 700 mV between the protection potential and the corrosion potential and the absence of visible localized attack, Trial 35 was determined to be a passing condition, also in accordance with pitting factor control limit of pitting factor greater than 1.2.
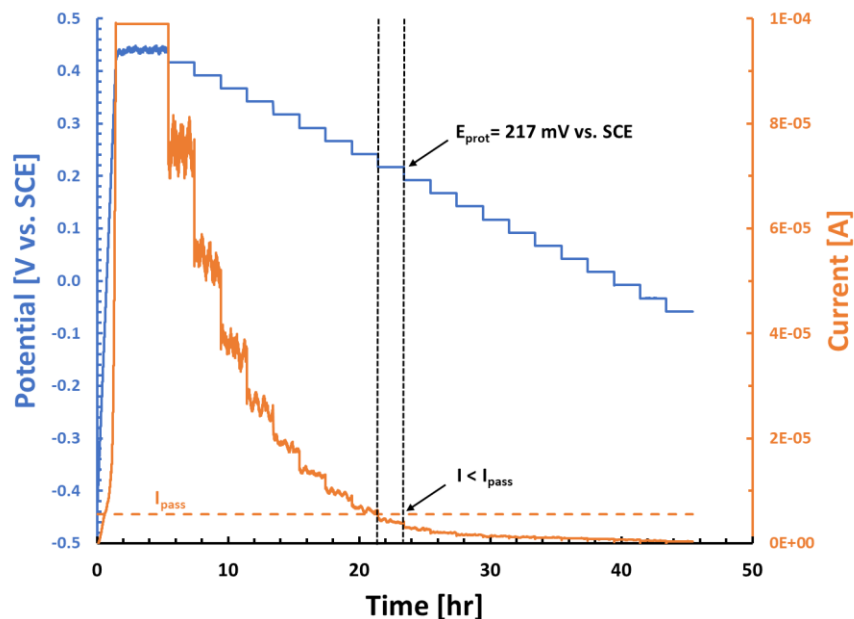
**Figure 3-9: Modified ASTM G192 data for Trial 35 for A537**

The majority of slow strain rate tests were conducted at open circuit, meaning that the tensile specimen was not polarized, and the potential was allowed to change as the system evolved. However, decades-long exposures involving changes to surface condition, waste chemistry, temperature, or other factors that contribute to changes in electrochemical reaction rates can result in meaningful shifts in OCP over time [9]. For this reason, overpotentials were applied during some trials to evaluate whether an anodic (or positive) shift in OCP would result in susceptibility to SCC that was not observed at open circuit. An example of the current-potential relationship during these tests is presented in Figure 3-10.
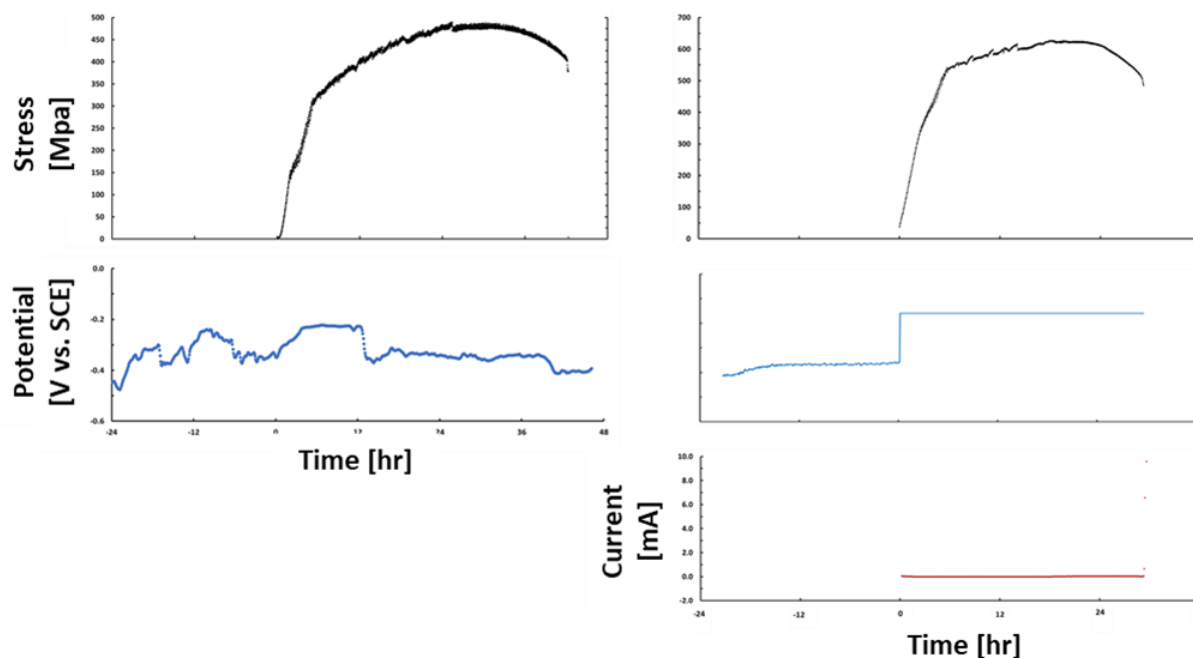


**Figure 3-10: Example of current-potential relationship during slow strain rate tests at open circuit (left) and with an applied overpotential (right).**
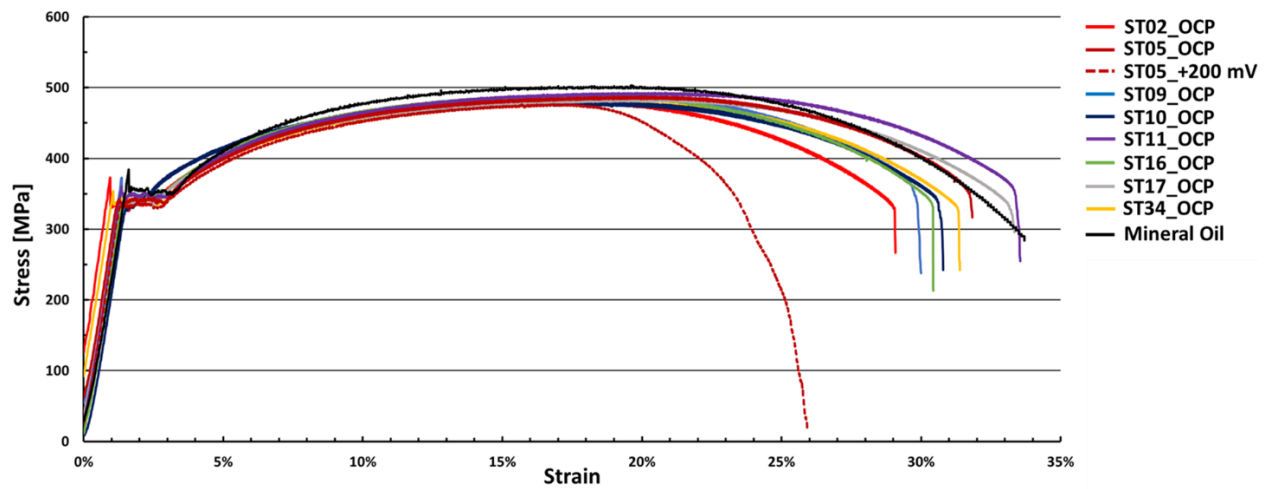
**Figure 3-11: Stress-Strain plots for slow strain rate tests of A537 with a gage diameter of 0.25 inches.**
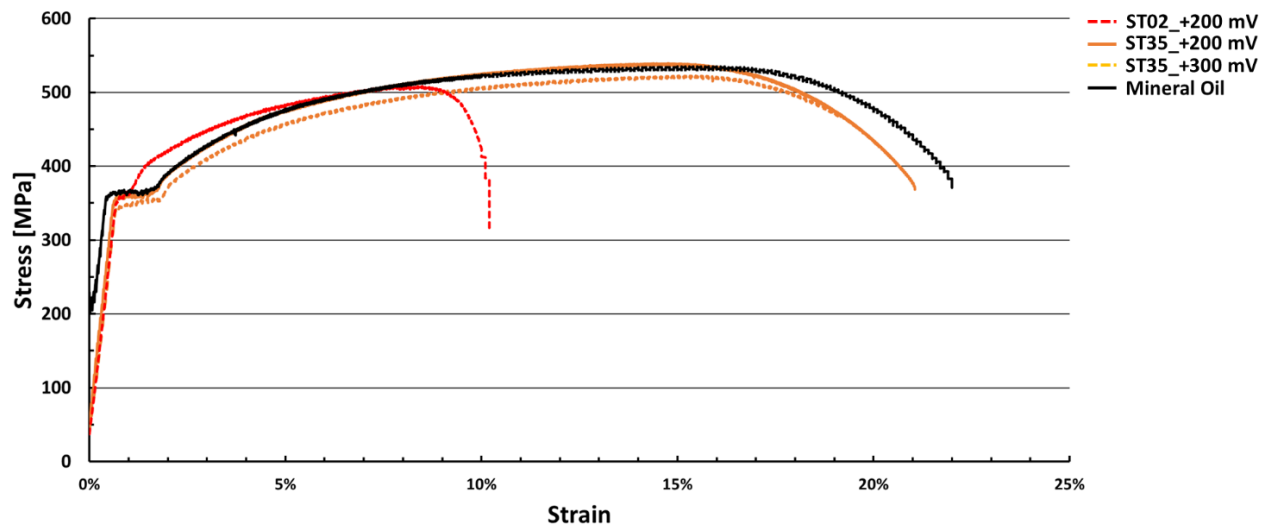


**Figure 3-12: Stress-Strain plots for slow strain rate tests of A537 with gage diameter of 0.16 inches.**

**Table 3-7: Summary of Slow Strain Rate Testing Results.**

| Trial | Pitting Factor | OCP @24 hr [mV vs. SCE] | Potential [mV vs. SCE] | UTS [Mpa] | Elongation | Elongation Ratio |
|---|---|---|---|---|---|---|
| A537 - 0.25" diameter | | | | | | |
| Mineral Oil | - | - | - | 503 | 0.337 | - |
| 2 | 0.86 | - | - | 481 | 0.291 | 86.4% |
| 5 | 0.86 | -404 | -404 | 488 | 0.318 | 94.4% |
| 5 (+200 mV) | 0.88 | -308 | -108 | 477 | 0.259 | 76.9% |
| 9 | 0.88 | - | - | 490 | 0.300 | 89.0% |
| 10 | 1.02 | -248 | -248 | 479 | 0.308 | 91.4% |
| 11 | 1.4 | -303 | -303 | 493 | 0.336 | 99.7% |
| 16 | 0.55 | -108 | -108 | 489 | 0.304 | 90.2% |
| 17 | 2.02 | -316 | -316 | 483 | 0.333 | 98.8% |
| 34 | 0.61 | -225 | -225 | 479 | 0.314 | 93.2% |
| A537 - 0.16" diameter | | | | | | |
| Mineral Oil | - | - | - | 535 | 0.220 | - |
| 2 (+200 mV) | 0.86 | -335 | -135 | 508 | 0.102 | 46.4% |
| 35 (+200 mV) | 2.88 | -442 | -242 | 540 | 0.211 | 95.9% |
| 35 (+300 mV) | 2.88 | -366 | -66 | 523 | 0.192 | 87.3% |
| A285 - 0.16" diameter | | | | | | |
| Mineral Oil | - | - | - | 474 | 0.133 | - |
| 5 | 0.86 | -347 | -347 | 489 | 0.118 | 88.7% |
| 5 (+200 mV) | 0.86 | -360 | -160 | 628 | 0.083 | 62.4% |
| 11 (+200 mV) | 1.4 | -299 | -99 | 499 | 0.121 | 91.0% |
| 11 (+300 mV) | 1.4 | -428 | -128 | 563 | 0.069 | 51.9% |
| 34 (+200 mV) | 0.61 | -331 | -131 | 618 | 0.067 | 50.4% |

The results of the slow strain rate tests conducted for A537 carbon steel are shown in Figures 3-11 and 3-12. Additionally, a summary of the results for both materials is presented in Table 3-7. In this table, UTS represents the ultimate tensile strength during the slow strain rate test and the elongation ratio is the ratio between the elongation achieved during the screening trial compared to that of the mineral oil standard. Of all of the tests conducted at open circuit, none of these tests showed a significant reduction in elasticity from the mineral oil standard, including those with pitting factors of less than 1.2, despite these solution chemistries being deemed out of specification and aggressive in terms of susceptibility to localized corrosion. Trials 2, 5, and 35 were then selected to determine if anodic overpotentials would affect the susceptibility to SCC. Trials 2 and 5, with pitting factors equal to 0.86, were selected as they represent identical, failing chemistries with the exception of the presence of 0.3 M sulfate in Trial 2. Trial 35 was selected as it represented a benign solution with respect to pitting corrosion, is within current SRS corrosion control limits, and has a high pitting factor of 2.88. All three trials were exposed to an anodic overpotential of +200 mV vs OCP. Trials 2 and 5 displayed significant reduction in elasticity with an overpotential of +200 mV, with an elongation ratio with respect to the mineral oil standard of less than 80 %. Images of the fracture surface and secondary cracking can be seen in Figure 3-13 for Trial 5. This indicated that these chemistries could result in susceptibility to SCC if the OCP were to depart significantly from the OCP at the beginning of exposure. However, this trend was not observed with Trial 35. The mechanical response of the trial with an overpotential of +200 mV closely resembled that of the mineral oil standard, with an elongation ratio compared to the control of 95.9%. An additional test was conducted with an overpotential of +300 mV to determine if additional polarization would lead to a reduction in performance. As was the case with the +200 mV polarization, a significant reduction in elongation was not observed for the +300 mV polarization. This indicated that for Trial 35 with a pitting factor well above a 1.2 control limit, a lack of susceptibility to SCC was maintained even with exposure to large anodic overpotentials and the validity of pitting factor as a predictive metric was maintained.
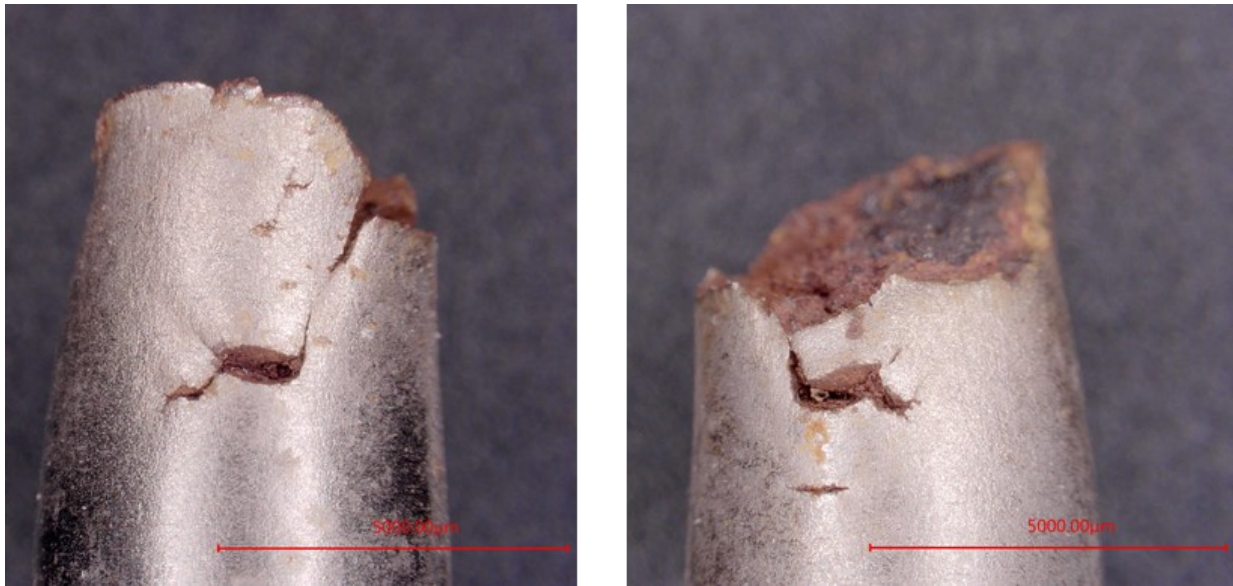
**Figure 3-13: Images of fracture surface and secondary cracking for A537 Trial 5 with an overpotential of +200 mV.**
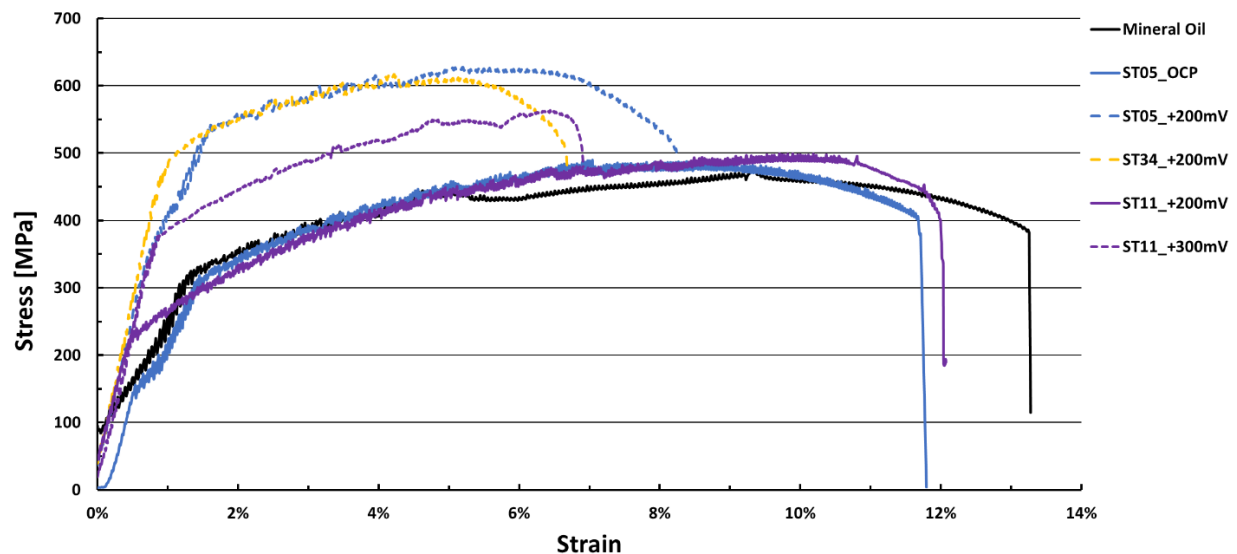


**Figure 3-14: Stress-Strain plots for slow strain rate tests of A285 with gage diameter of 0.16 inches**

Trials 5, 11, and 34 were also selected for SSRT of A285 carbon steel. These results are presented in Figure 3-14. Trials 5 and 11 provided chemistries near the pitting factor threshold of 1.2, with one being higher (ST11, pitting factor = 1.40) and one lower (ST05, pitting factor = 0.86). Trial 34 was also selected as it represented a very aggressive chemistry based upon the pitting factor metric. As was the case with SSRT of A537, the test conducted at open circuit for A285 (Trial 5) also resulted in a pass, with an elongation ratio of 88.7 % compared to the mineral oil standard. A failure occurred however when Trial 5 was conducted with an overpotential of +200 mV. This result was predicted based upon the pitting factor metric. The metric also proved adequate in predicting a passing condition in Trial 11 with an overpotential of +200 mV. However, increasing the overpotential to +300 mV resulted in a failure. This result bears significance,

as Trial 11 represents a chemistry that is within the current minimum inhibitor requirements with a hydroxide concentration greater than 0.3 M and the sum of hydroxide plus nitrite concentrations greater than or equal to 1.1 M. This result is contrary to the prediction based upon the pitting factor, however, a polarization of +300 mV, or even +200 mV, from open circuit is substantial, with polarization of low carbon steel in waste tank supernates to -128 mV vs. SCE being unlikely. Lastly, a large reduction in elasticity and secondary cracking were observed for Trial 34 with an overpotential of +200 mV. As was the case with Trial 5, this result was anticipated based upon the pitting factor (0.61) being less than 1.2.

No difference between the susceptibility to SCC of A537 and A285 could be discerned from the results of this testing matrix. However, differences in other aspects of the data warrant further discussion and/or future evaluation. First, A537 displayed increased ductility compared to A285. While a discernable difference was not determined in this study, the more brittle nature of A285 could manifest in an increase vulnerability to SCC. The measured ultimate tensile strength during testing also produced intriguing results. For A537, the ultimate tensile strength was very consistent at approximately 500 MPa and within the expected range of values in all tests. For A285, the samples that did not experience premature failure behaved as expected, with an ultimate tensile strength that was consistent and slightly less than that of the A585 carbon steel. However, each of the failures exhibited ultimate tensile strengths that were significantly higher and outside of the expected range for this material. An explanation of this phenomenon has not yet been determined, but future evaluation of this issue is recommended as this was not observed for testing of A537 samples of either diameter with the same testing protocol. The potential at which the tensile tests were carried out is also noteworthy. Consistent OCP values were not always reproducible during testing of identical chemistries. While some variation in OCP is expected, the large difference from test-to-test resulted in cases where comparison of different applied overpotentials were problematic. This could be attributed to another phenomenon observed during testing, failures occurring at the liquid-air interface and not along the fully immersed portion of the gage length. Trials A537 ST02 (+200 mV), A285 ST05 (+200 mV), A285 ST11 (+300 mV), and A285 ST34 (+200 mV) all failed at the liquid-air interface near the shoulder of the test specimen. This results in two issues in the evaluation of the results. First, the conditions at the liquid-air interface can differ from that of the bulk chemistry. Differences in localized chemistry and kinetics of electrochemical reactions could result in changes in the measured open circuit potential and therefore the applied potential at which the test is carried out. In addition, the localized chemistry could represent a more aggressive condition than that of the bulk chemistry conditions in full immersion. Secondly, the failure occurring outside of the gage length results in a change to the cross-sectional area. An increase in cross-sectional area that is not accounted for in the calculation of stress would result in an increase in the calculated stress in the stress-strain curve. Reevaluating the testing protocol is recommended to evaluate the underlying reason for non-reproduceable OCP values and to insert a checkpoint to ensure that trials with different overpotentials can be compared accurately. In addition, the impact of the liquid-air interface should be evaluated, and the testing protocol should be changed accordingly such that the liquid-air interface does not result in failures outside of the gage length.

## 4.0 Conclusions

An experimental matrix was designed to evaluate the use of the pitting factor for supernate chemistries characteristic to SRS, particularly during the salt dissolution process. Two electrochemical test methods were utilized to determine the susceptibility of A537 and A285 low-carbon steels to pitting corrosion with this chemistry envelope at temperatures up to 75 °C. The predominant test method was CPP studies. Through CPP, the pitting factor was determined to accurately identify pitting susceptibility within the compositional range investigated. Additionally, sulfate was determined to have no significant influence on pitting behavior, at concentrations up to 0.6 M. Modified ASTM G192 was successfully used to evaluate conditions where CPP was inconclusive and allowed for a pass/fail result to be determined. In all cases the

pitting factor was determined to be applicable to the simulants tested, with this metric accurately predicting incidences in which pitting occurred.

Table 4-1 summarizes the chemistry envelope over which pitting behavior was examined and recommends a minimum pitting factor of 1.2 for temperatures up to 75 °C. The chemistry envelope tested includes both the testing performed for this program and that performed for Hanford [8]. While a minimum pitting factor threshold of 1 was determined to be sufficient for the prediction of pitting corrosion, a pitting factor of 1.2 is being proposed to build in a safety factor and remain consistent with the Hanford Site approach [8]. Additionally, a minimum pH limit of 12 is proposed. Therefore, a pH limit of 12 is proposed to ensure passivity and that localized corrosion is the primary form of corrosion degradation

Susceptibility to SCC was evaluated using a reduced matrix of tests at temperatures up to 75 °C. No failures due SCC were observed at the OCP. In addition, tests polarized anodically to +200 mV compared to the 24 hour open circuit value, only resulted in failures for trials with pitting factors less than 0.86. However, a test with a passing condition based upon the pitting factor metric (pitting factor = 1.40) did exhibit a failure with an applied potential of +300 mV vs. OCP (-128 mV vs. SCE). This result bears additional significance, as Trial 11 represents a chemistry that is within the current minimum inhibitor requirements with a hydroxide concentration greater than 0.3 M and the sum of hydroxide plus nitrite concentrations greater than or equal to 1.1 M. This result is contrary to the prediction based upon the pitting factor, however, a polarization of +300 mV, or even +200 mV, from open circuit is substantial. The relationship between these testing parameters and service environment/conditions and the desired level of conservatism in the metric should be further evaluated with additional testing in the determination of the significance of this result. While the pitting factor accurately predicted susceptibility to SCC at temperatures up to 75 °C and with positive overpotentials up to +200 mV, the relatively small sample matrix and failure of a passing pitting factor with a +300 mV polarization resulted in an inconclusive determination of whether the pitting factor may be used for predicting susceptibility to SCC at temperatures between 50 °C and 75 °C. Additionally, failure occurring at the shoulder of the test specimen along the liquid-air interface presented issues with the interpretations of these results.

**Table 4-1: Summary of chemistry envelope and proposed control limits**

| Chemistry Envelope Tested | |
|---|---|
| Nitrate (M) | 0 to 7.0 |
| Chloride (M) | 0 to 0.4 |
| Hydroxide (M) | 0.0001 to 6 |
| Nitrite (M) | 0 to 1.2 |
| Sulfate (M) | 0 to 0.6 |
| | |
| Proposed Control Limits | |
| Minimum pH | 12 |
| Minimum Pitting Factor | 1.2 |
| Minimum Nitrite (M) | 0.2 |
| Minimum Nitrite/Nitrate Ratio | 0.15 |
| Maximum Temperature (°C) | Pitting - 75 °C<br>SCC - 50 °C |

**5.0 Recommendations, Path Forward or Future Work**

The use of the pitting factor as a predictive tool for SCC was evaluated using a matrix of nine waste tank simulants in the course of this work. However, more information is needed for making a more definitive determination as to the efficacy of the pitting factor for predicting SCC in the temperature range of 50 °C to 75 °C. It is recommended that additional work be conducted to further refine the testing protocol for SSRT to determine the level of conservatism desired in terms of overpotentials used. In this study, the pitting factor was 100% accurate at predicting failures at open circuit and with an overpotential of 200 mV. However, one failure was missed with a predicted passing condition at an overpotential of 300 mV. This failure occurred at a potential of -128 mV vs. SCE, significantly above the 24-hour OCP value measured between -430 and -300 mV vs. SCE. The final value for the OCP of a solution with a pH of 12 or greater is expected to be less than approximately -150 mV vs. SCE based upon previous studies [9]. This illustrates that shifts in OCP do occur in service and the use of an overpotential in this testing creates a level of conservatism that may be necessary to account for such changes. However, the overpotential must not be too large that test conditions no longer represent in-service conditions. For these reasons, it is recommended that additional work be conducted to evaluate the testing protocol for SSRT in regards to the predictive quality of the pitting factor, conduct additional testing near the pass/fail boundary, and to mitigate the complications in interpreting results due to impacts of the liquid-air interface to validate the use of the proposed control limits in Table 4-1 for the inhibition of SCC at temperatures between 50 and 75 °C. These limits are sufficient for the mitigation of SCC and pitting corrosion at temperatures up to 50 °C. However, if it is desired to operate at temperatures between 50 and 75 °C or determine if the proposed control limits are adequate, additional SCC testing is recommended.

## 6.0 References

1.  K.B. Martin, "CSTF Corrosion Control Program: Program Description Document", WSRC-TR-2002-00327, Rev. 9, December 16, 2015.

2.  B. J. Wiersma, J. I. Mickalonis "Determination of Corrosion Inhibitor Criteria for Type III/IIIA Tanks During Salt Dissolution Operations", WSRC-STI-2006-00029, Rev. 0, September 2007.

3.  K. M. Counts, B. J. Wiersma, J. I. Mickalonis, "Determination of Corrosion Inhibitor Criteria for Type III/IIIA Tanks During Salt Dissolution Operations-Interim Report", WSRC-STI-2007-00552, Rev. 0, December 2007.

4.  B. L. Garcia-Diaz, J. I. Mickalonis, B. J. Wiersma, "Determination of Corrosion Inhibitor Criteria for Type III/IIIA Tanks During Salt Dissolution Operations-Summary Document", SRNL-STI-2009-00600, Rev. 0, October 2009.

5.  T. Martin, "Tank Integrity Expert Panel Corrosion Subgroup March 2016 Meeting Outcomes", RPP-ASMT-60833, Washington River Protection Solutions LLC, Richland, WA, May 2016.

6.  K.J. Evans, S. Chawla, K. Sherer, J. Gerst, J.A. Beavers, K. Boomer. The Use of ASTM G192 (Tsujikawa-Hisamatsu Electrochemical Method) to Evaluate the Susceptibility of Hanford Tank Steels to Pitting Corrosion. *Corrosion.* 2016.

7.  J.T. Boerstler, "Slow Strain Rate Testing in Tank Farm Simulants", Electronic Laboratory Notebook Experiment G1720-00424-01.

8.  B.J. Wiersma, R.E. Fuentes, L.M. Stock, "Chemistry Envelope for Pitting and Stress Corrosion Cracking Mitigation", SRNL-STI-2019-00217, Rev. 0, September 2019.

9.  K. J. Evans, N. Sridhar, B.C. Rollins, S. Chawla, J.A. Beavers, and J. Page. Long Term Evolution of Corrosion Potentials of Carbon Steel in Alkaline Radioactive Environments. *Corrosion.* 2019

### Appendix A.  Cyclic potentiodynamic polarization curves for each screening trial

The following pages contain the cyclic potentiodynamic polarization curves for each screening trial.  The data in blue represent data for A537 carbon steel and the green represent A285 carbon steel.  Forward scans are indicated by a solid line, whereas the reverse scans are indicated by a dashed line.

## Screening Trial 1
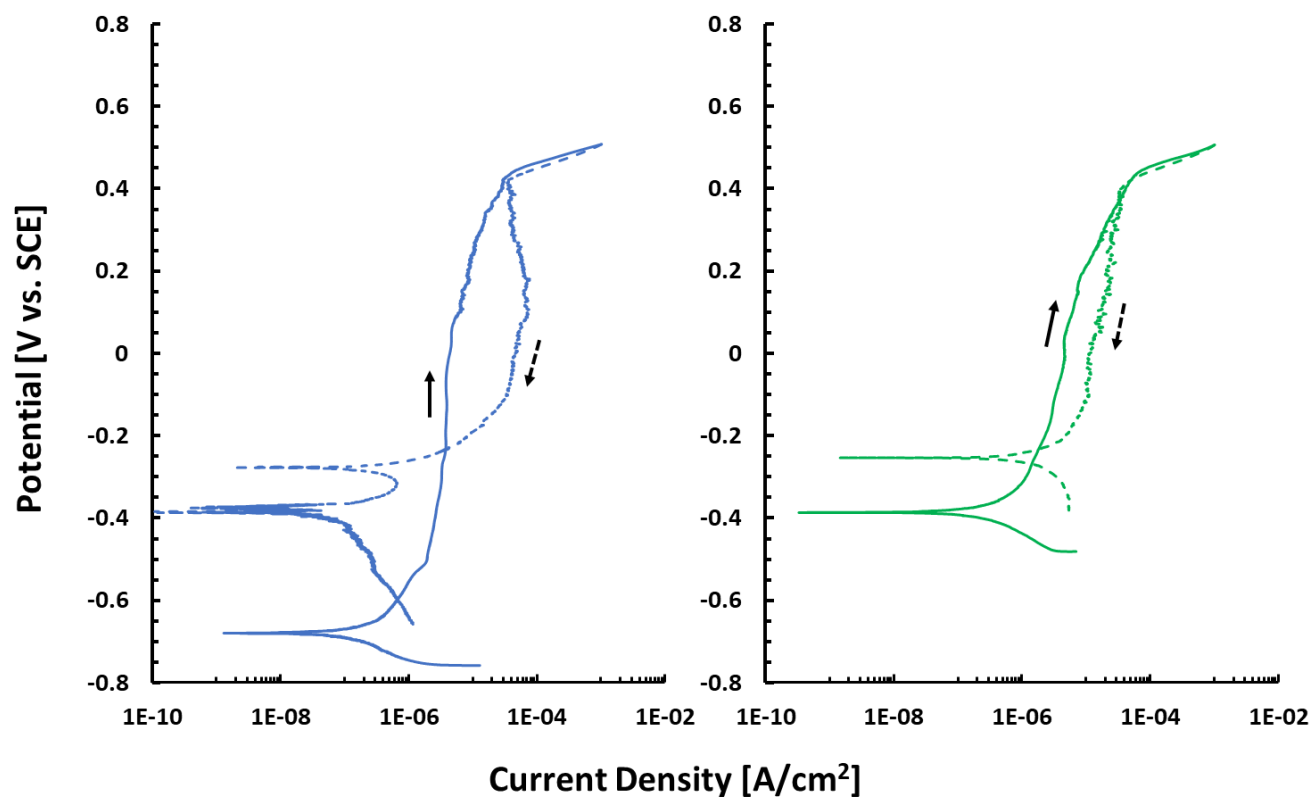
# Screening Trial 2
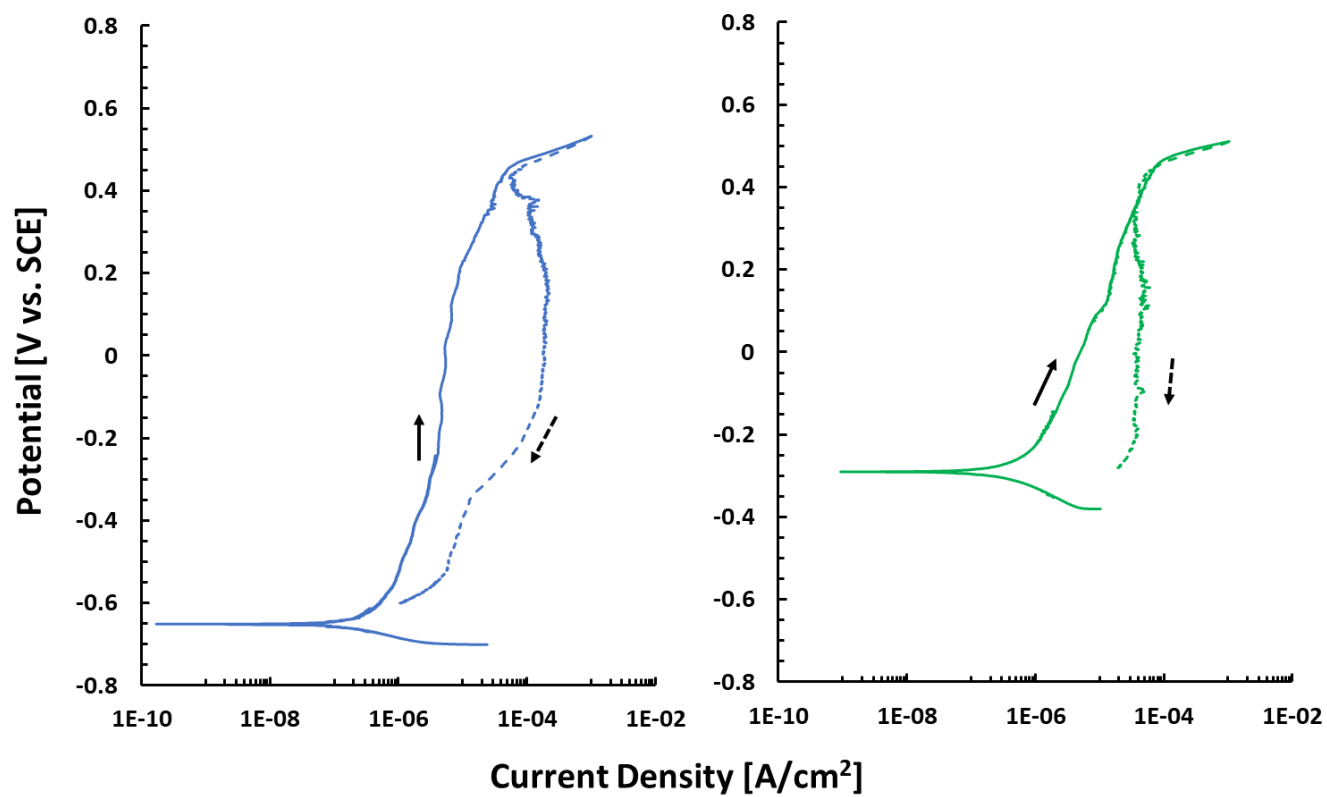
# Screening Trial 3
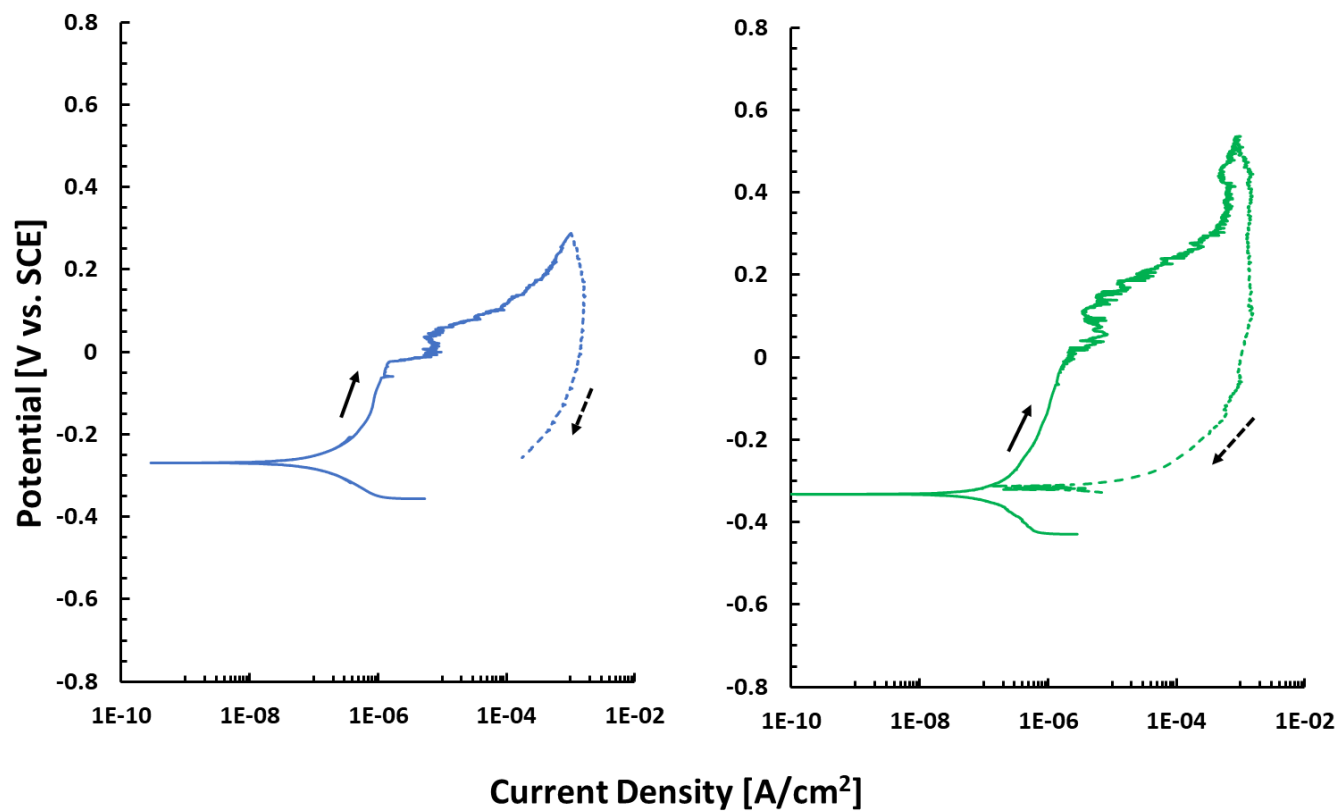
# Screening Trial 4
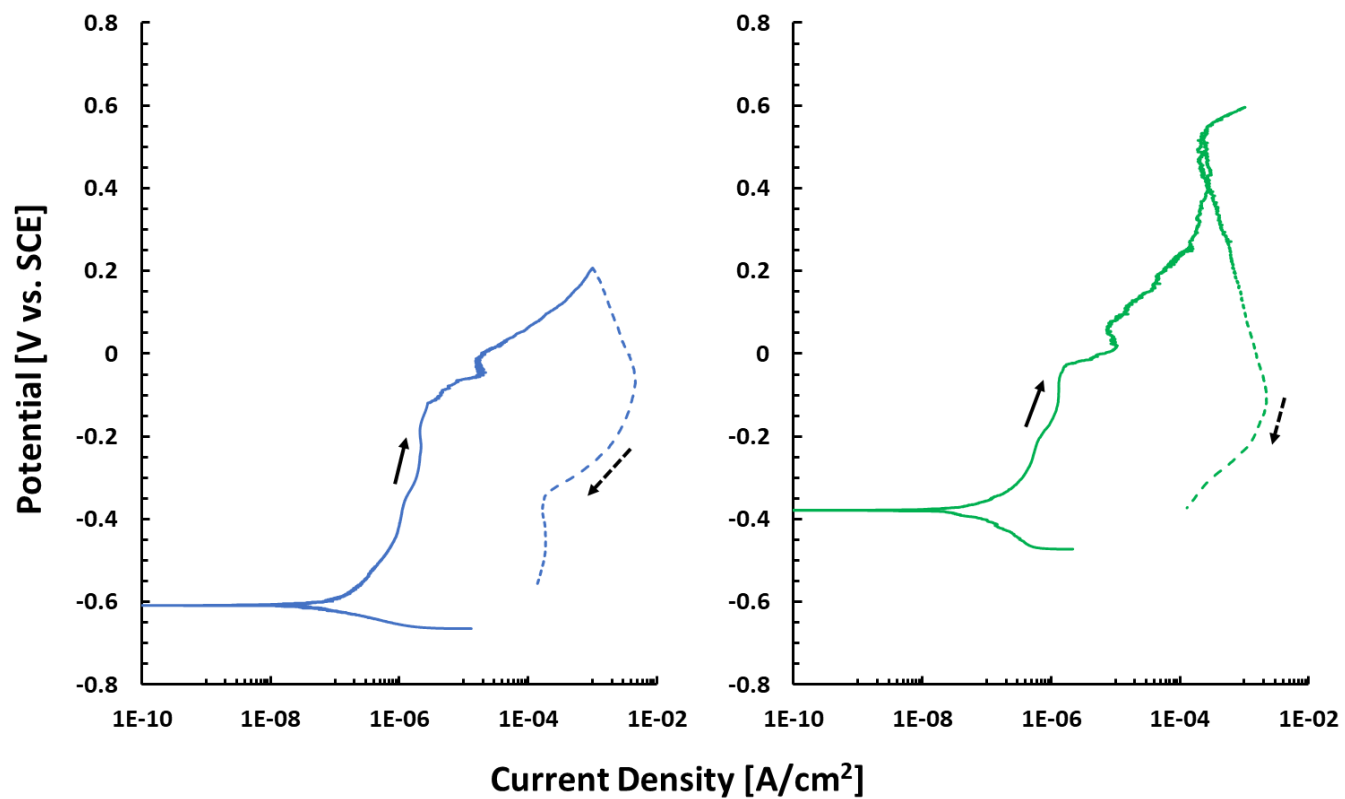
# Screening Trial 5
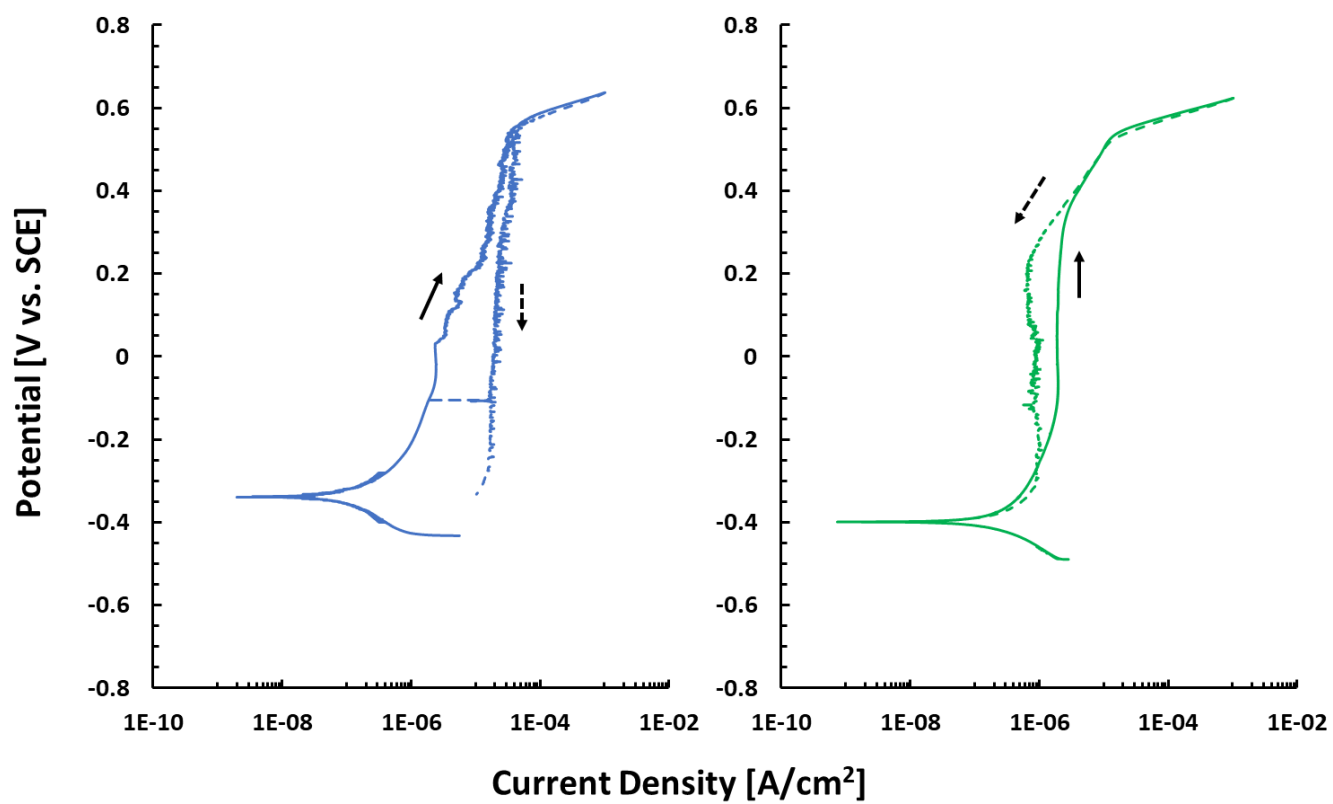
# Screening Trial 6
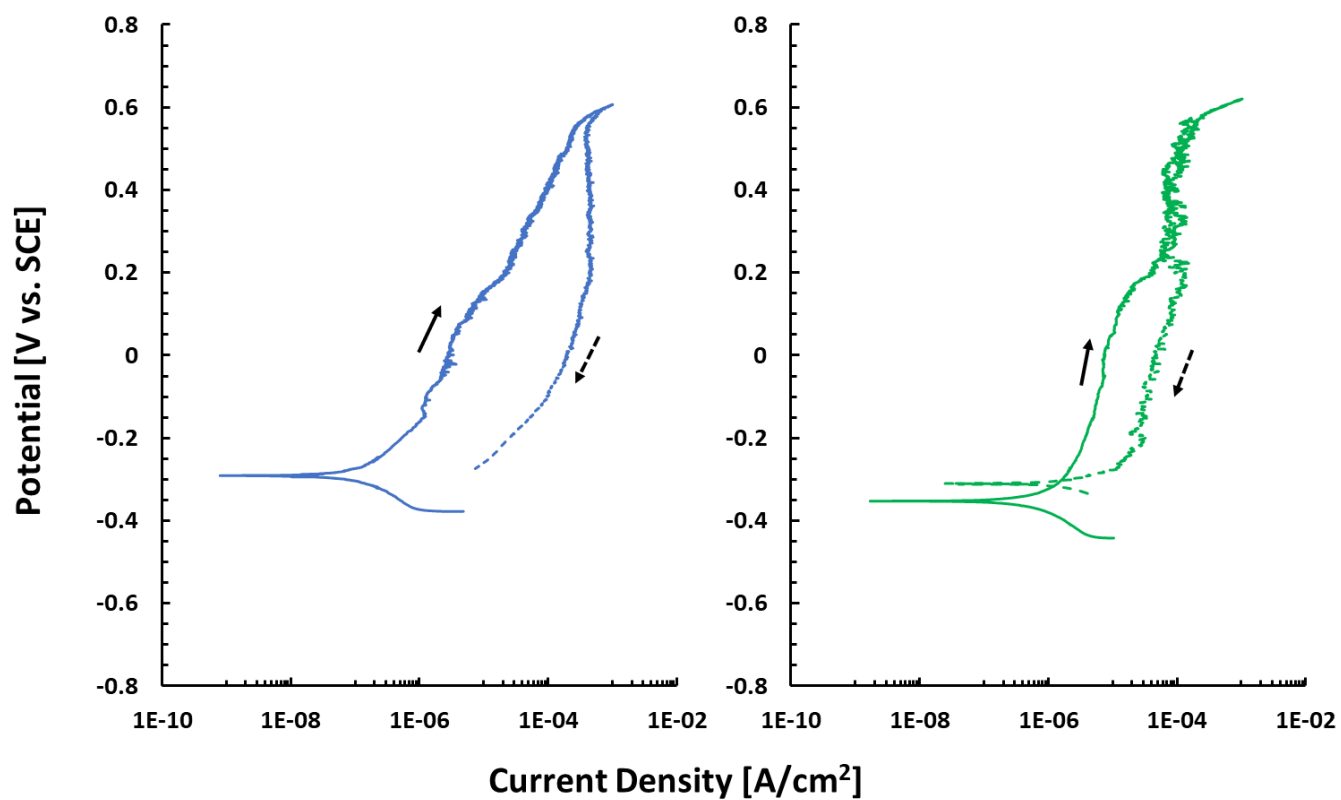
# Screening Trial 7

## Screening Trial 8



Current Density [A/cm²]

a)                                         b)
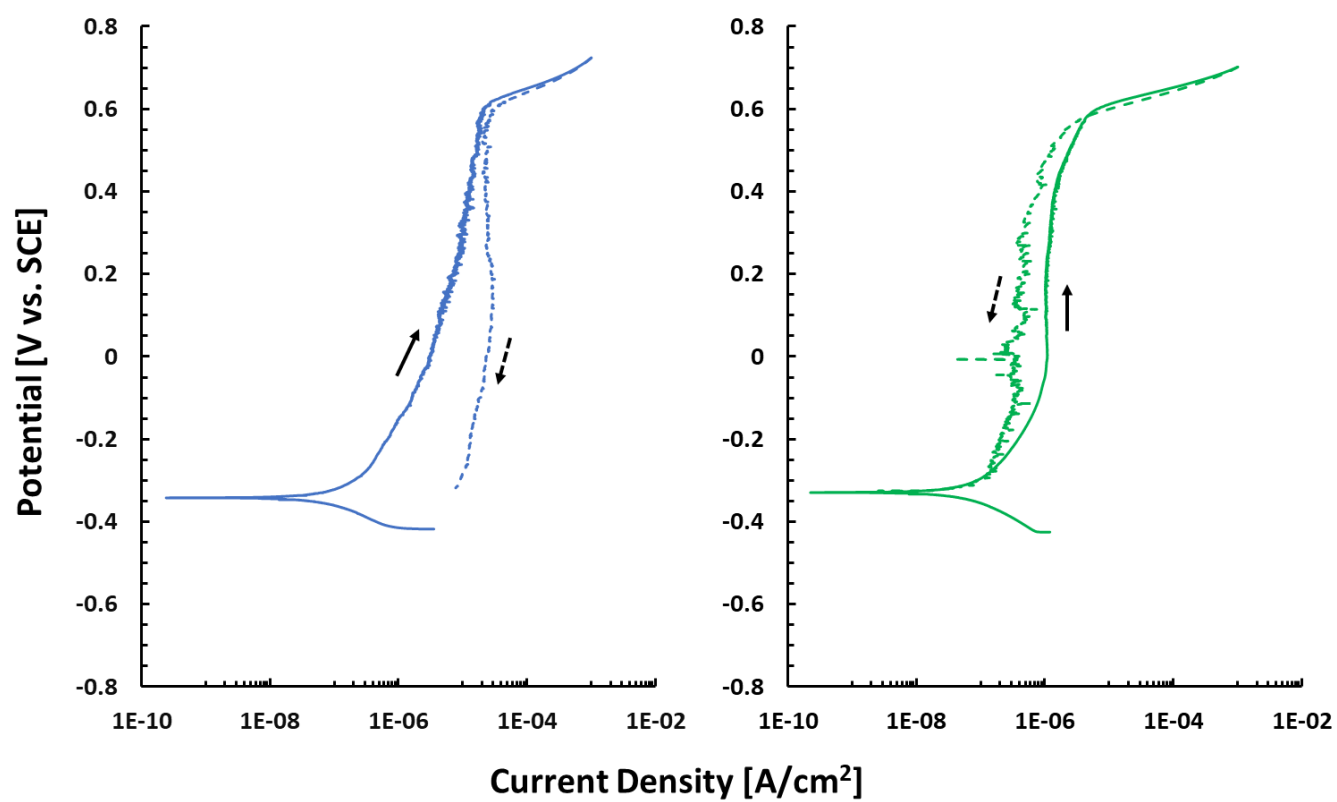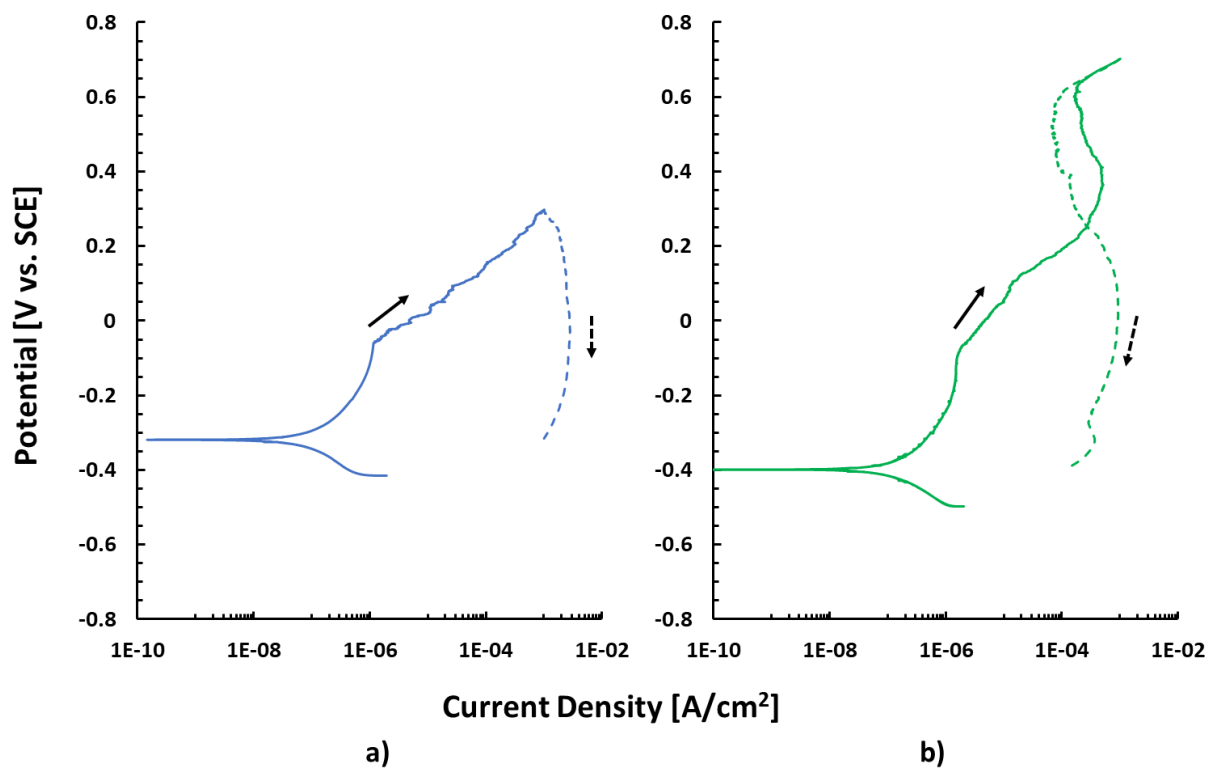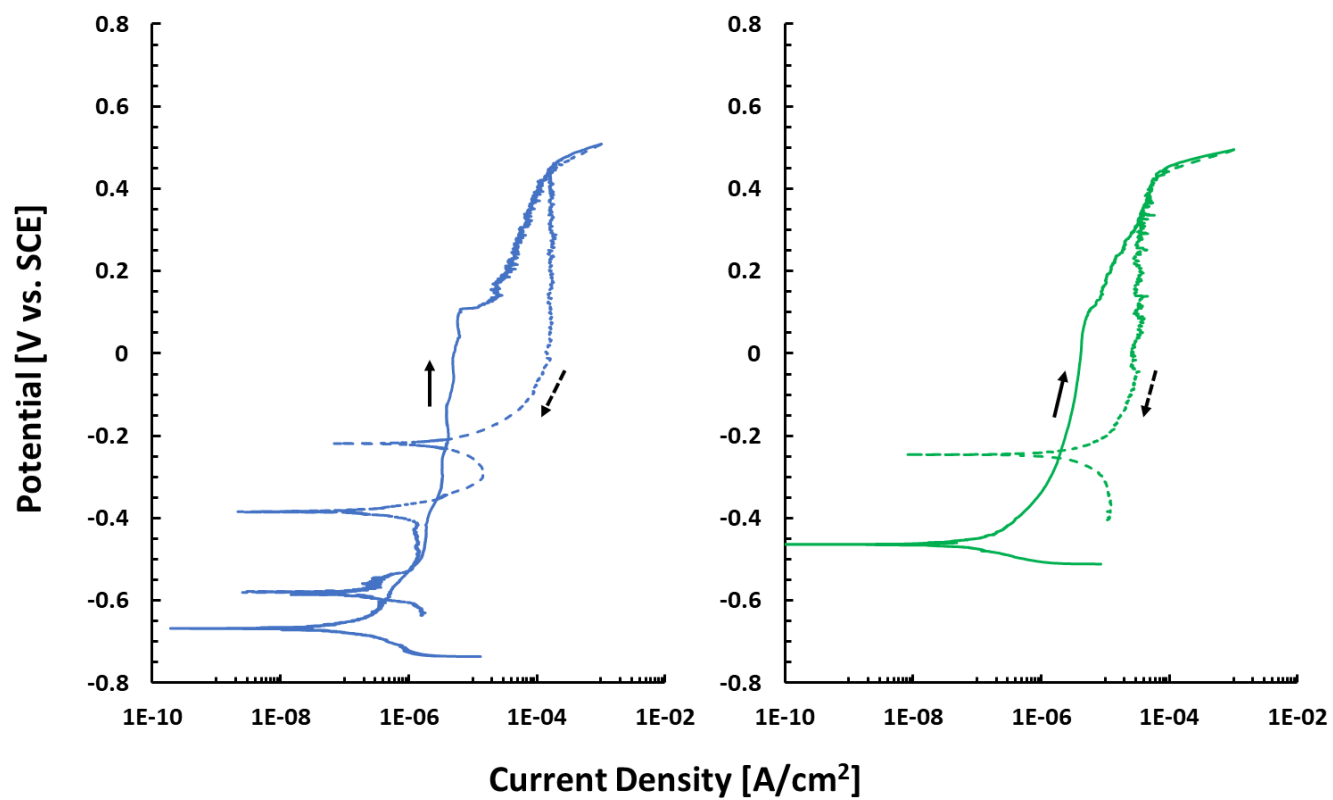
# Screening Trial 9

# Screening Trial 10
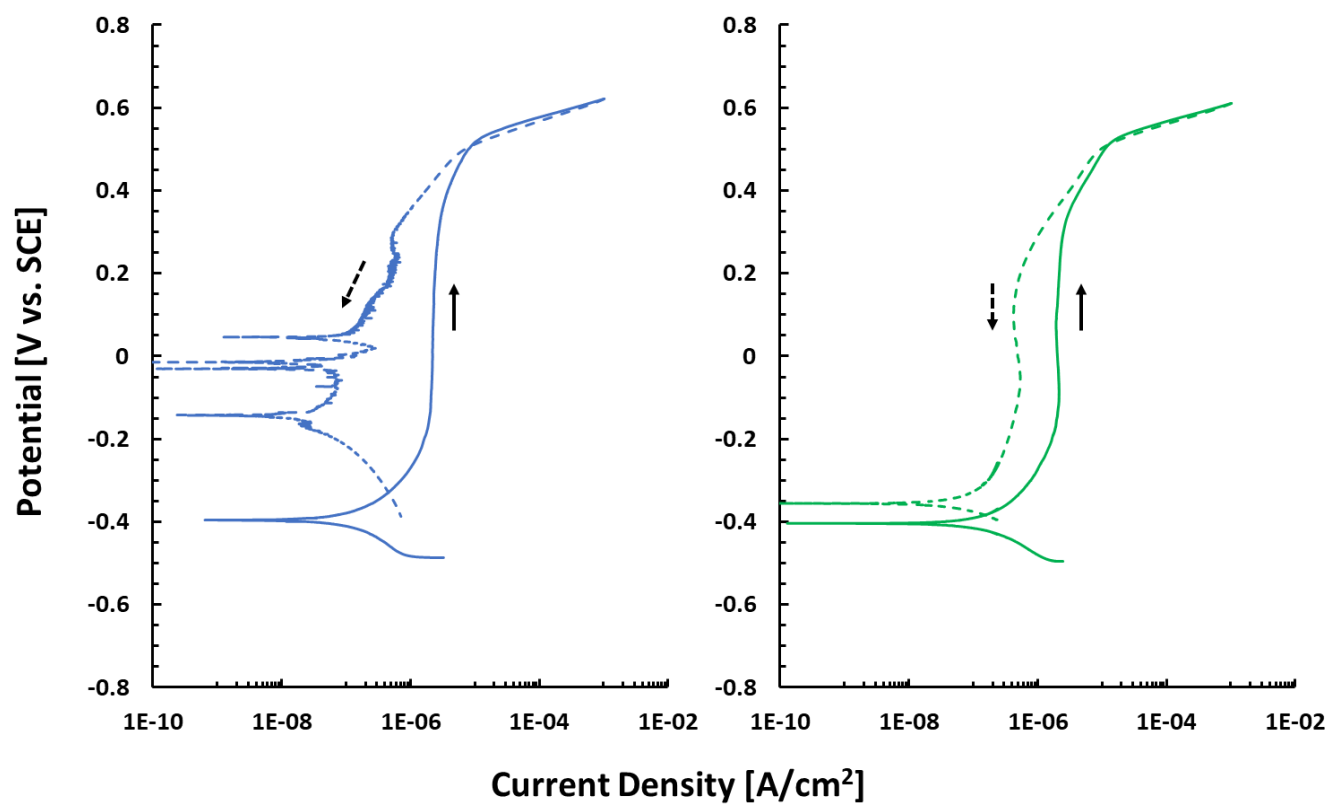
# Screening Trial 11



**Current Density [A/cm²]**
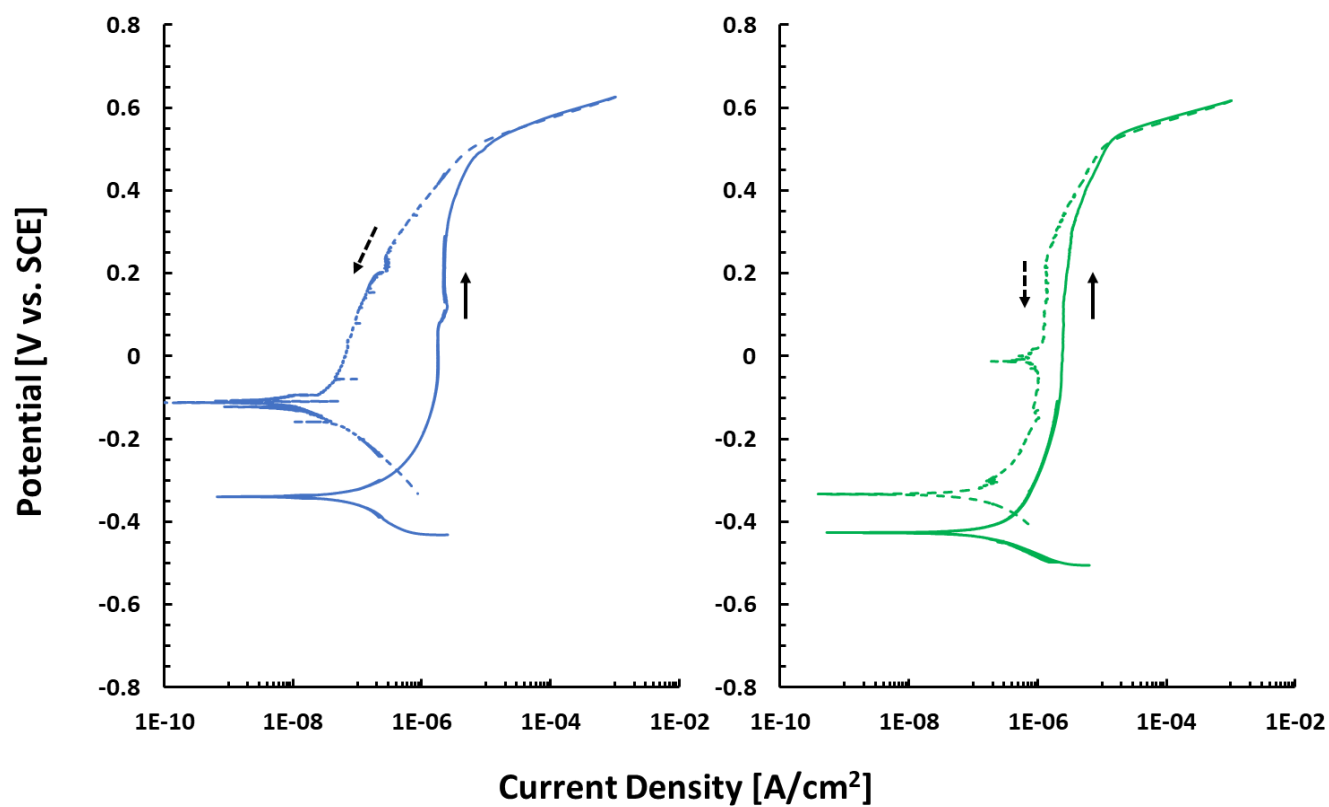
# Screening Trial 12
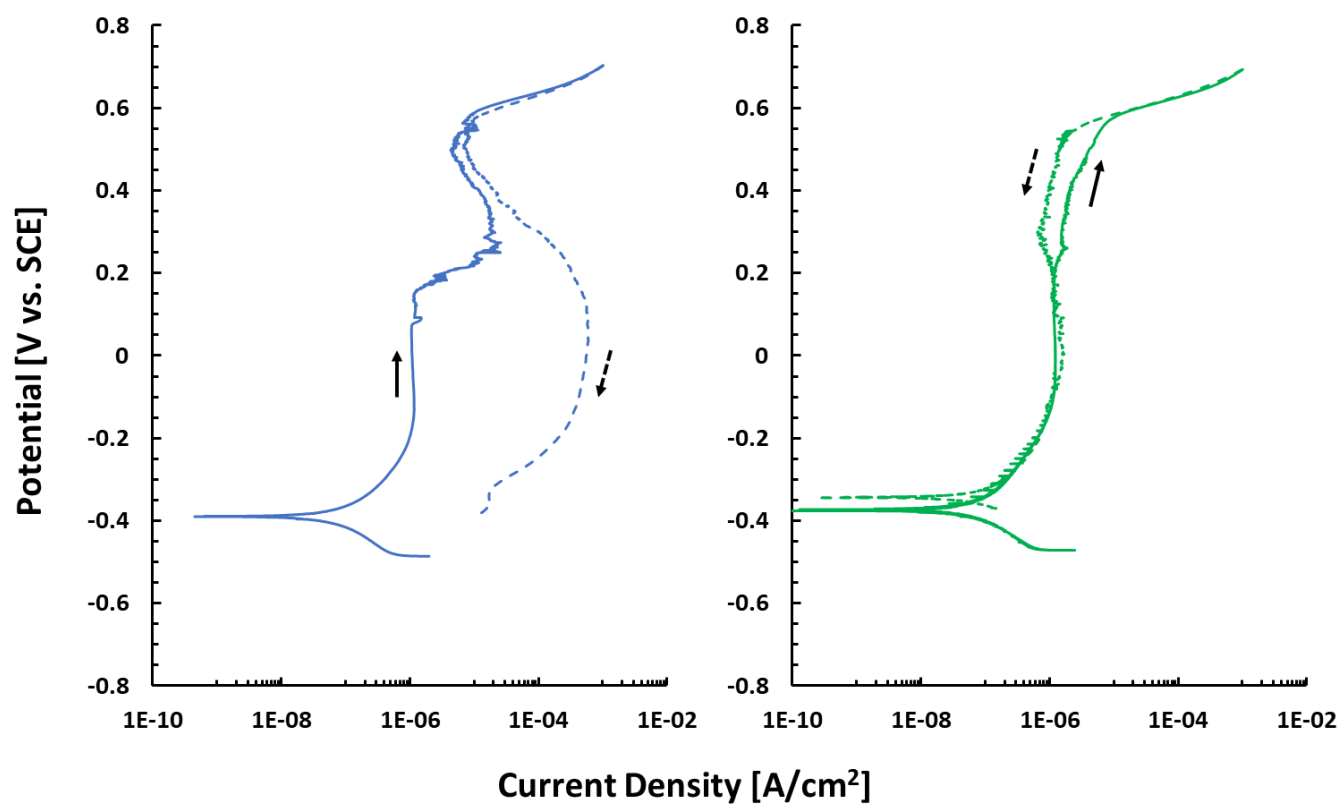
# Screening Trial 13
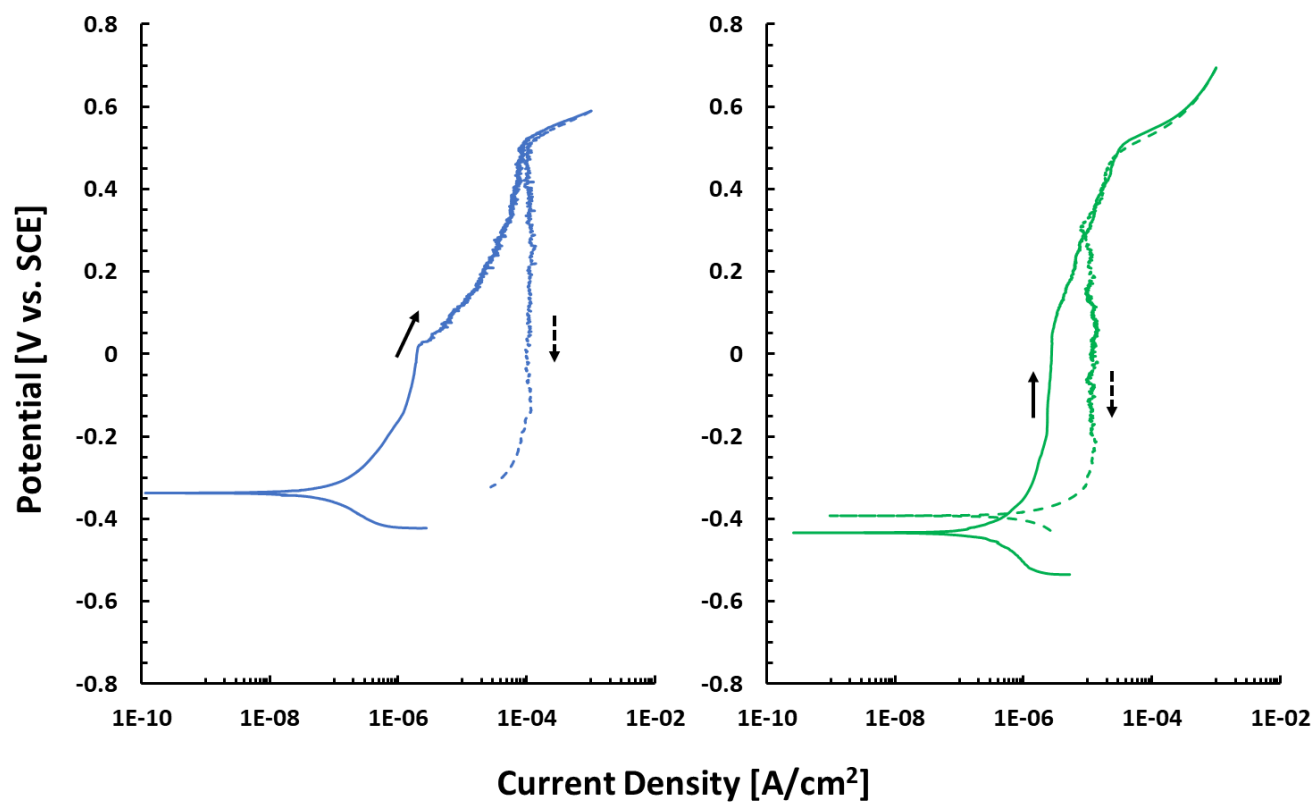
# Screening Trial 14
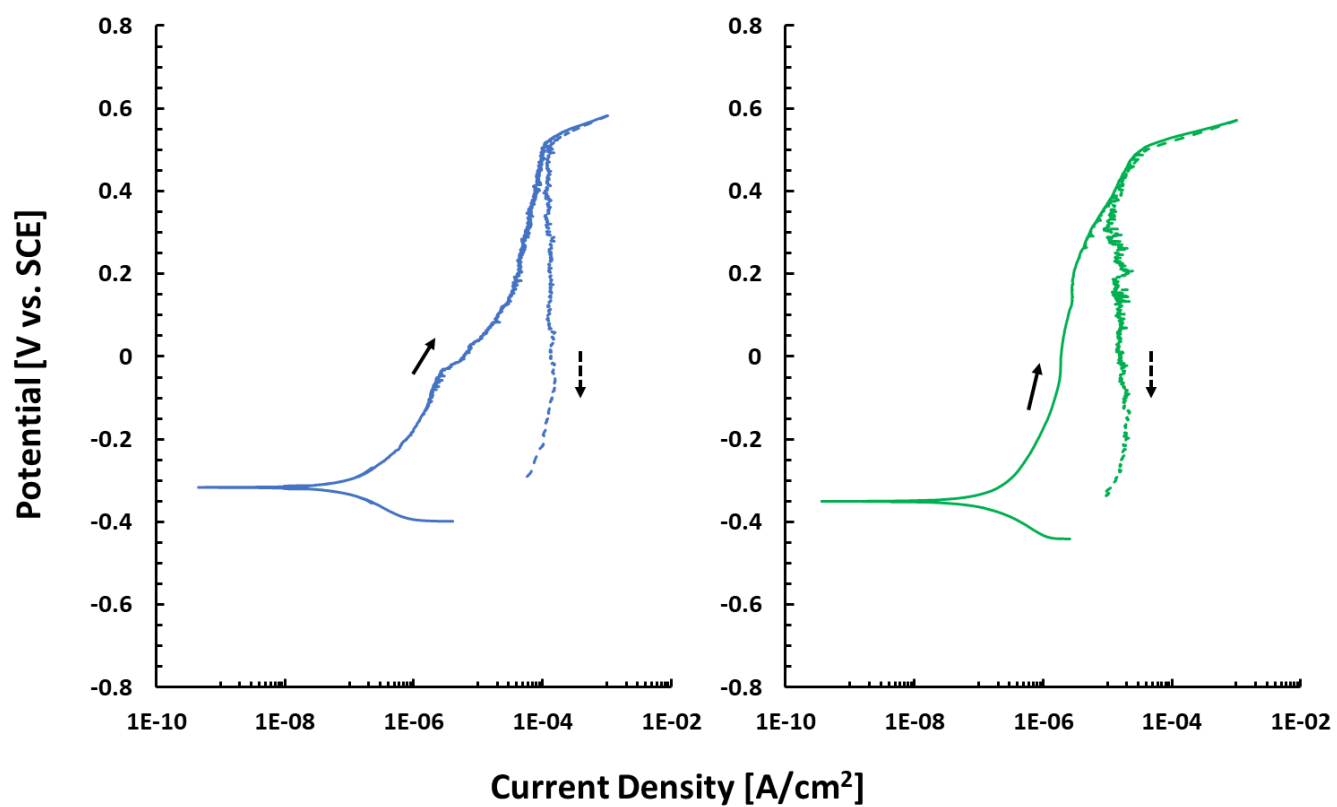
# Screening Trial 15
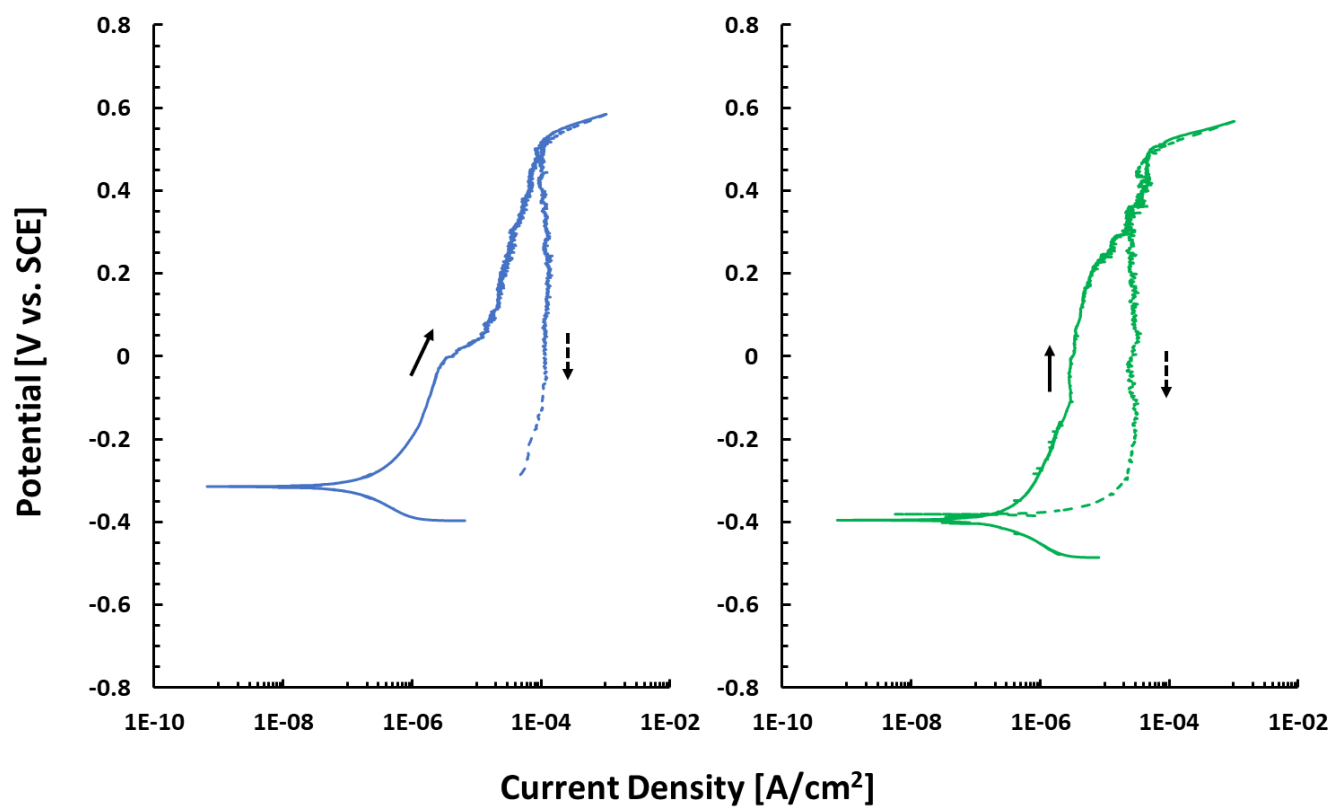
# Screening Trial 16
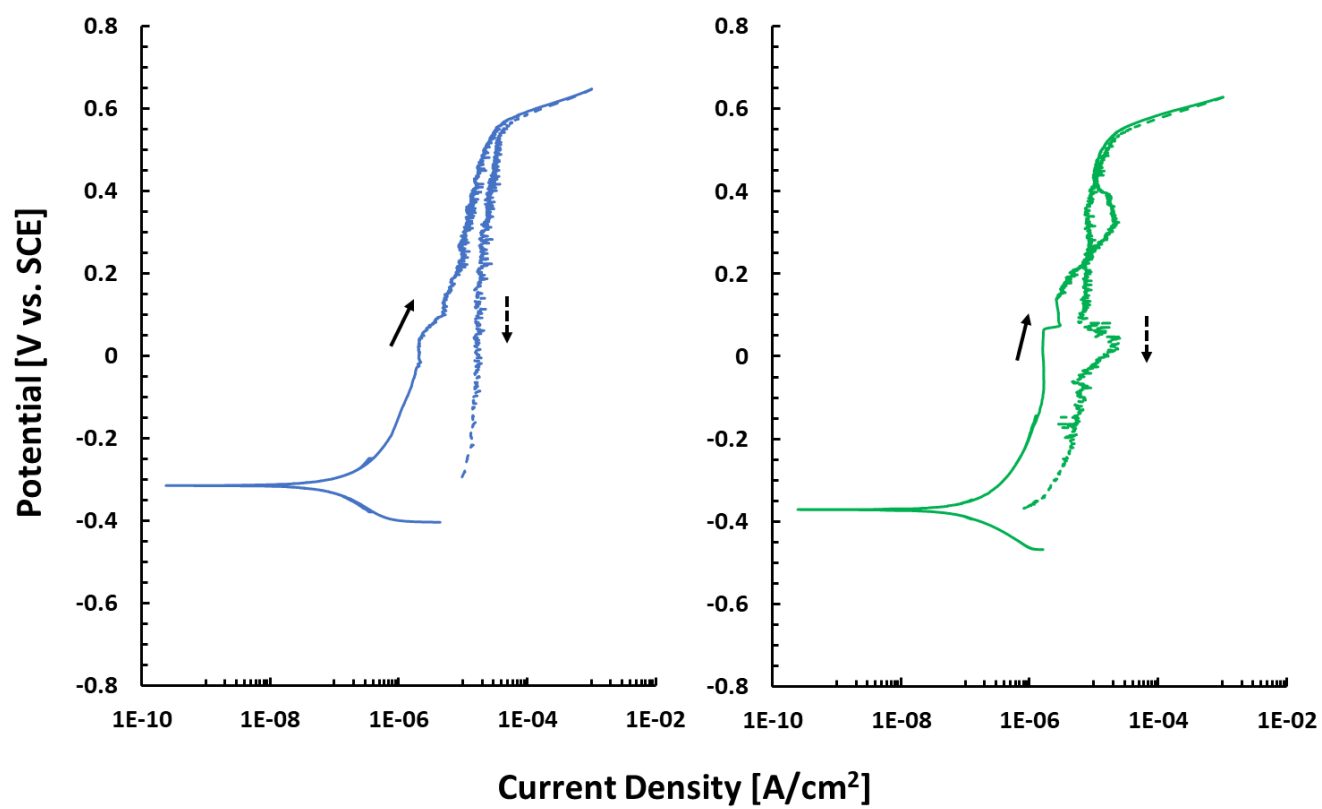
# Screening Trial 17
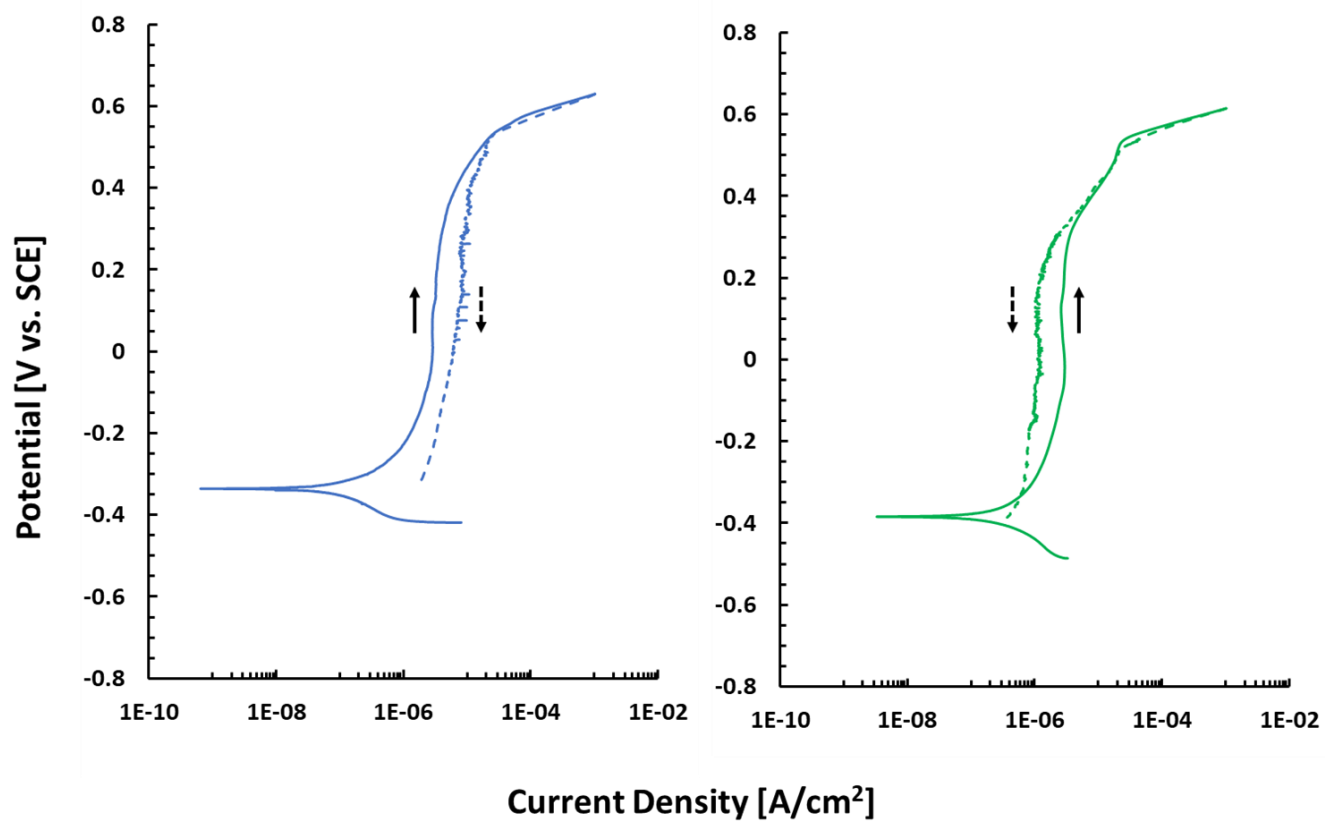
# Screening Trial 18
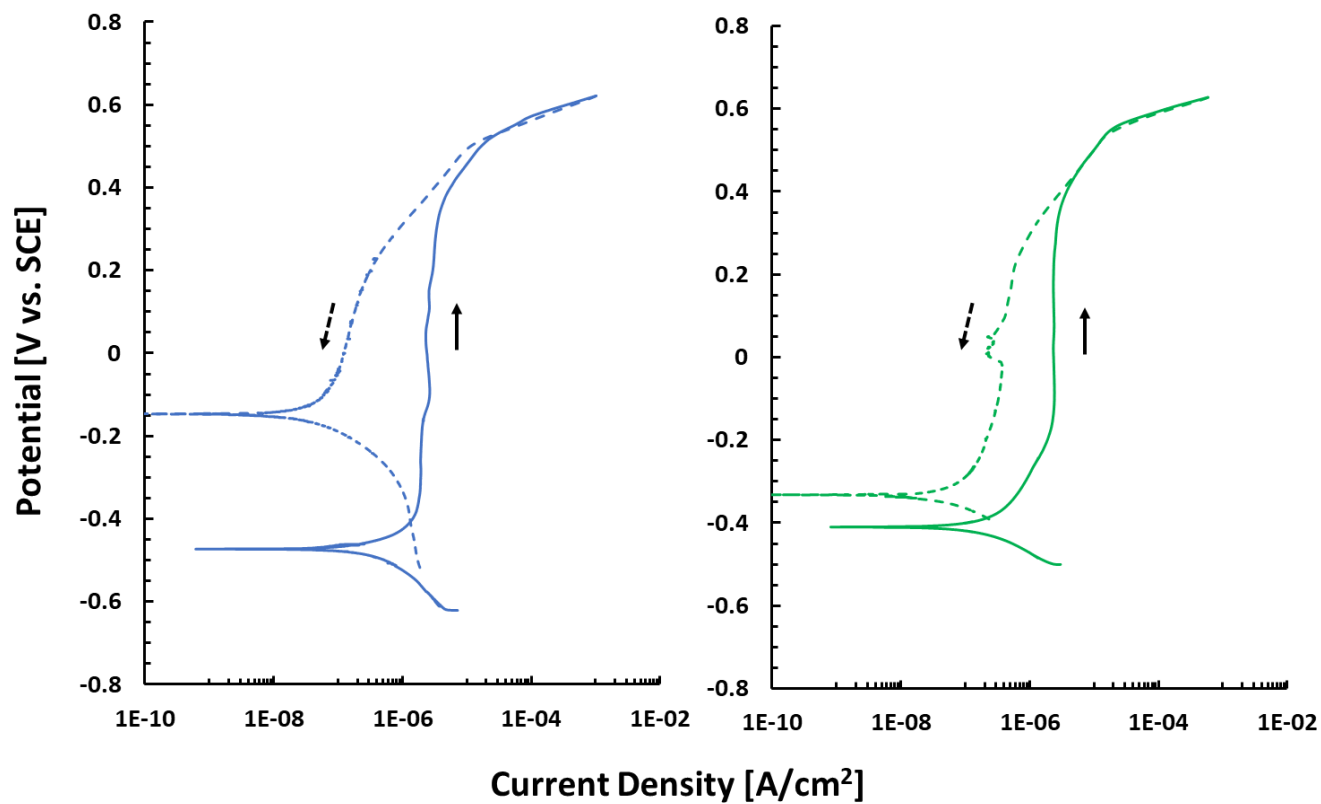
# Screening Trial 19
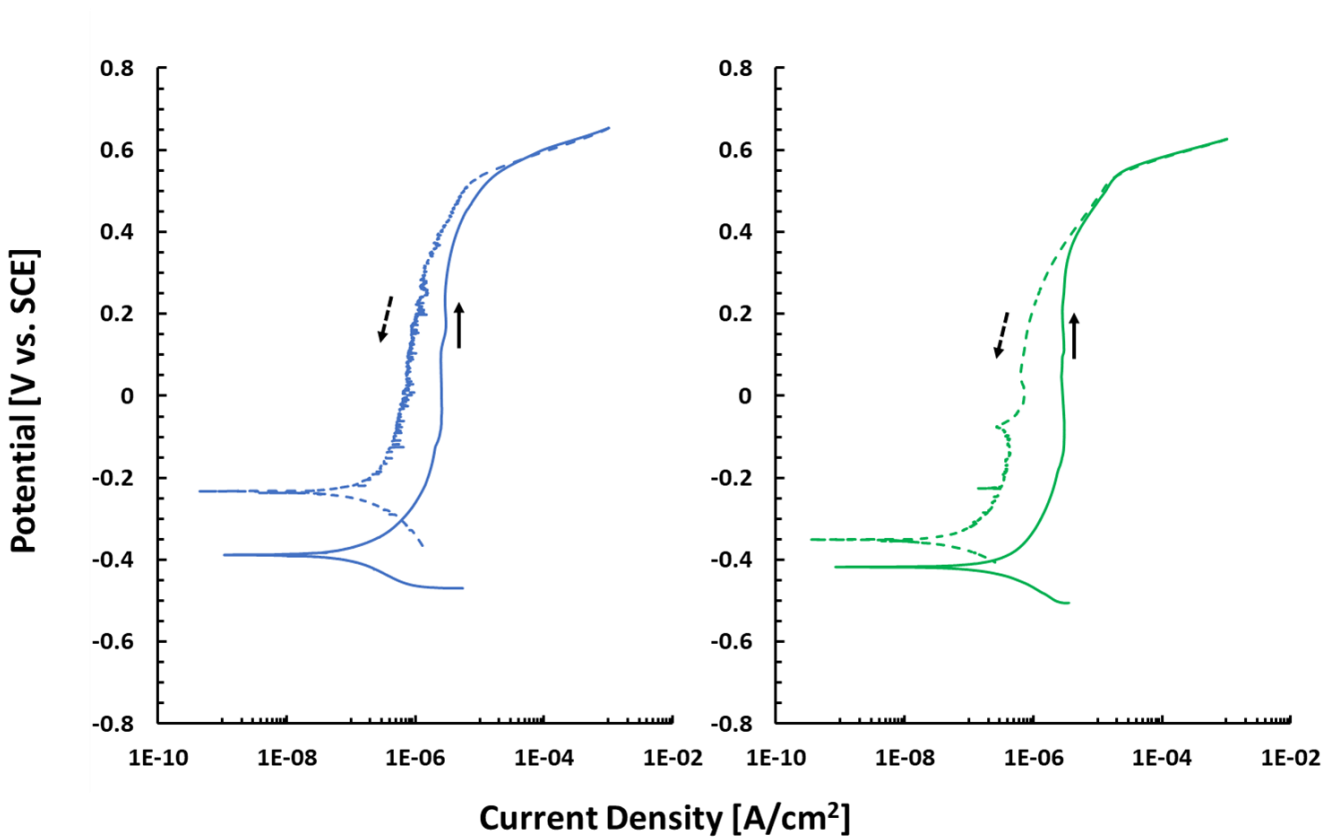
# Screening Trial 20
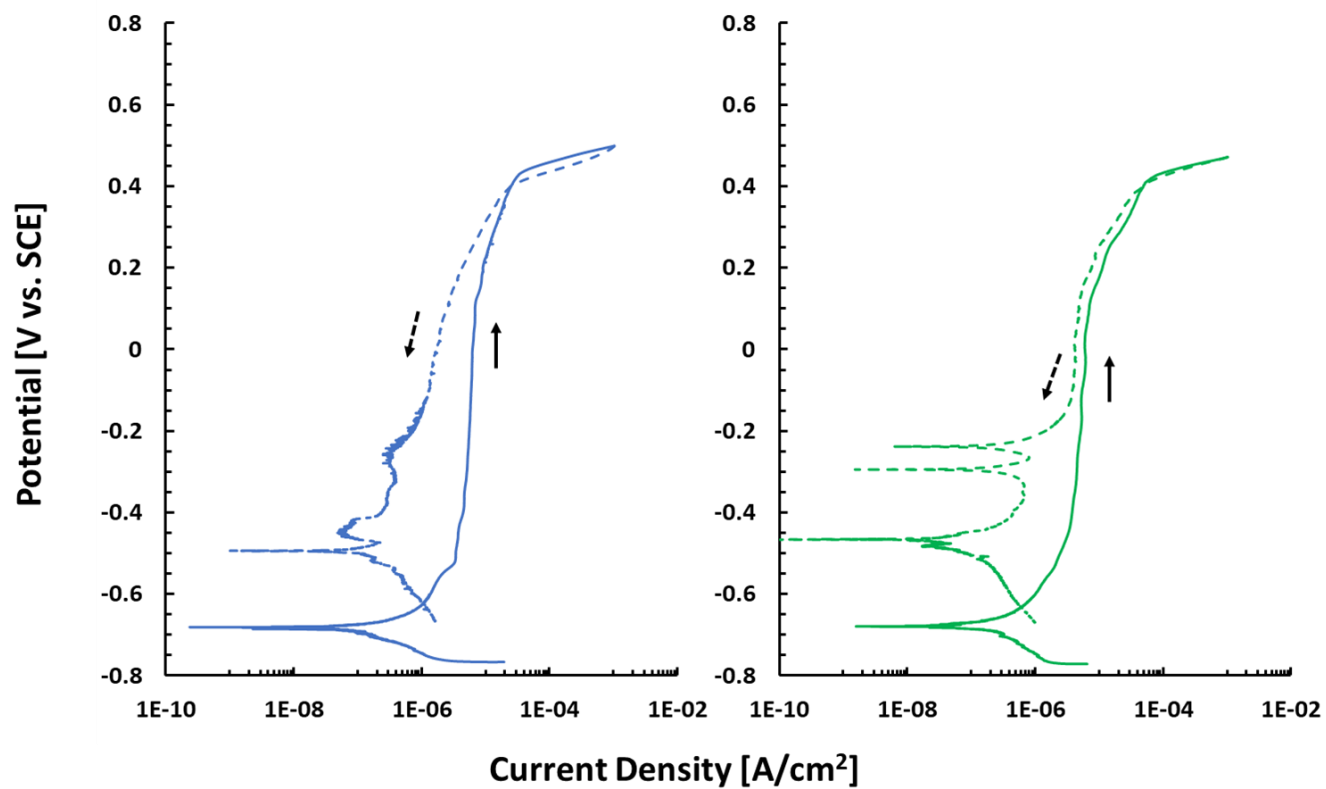
# Screening Trial 21
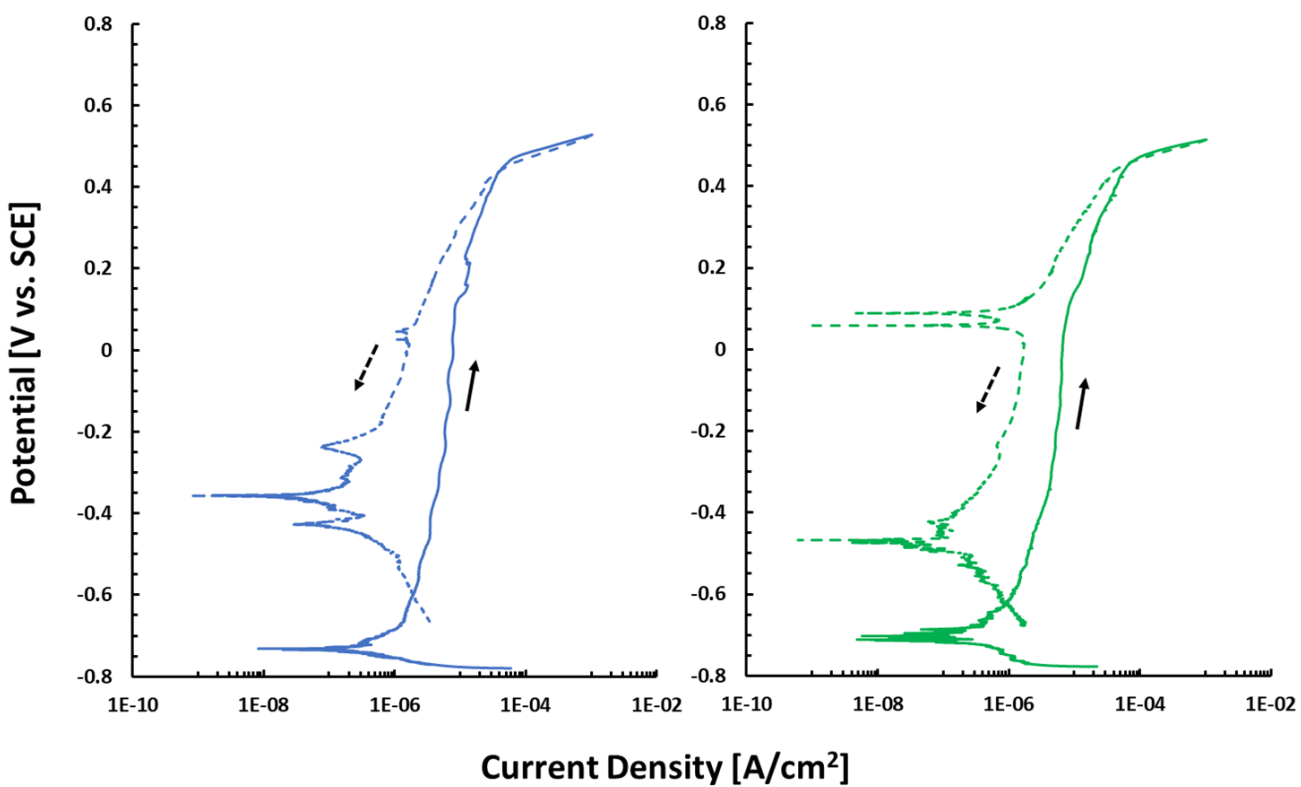
# Screening Trial 22
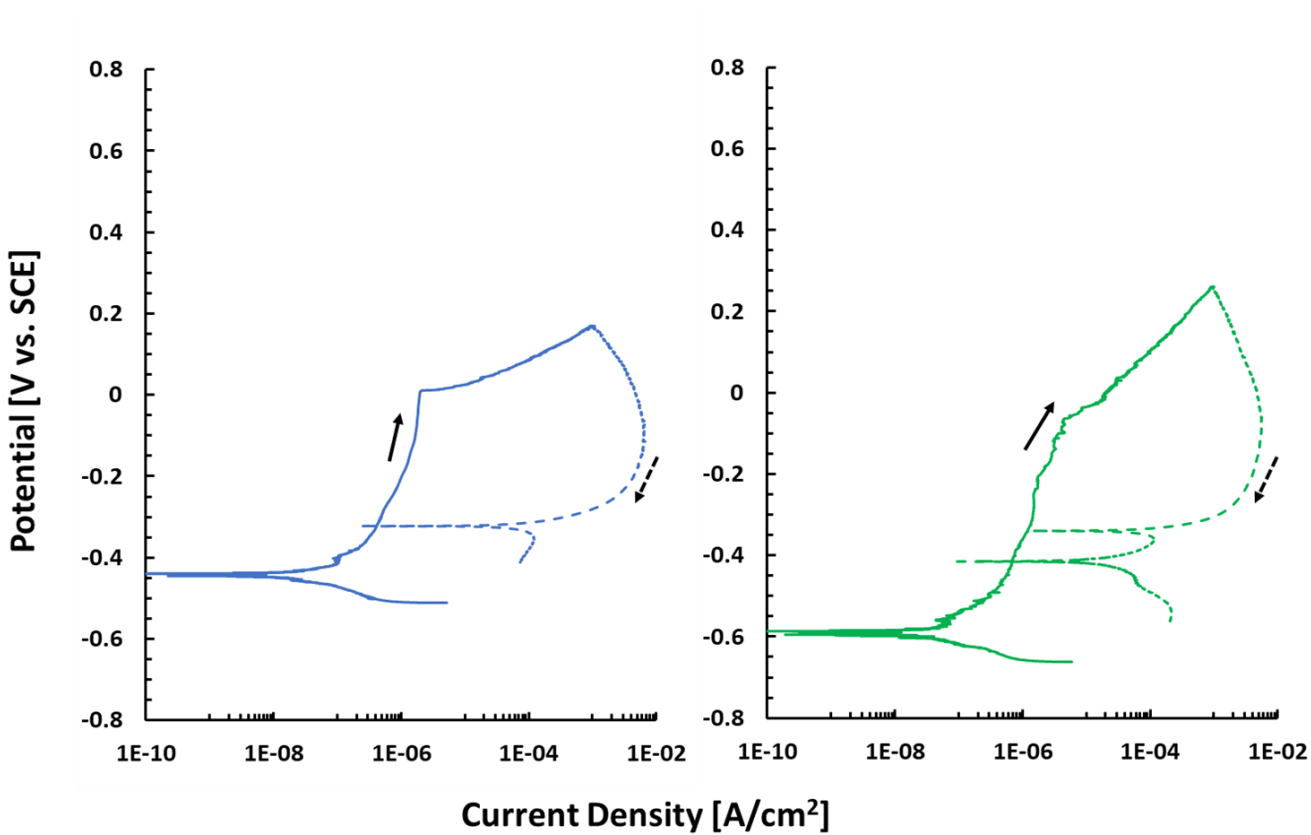
# Screening Trial 23
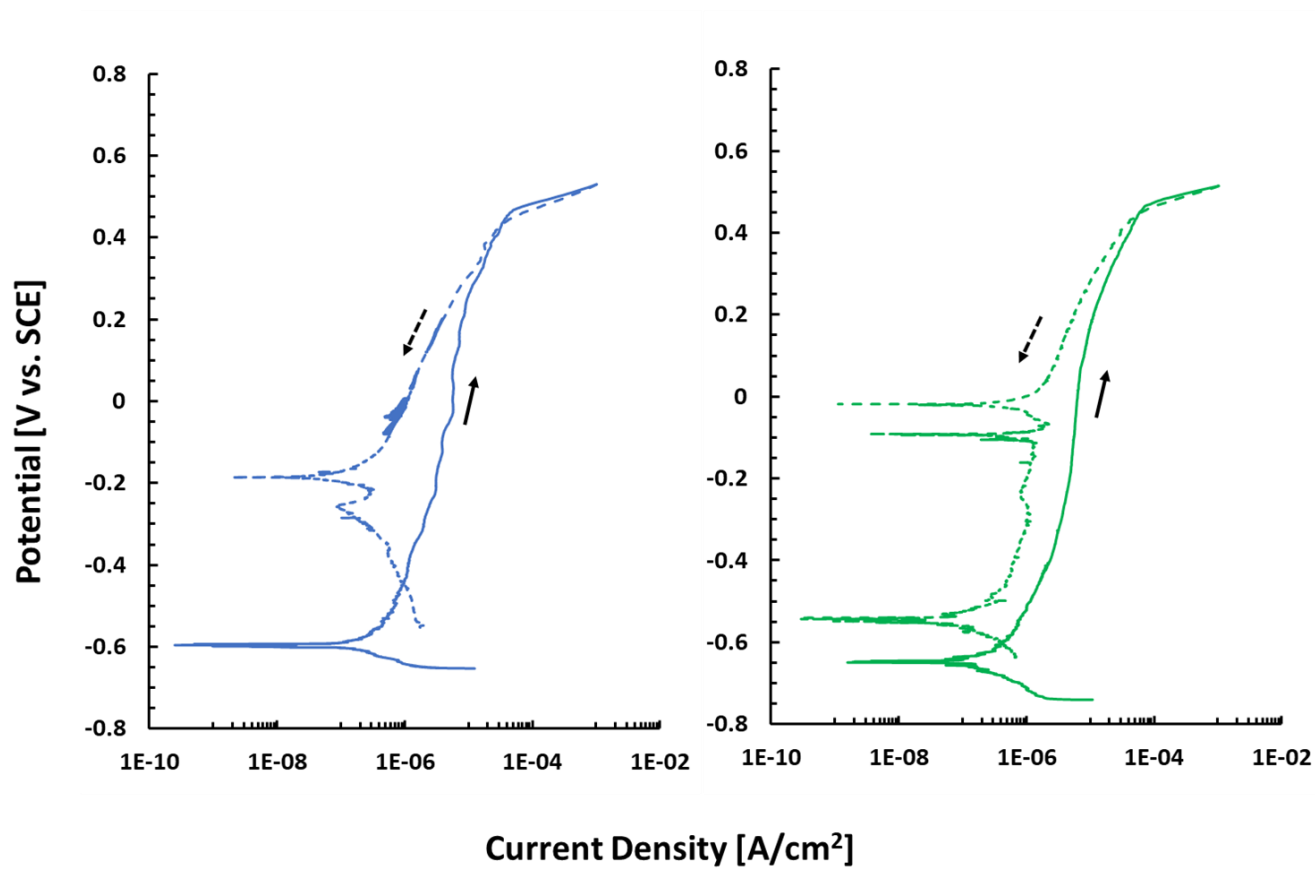
# Screening Trial 24
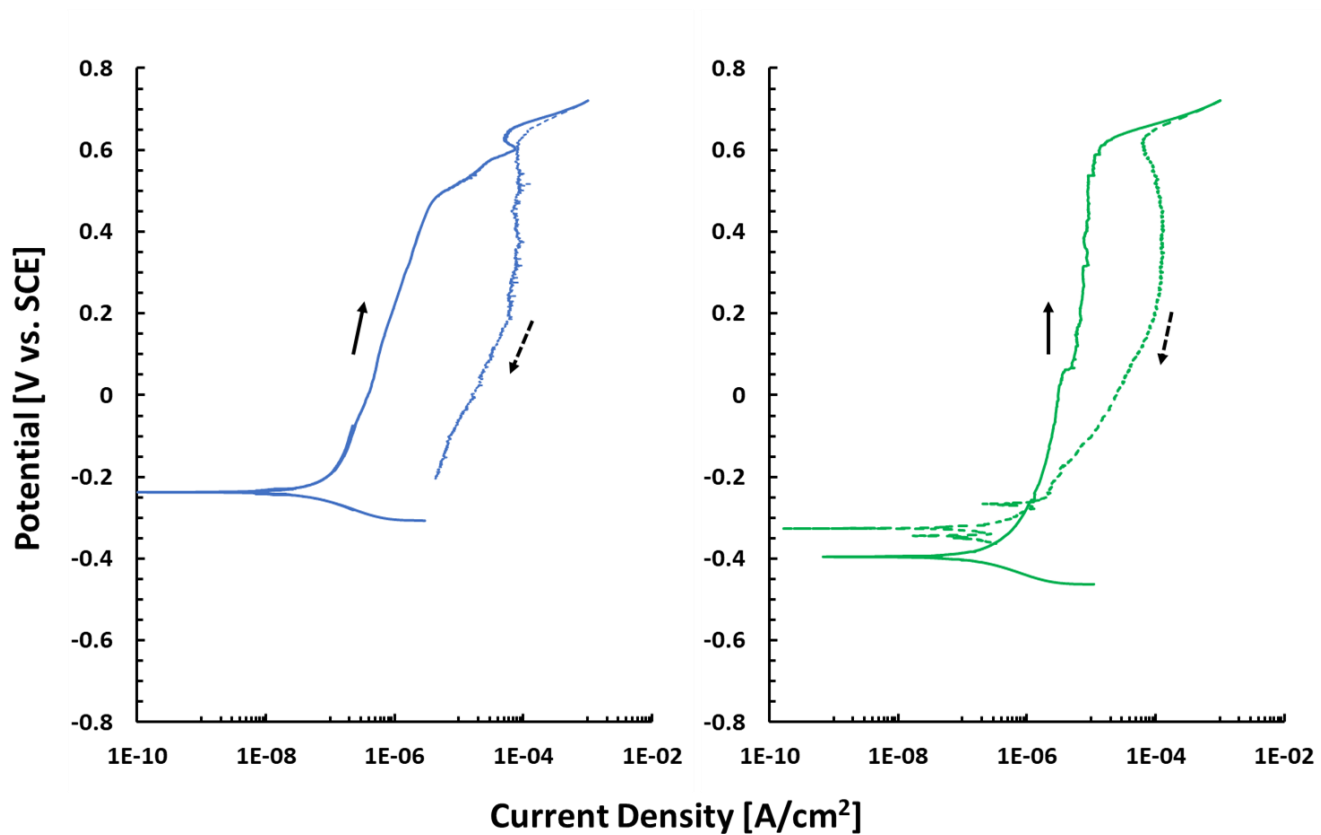
# Screening Trial 25
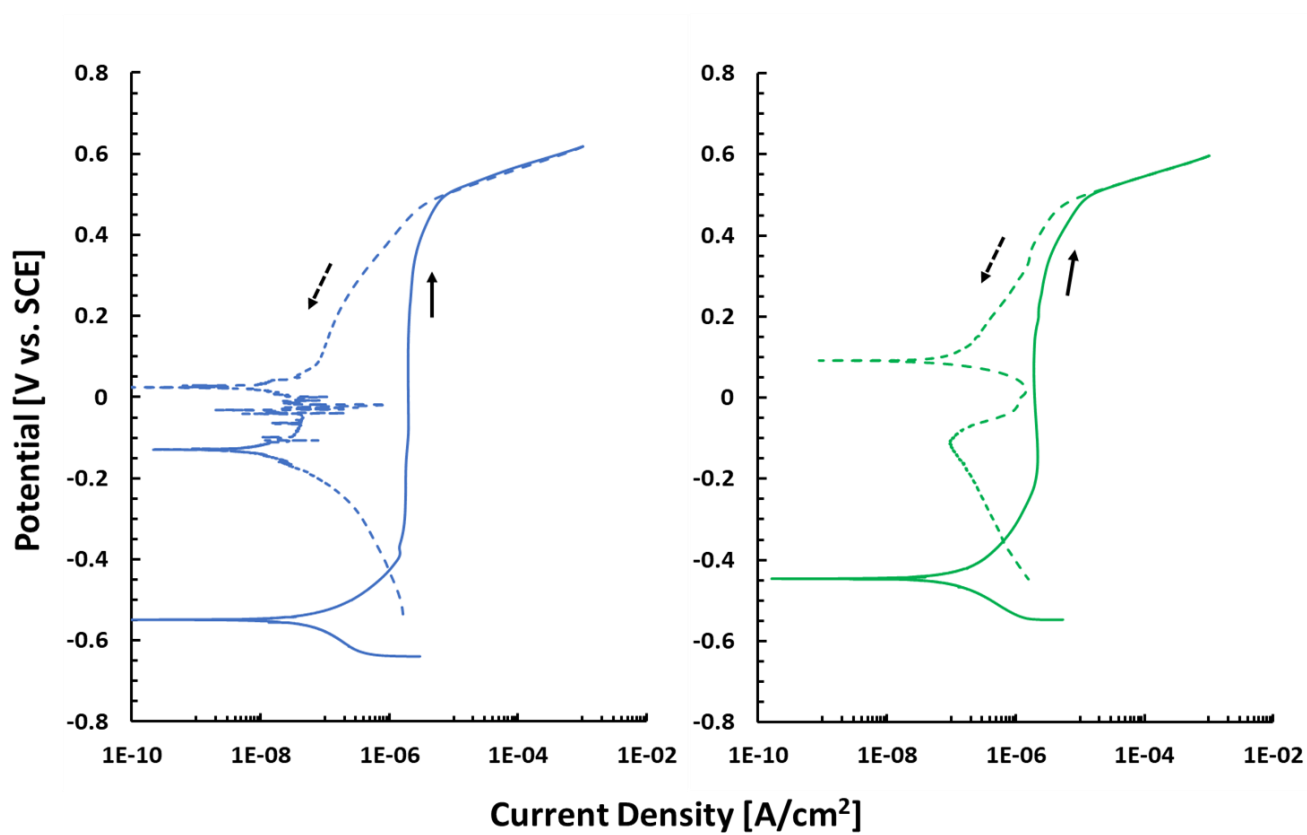
# Screening Trial 26
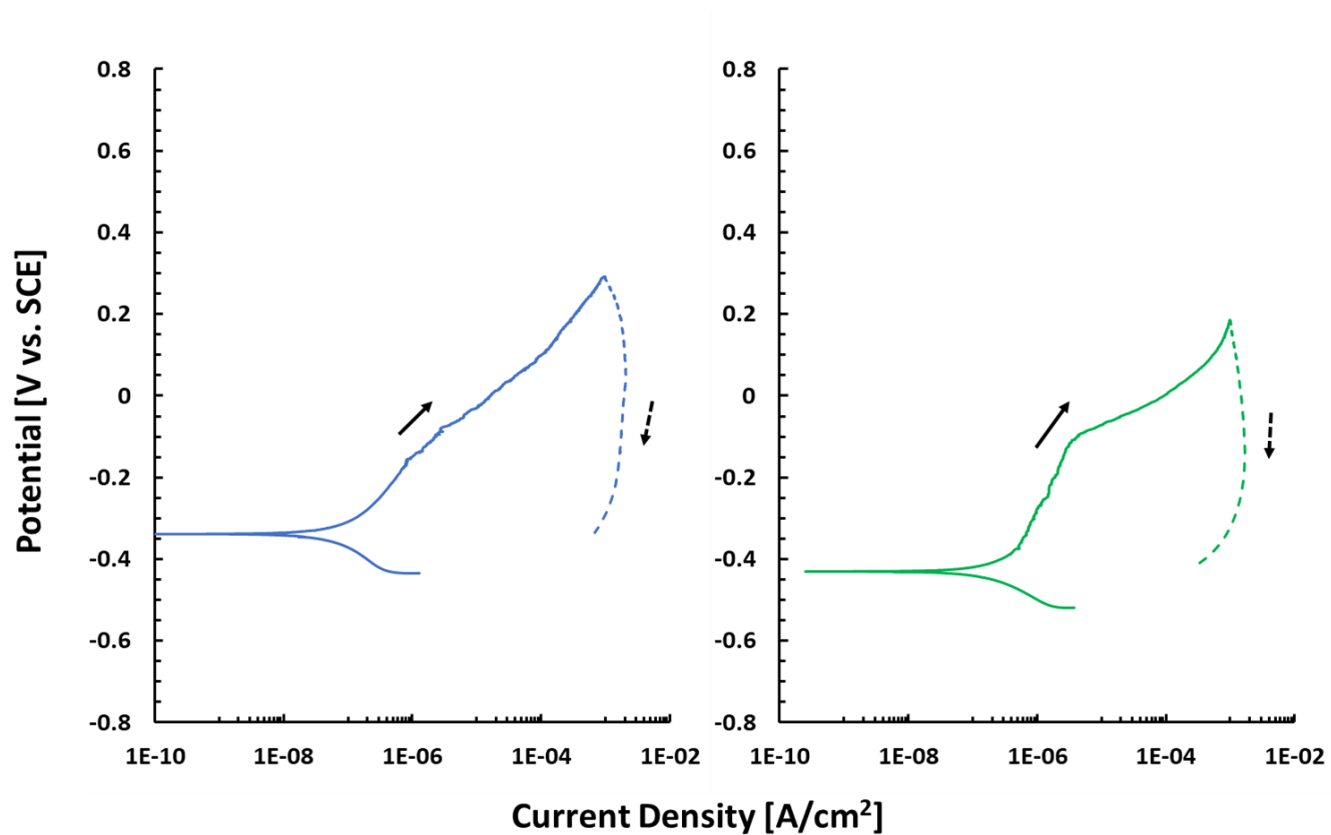
# Screening Trial 27
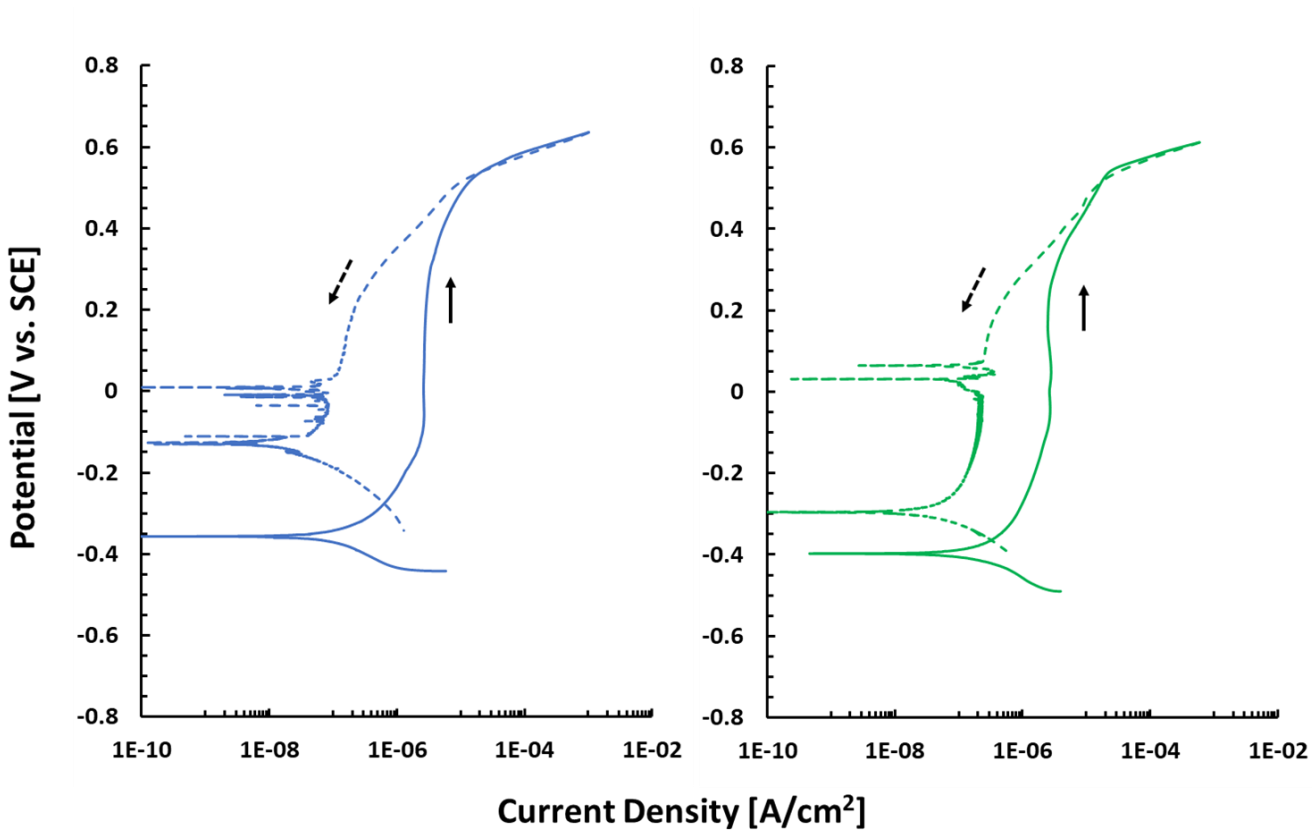
# Screening Trial 28
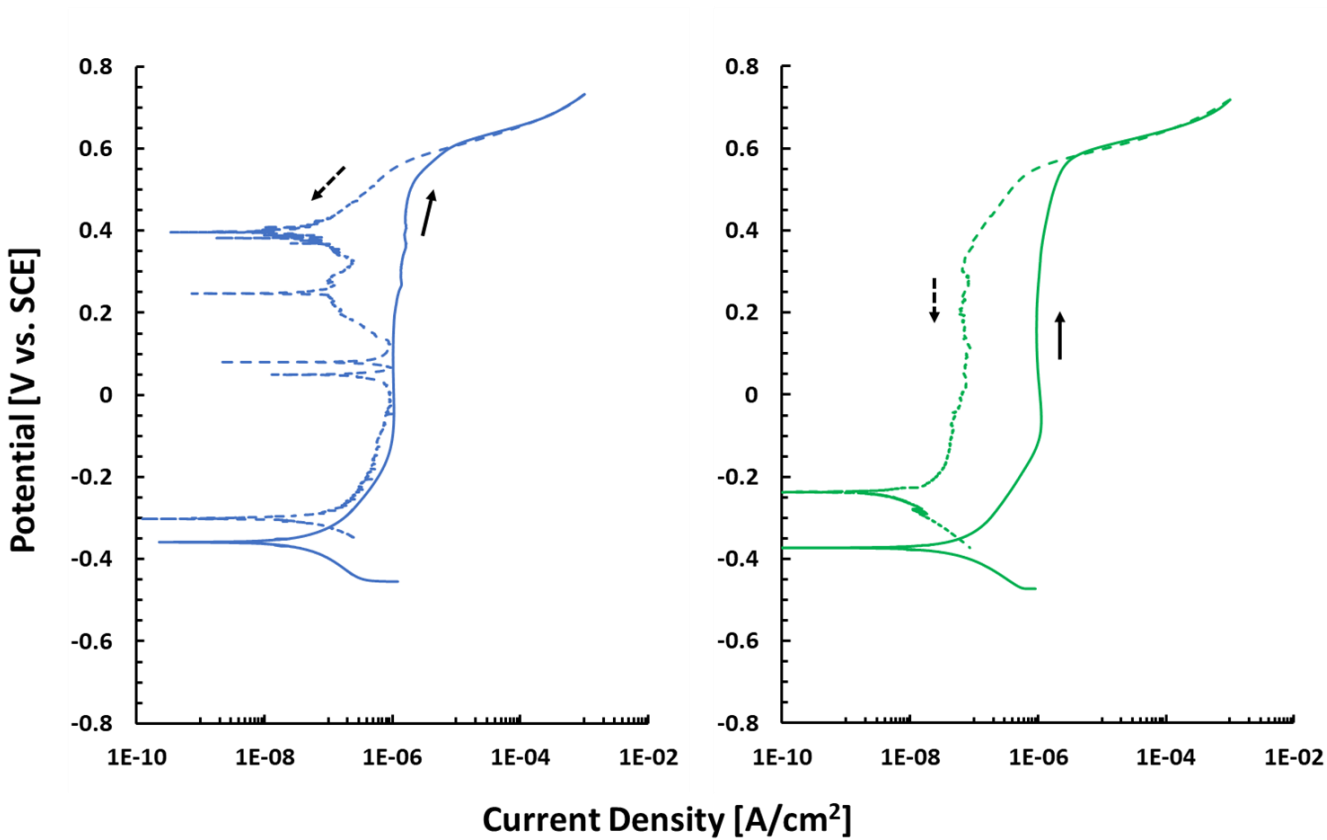
# Screening Trial 29
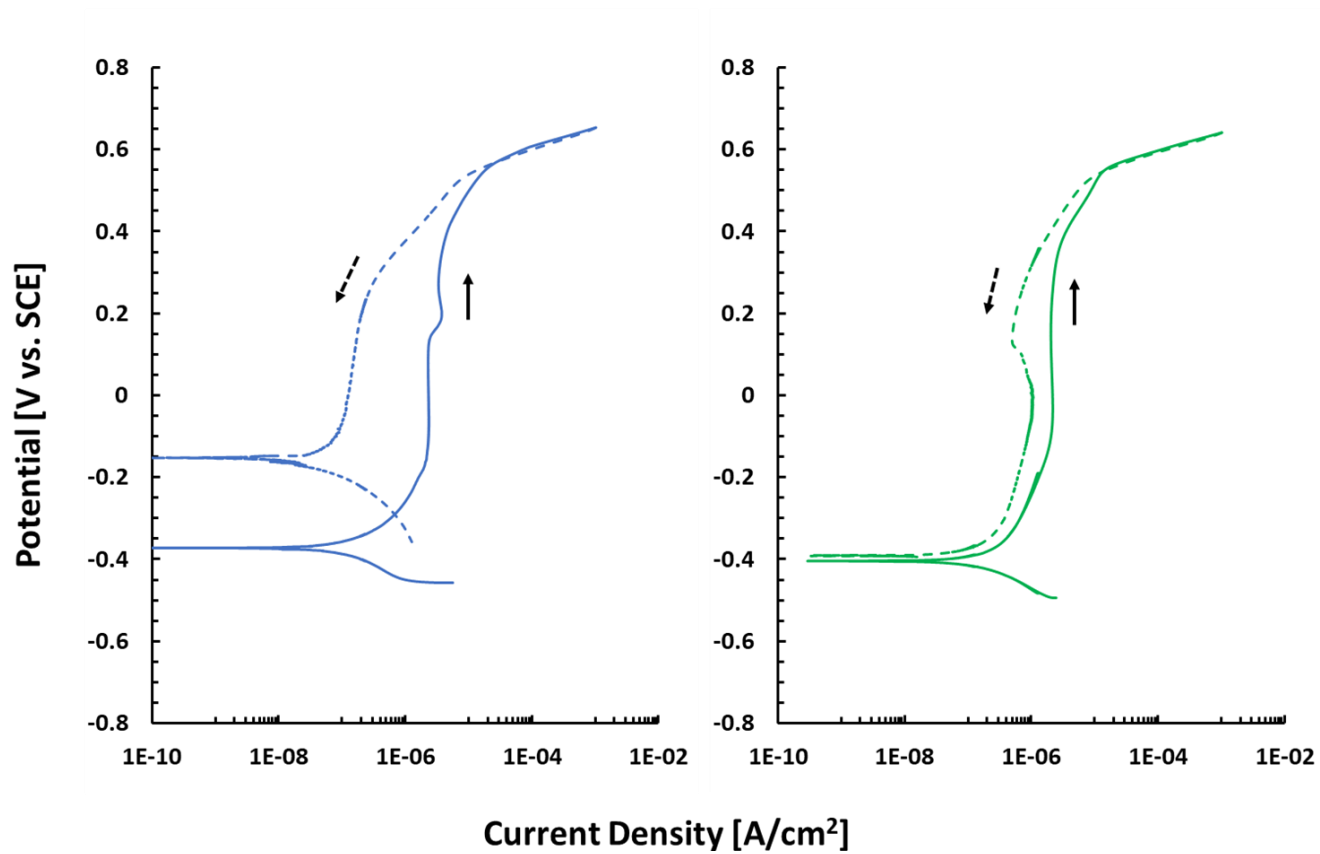
# Screening Trial 30
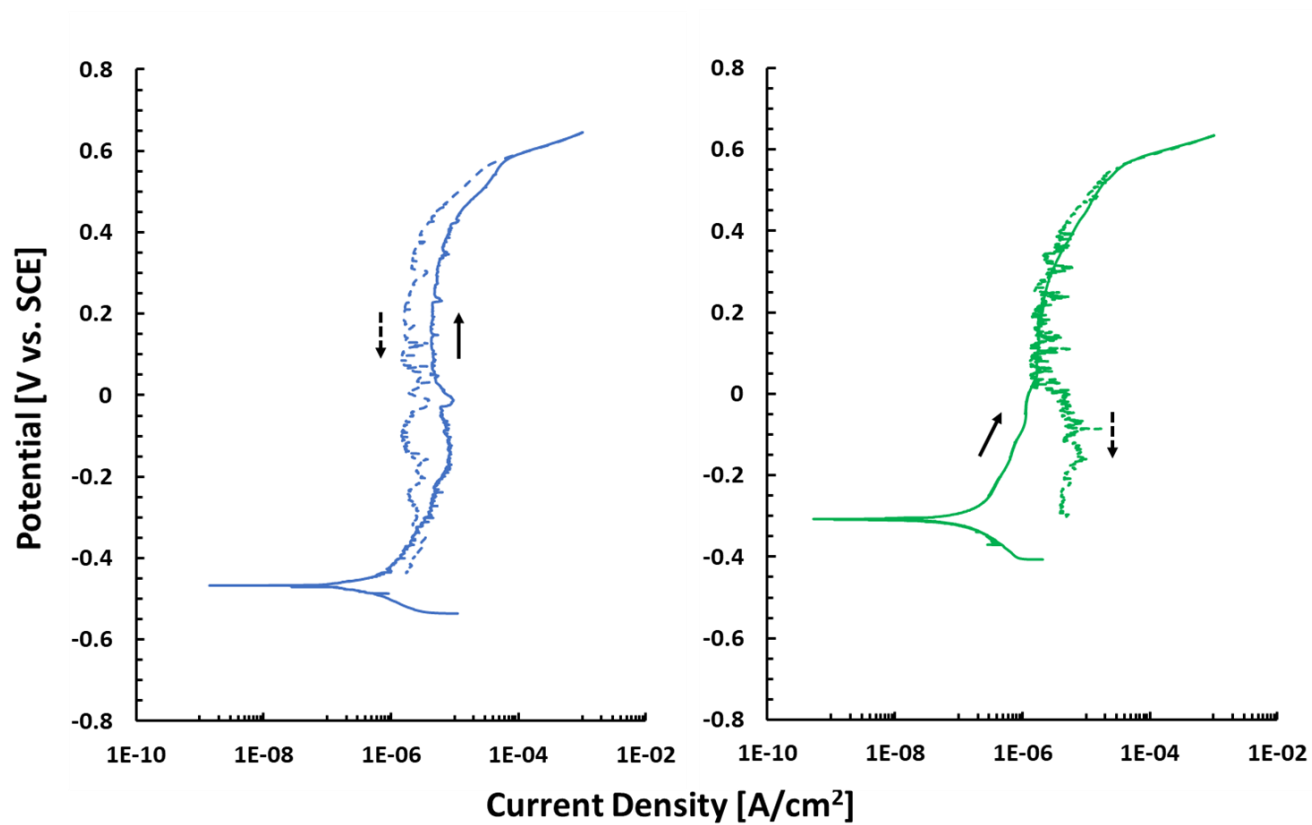
# Screening Trial 31
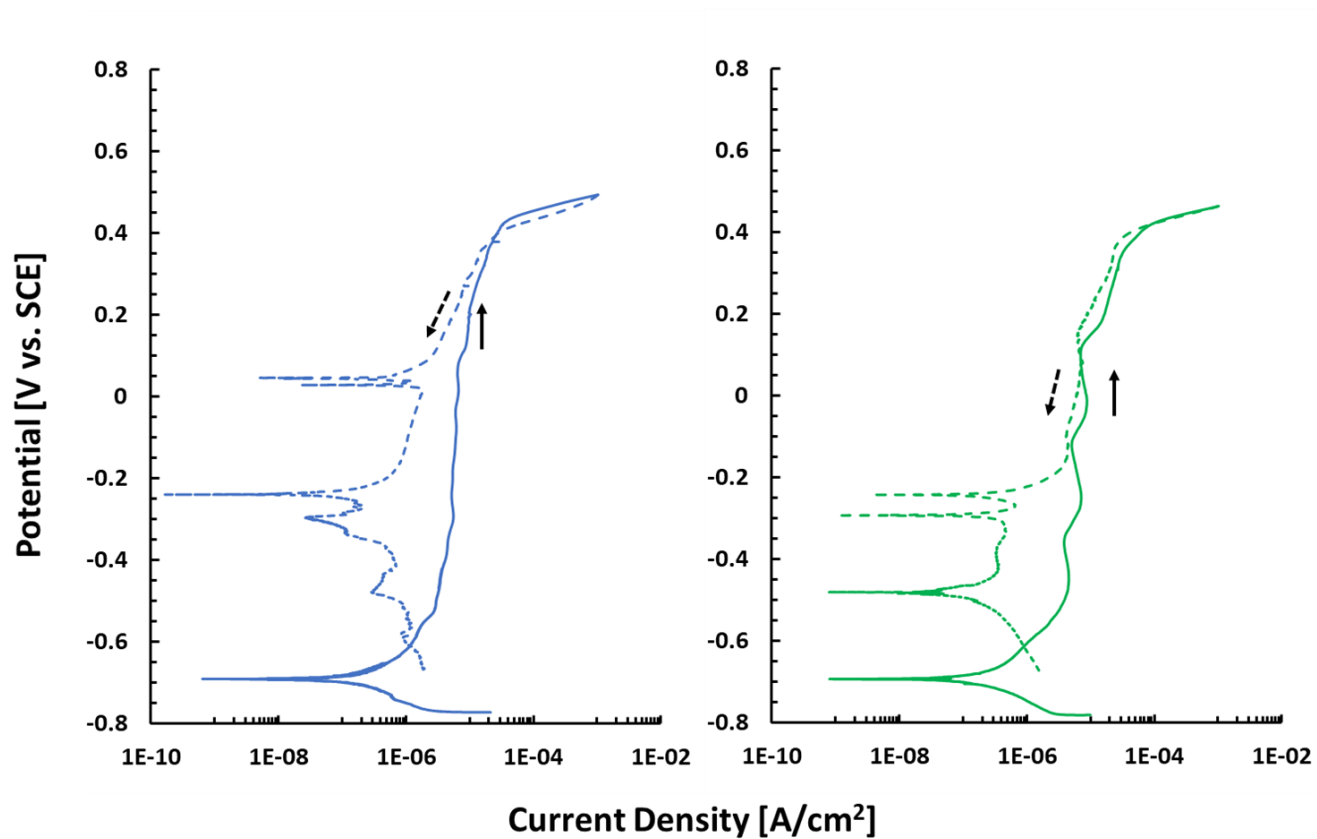
# Screening Trial 32
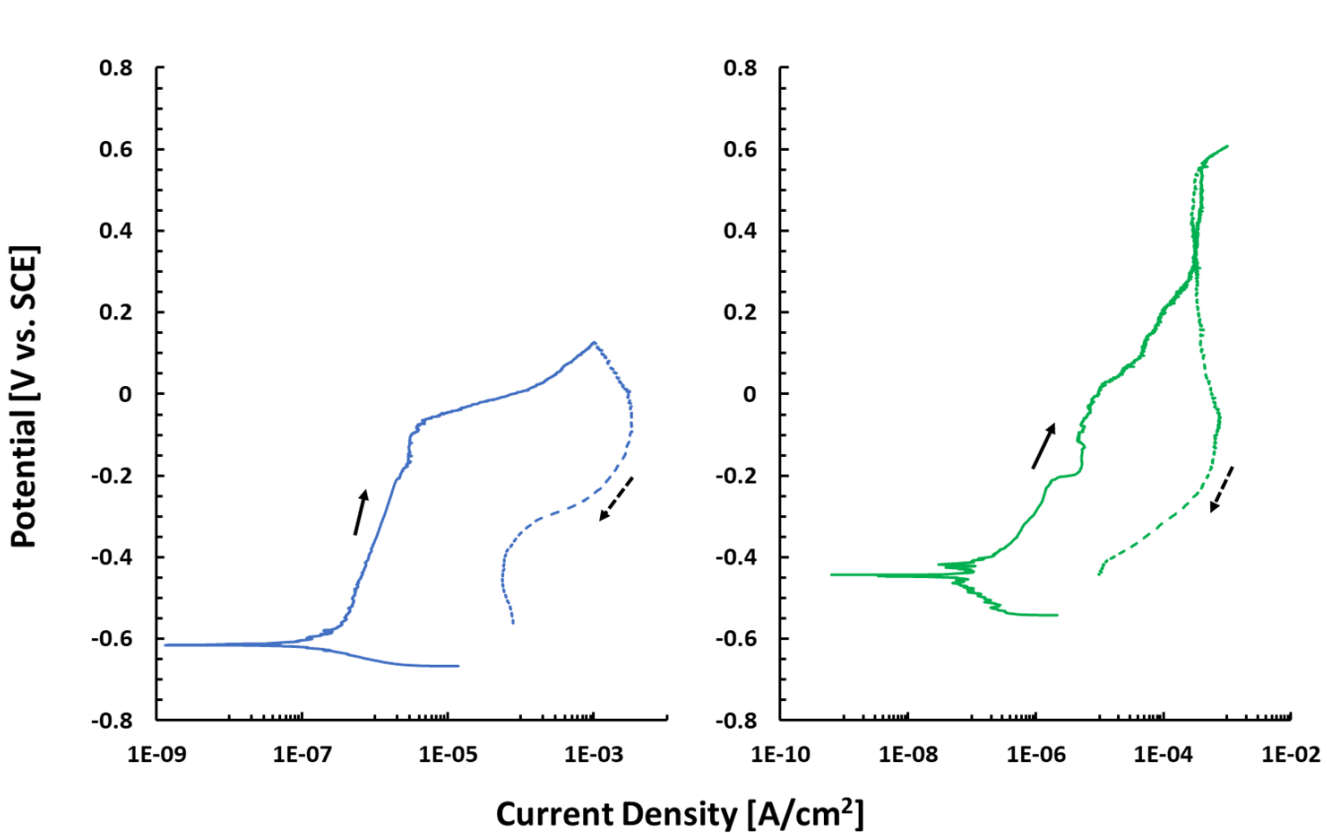
# Screening Trial 33
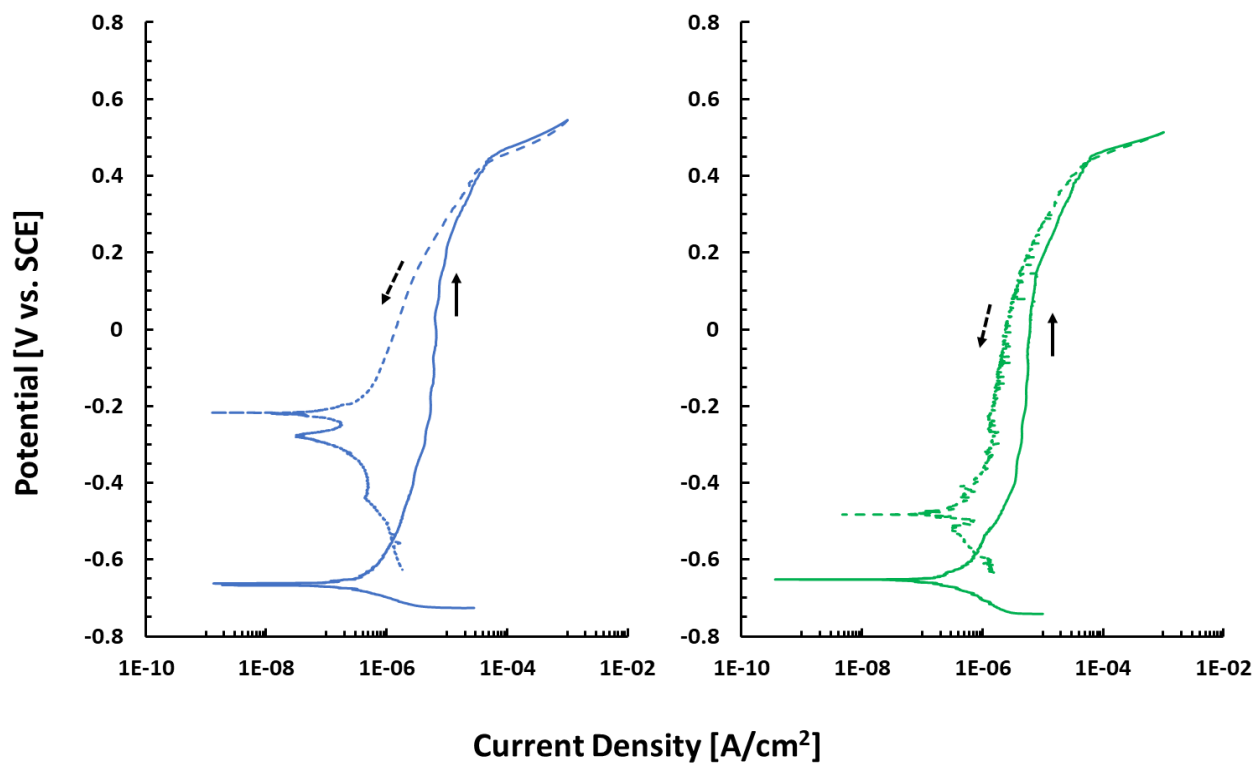
**Appendix B.  Micrographs of the fracture surface of slow strain rate tests.**

**A537 Mineral Oil**
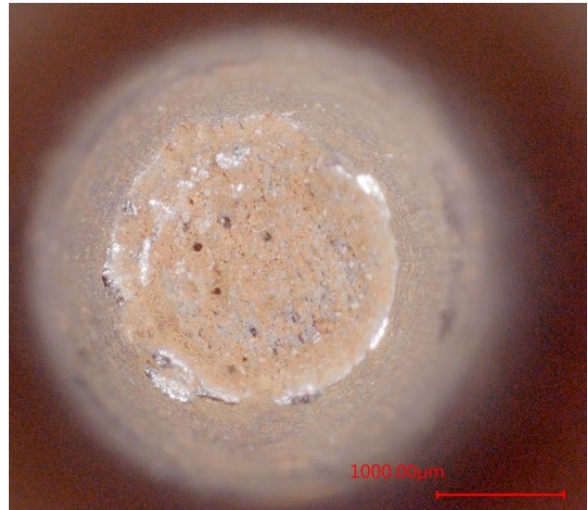
**A537 ST02 OCP**
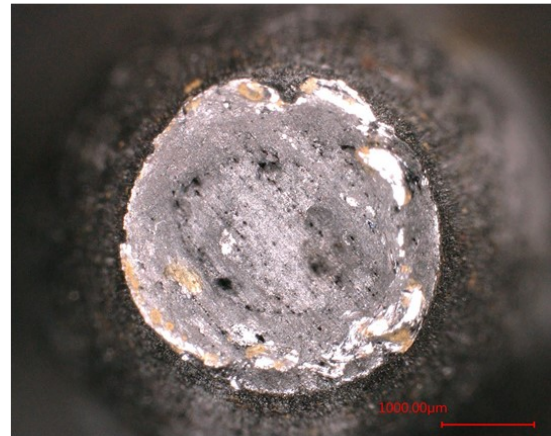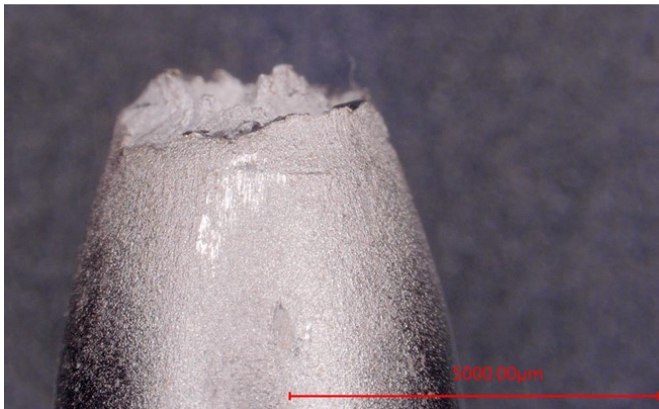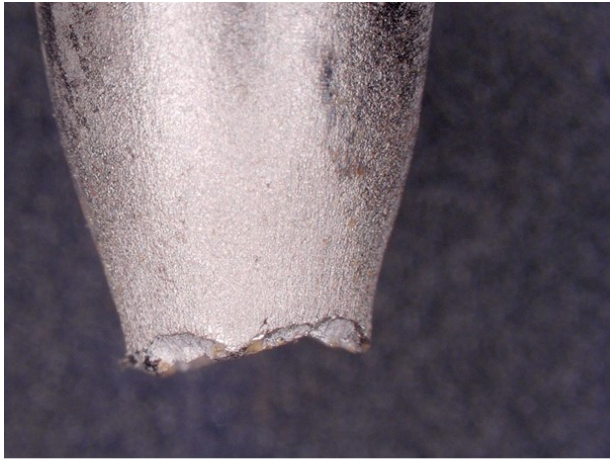
**A537 ST02 +200 mV vs. OCP**
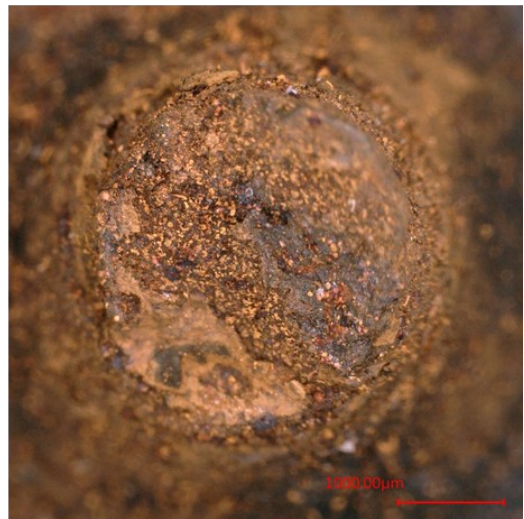
**A537 ST05 OCP**
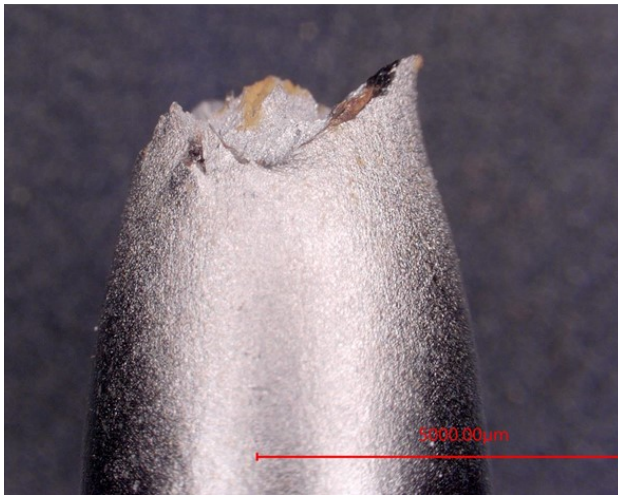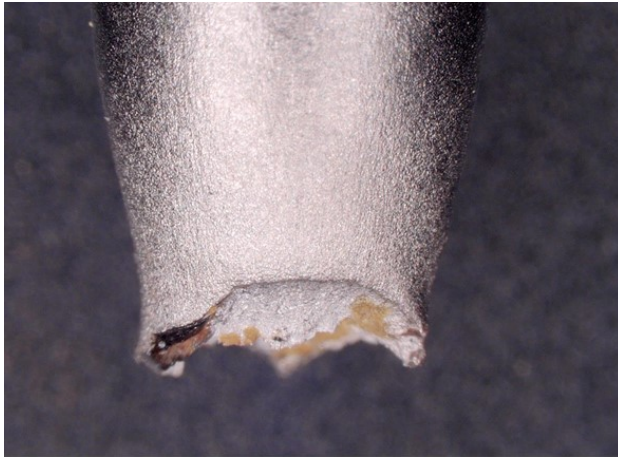
**A537 ST05 +200 mV vs. OCP**
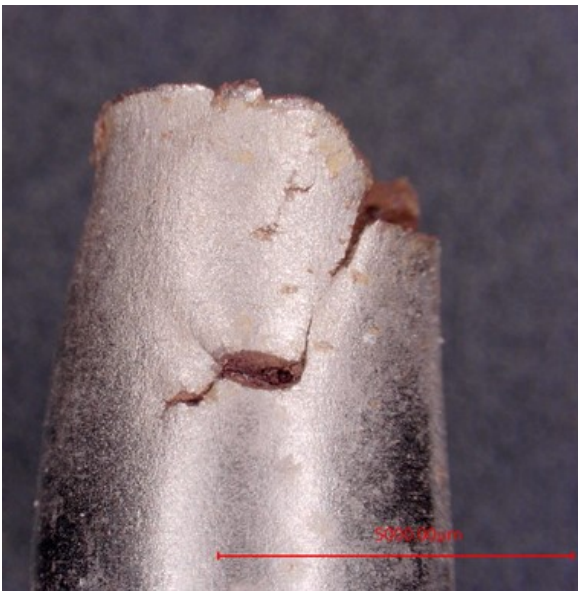
**A537 ST09 OCP**

**A537 ST10 OCP**

**A537 ST11 OCP**
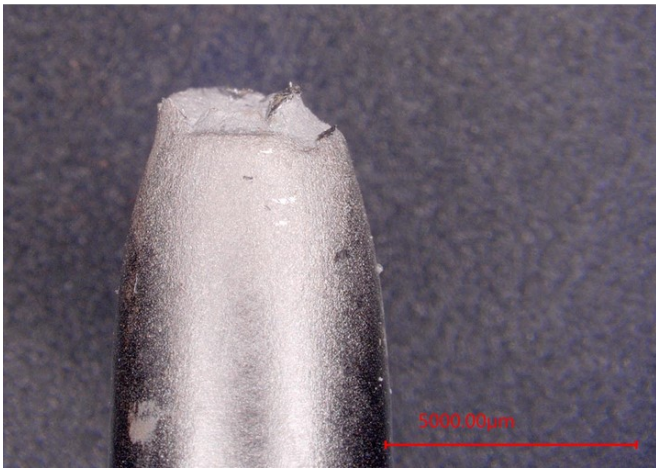
**A537 ST16 OCP**
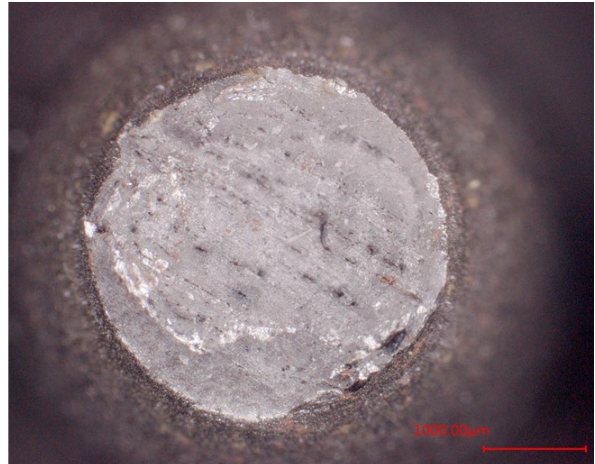
**A537 ST17 OCP**
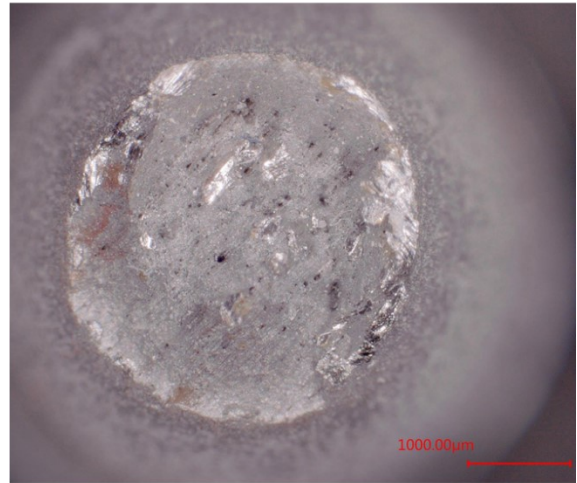
**A537 ST34 OCP**
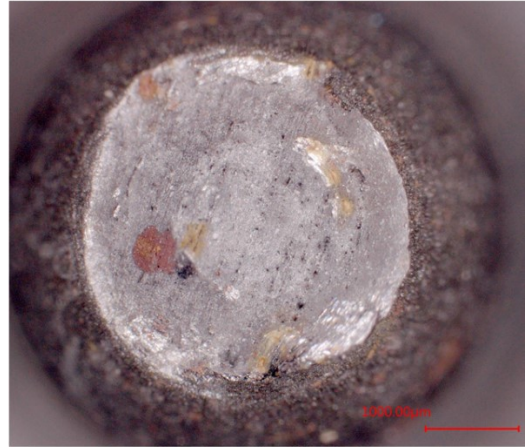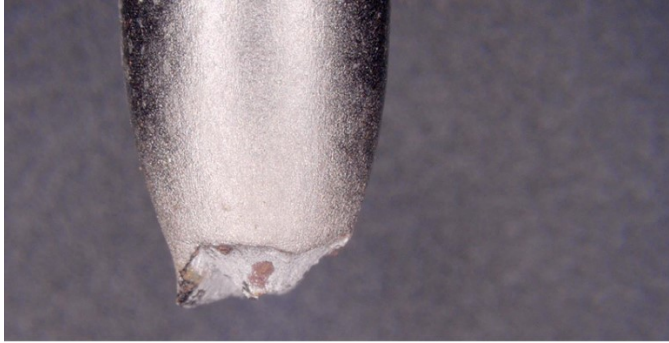
**A537 ST35 +200 mV vs. OCP**
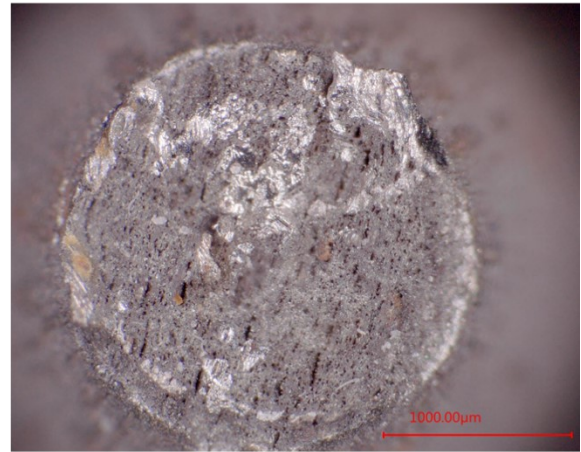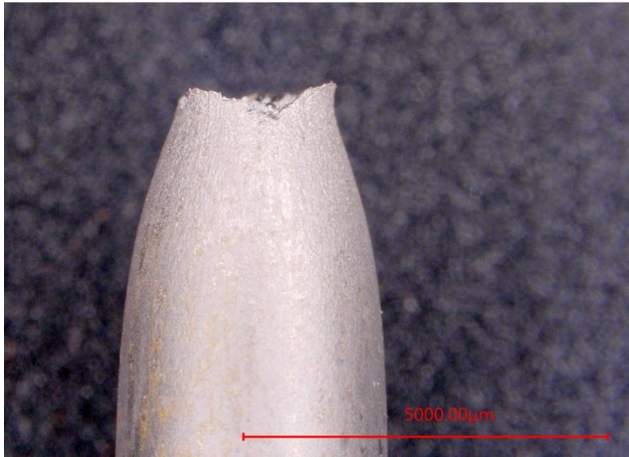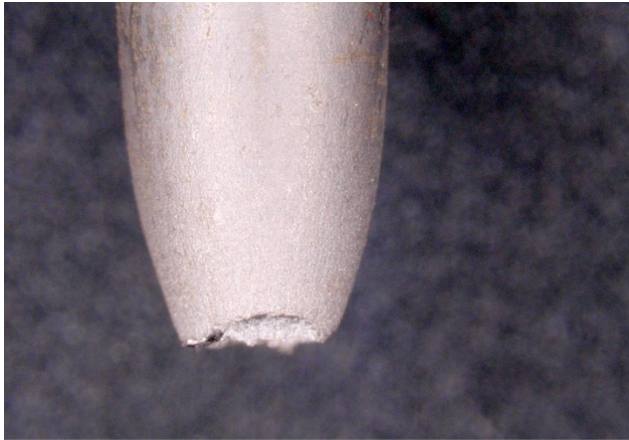
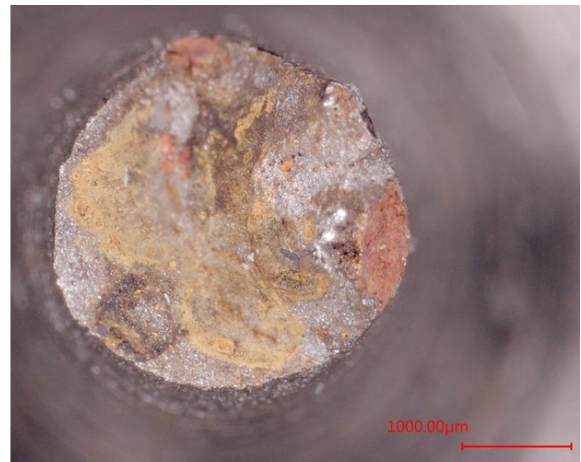**A537 ST35 +300 mV vs. OCP**
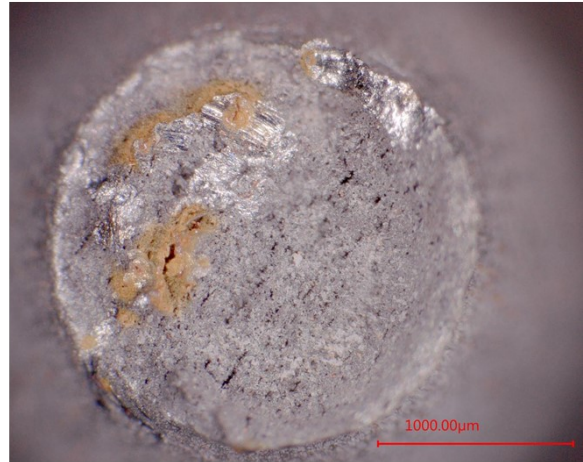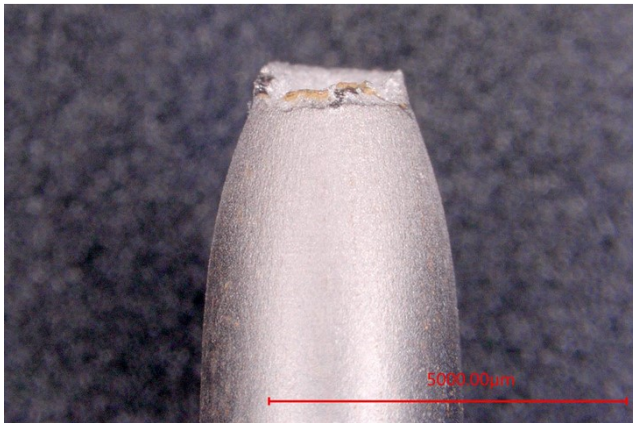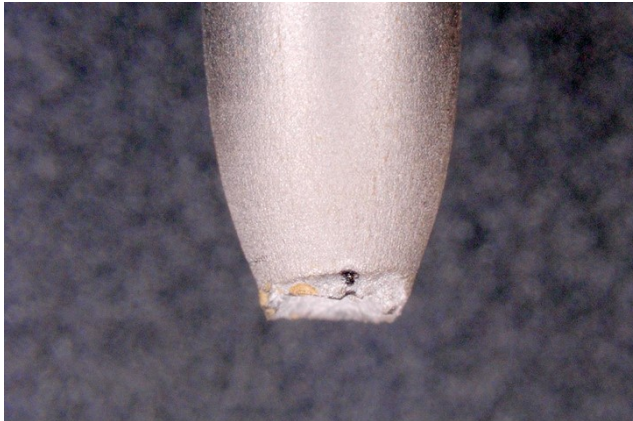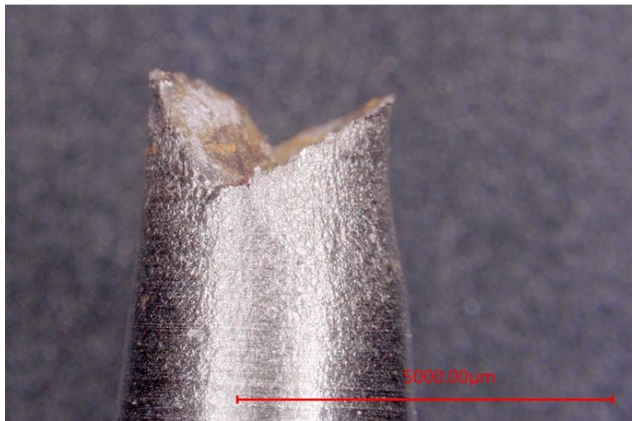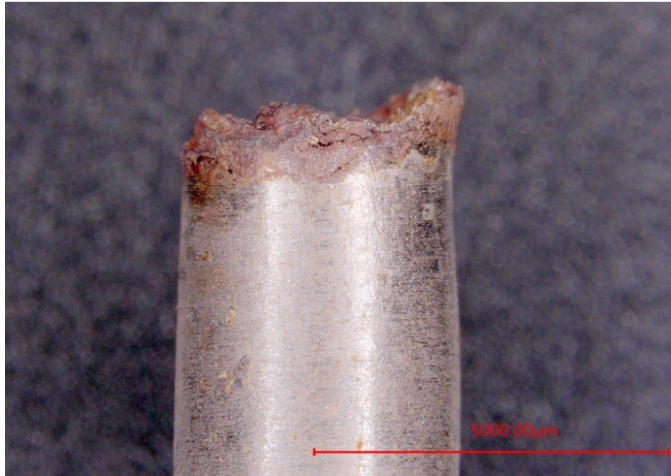
**A285 Mineral Oil**
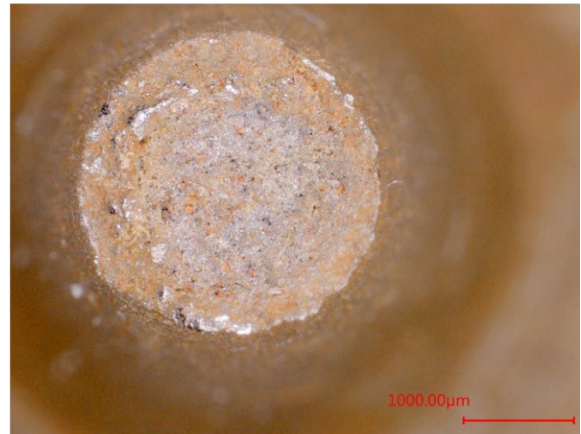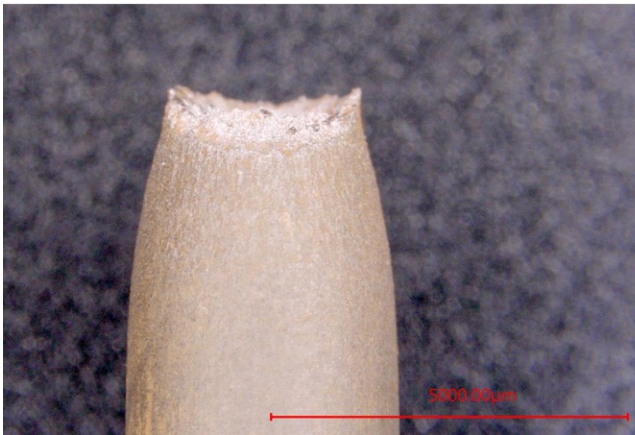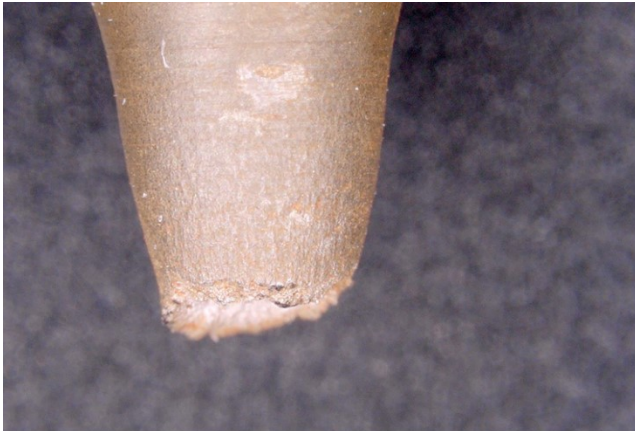
**A285 ST05 OCP**
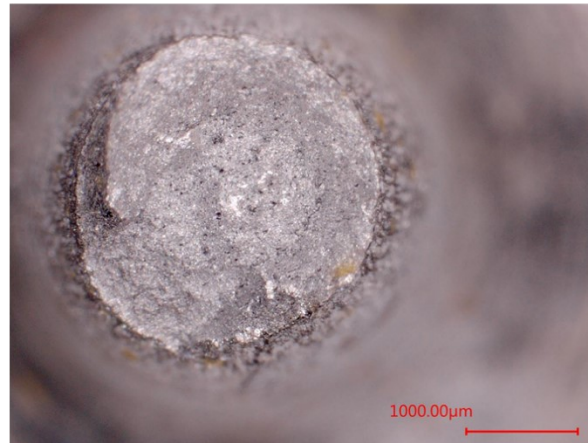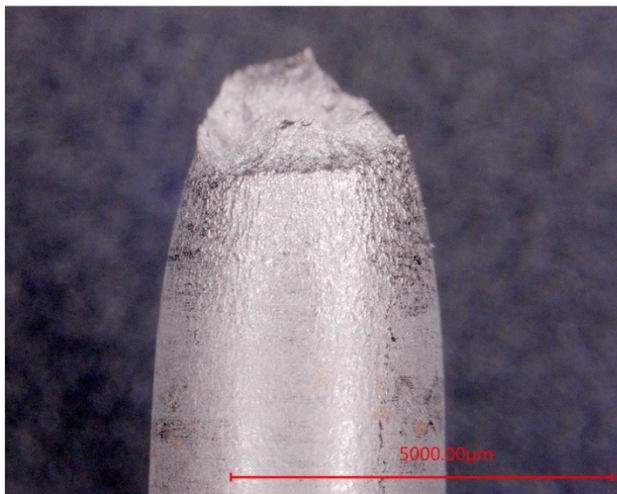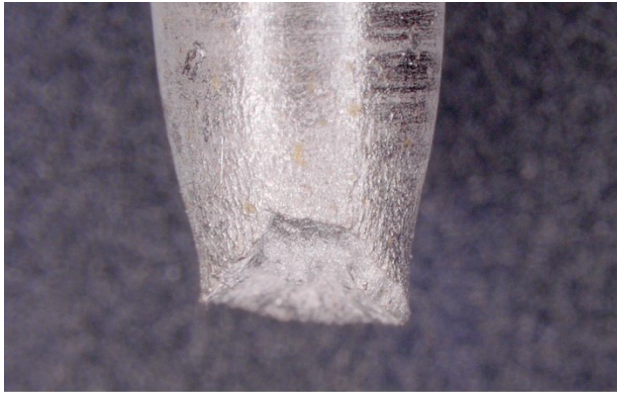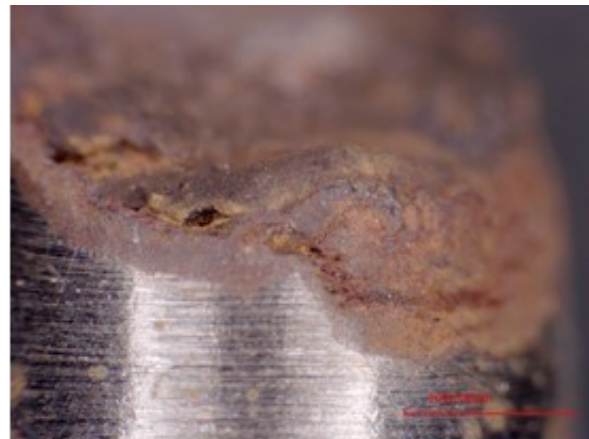
**A285 ST05 +200 mV vs. OCP**
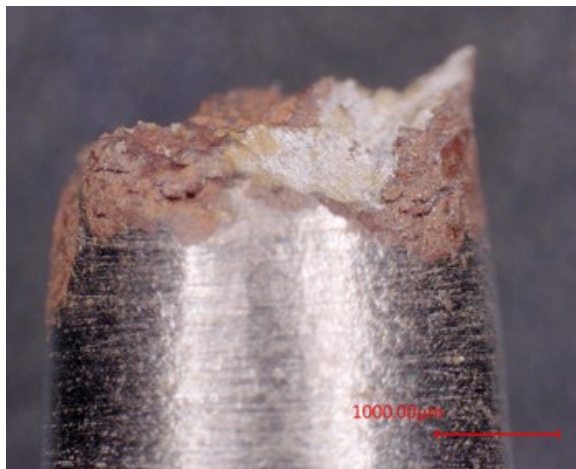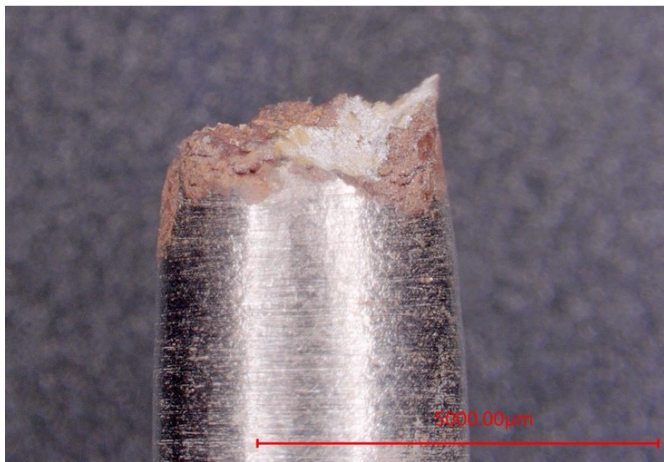
**A285 ST11 +200 mV vs. OCP**

**A285 ST11 +300 mV vs. OCP**

**A285 ST34 +200 mV vs. OCP**

**Distribution:**

a.fellinger@srnl.doe.gov
alex.cozzi@srnl.doe.gov
Amy.Ramsey@srnl.doe.gov
Andrea.bridges@srs.gov
arthur.wiggins@srs.gov
Azadeh.Samadi-Dezfouli@srs.gov
Azikiwe.hooker@srs.gov
bill.wilmarth@srnl.doe.gov
Boyd.Wiedenman@srnl.doe.gov
Brenda.Garcia-Diaz@srnl.doe.gov
Bruce.Wiersma@srnl.doe.gov
c.diprete@srnl.doe.gov
celia.aponte@srs.gov
Christie.sudduth@srs.gov
Christine.Ridgeway@srs.gov
connie.herman@srnl.doe.gov
daniel.mccabe@srnl.doe.gov
david.crowley@srnl.doe.gov
earl.brass@srs.gov
eric.skidmore@srnl.doe.gov
erich.hansen@srnl.doe.gov
frank.pennebaker@srnl.doe.gov
Gregg.Morgan@srnl.doe.gov
james.folk@srs.gov
jeffrey.crenshaw@srs.gov
john.mayer@srnl.doe.gov
Joseph.Manna@srnl.doe.gov
Keisha.martin@srs.gov
michael.stone@srnl.doe.gov
nancy.halverson@srnl.doe.gov
patricia.suggs@srs.gov
phillip.norris@srs.gov
Records Administration (EDWS)
Richard.Edwards@srs.gov
Roderick.Fuentes@srnl.doe.gov
Ryan.McNew@srs.gov
Frank.Pennebaker@srnl.doe.gov
Stephen.harris@srnl.doe.gov
Thomas.Huff@srs.gov
timothy.baughman@srs.gov
timothy.brown@srnl.doe.gov
tony.polk@srs.gov
Vijay.Jain@srs.gov
William.Ramsey@SRNL.DOE.gov